



저작자표시-비영리-변경금지 2.0 대한민국

이용자는 아래의 조건을 따르는 경우에 한하여 자유롭게

- 이 저작물을 복제, 배포, 전송, 전시, 공연 및 방송할 수 있습니다.

다음과 같은 조건을 따라야 합니다:



저작자표시. 귀하는 원저작자를 표시하여야 합니다.



비영리. 귀하는 이 저작물을 영리 목적으로 이용할 수 없습니다.



변경금지. 귀하는 이 저작물을 개작, 변형 또는 가공할 수 없습니다.

- 귀하는, 이 저작물의 재이용이나 배포의 경우, 이 저작물에 적용된 이용허락조건을 명확하게 나타내어야 합니다.
- 저작권자로부터 별도의 허가를 받으면 이러한 조건들은 적용되지 않습니다.

저작권법에 따른 이용자의 권리는 위의 내용에 의하여 영향을 받지 않습니다.

이것은 [이용허락규약\(Legal Code\)](#)을 이해하기 쉽게 요약한 것입니다.

[Disclaimer](#)

Chapter 1

Introduction

1. Introduction

Recently, cellulose nanofiber has been the subject of extensive scientific researches (Ghanadpour et al. 2015; Zhang et al. 2015). ‘Cellulose nanofiber’ is classified as cellulose nanocrystal (CNC) which produced by acid hydrolysis and cellulose nanofibrils (CNF) that made by mechanical disintegration with/without various pre-treatment. In case of CNC, concentrated sulfuric acid is commonly used to produce stable suspension by sulfuric acidic groups, which provide some electrostatic repulsion among the CNC (Espinosa et al. 2013). Acid hydrolysis degrades amorphous regions of cellulose and remains rod-like crystals with typical diameters of 5-50 nm and length scale of 100-300 nm (Candanedo et al. 2005). Homogenization, microfluidization, and micro-grinding are mechanical methods for the production of CNF, which has both crystalline and amorphous regimes (Nakagaito and Yano 2004; Zimmermann et al. 2004; Abe et al. 2007). Passing through such mechanical treatments, the pulp fiber disintegrated to strongly entangled networks CNF gels. The width of CNF is 5-100 nm and length is several micrometers depending on the source of cellulose (Henriksson et al. 2007). Even though, CNF has a potential application fields due to technically attractive properties, the isolation of CNF from pulp fiber by mechanical treatment still requires high-energy consumption and that is one of difficult issue to produce CNF by mill scale. The energy consumption to manufacture cellulose microfibril with suitable properties has been reported in the range of 5,580-31,000 kJ/kg (Henriksson et al. 2007; Spence et al. 2011).

Intensive research has been performed to easy fibrillation and to reduce energy consumption. Enzymatic hydrolysis and chemical pretreatment were commonly used for this matter. Pääkkö et al. (2007) reported about the use of

enzymatic hydrolysis with mechanical shearing to promote delamination of the fiber wall. Henriksson et al. (2007) used endoglucanase as enzymatic pretreatment. It was found that cellulose DP was decreased and crystallinity index was increased during enzymatic hydrolysis.

Chemical pretreatment such as TEMPO oxidation (Saito et al. 2006), carboxymethylation (Wågberg et al., 2008), and phosphorylation (Suflet et al. 2006) has also been studied as an option to enhance nano-fibrillation. The chemical pretreatment may provide an opportunity of decreasing energy consumption for CNF production by introducing charged groups onto pulp fiber, which enhance repulsive force inside fiber wall. Charge properties of pulp fiber such as zeta-potential and carboxyl group contents have strong influence on energy demand to isolate CNF. These charged groups also provide electrostatic repulsion between the fibrils, which creates the well-dispersed CNF suspensions that are necessary to form final products that have the uniform and mechanical properties (Ahola et al. 2008; Fujisawa et al. 2012).

Among the chemical pretreatments, the carboxymethylation is one of the most widely used methods as a chemical pretreatment. Carboxymethylation is carried out by etherification of the cellulose hydroxyl group with monochloroacetic acid (MCA) under alkaline conditions, which increases the water retention value and significantly decreases the ratio of crystalline to amorphous cellulose (Chen et al. 2013). The hornification caused by the formation of irreversible hydrogen bonding during drying can be reduced by replacing the hydroxyl groups with carboxymethyl groups in carboxymethylated CNF (Eyholzer et al. 2010).

In spite of the various benefits of carboxymethylation as a pretreatment for producing CNF, there are still limitations to applying mass production process. In the carboxymethylation process, water in the pulp suspension is normally solvent exchanged several times by ethanol (Naderi et al., 2017; Wang et al., 2011). Huge amounts of ethanol are consumed during this solvent exchange process, which increase the cost for the production of CNF. After the solvent exchange step, the carboxymethylation step is carried out in solvent mixtures such as methanol/isopropanol and ethanol/isopropanol, which are reaction mediums for producing carboxymethylated pulp. These organic solvents are usually discarded after carboxymethylation process. The use of a huge amount of organic solvent leads to the increase of production cost, although the mechanical energy consumption could be reduced by carboxymethylation. Therefore, it is important to optimize reaction conditions of carboxymethylation in terms of cost-effective and higher reactivity.

In addition, the characteristics of CNF such as surface charge, width, and length are important to its proper utilization. Because final product quality determines the characteristics of the CNF. The morphology of CNF is one of the factors to influence the fundamental properties of CNF-based materials. Microscopic techniques including scanning electron microscope (SEM), transmission electron microscope (TEM), and atomic force microscopes (AFM) can accurately measure the diameter of the fibers (Iwamoto et al. 2014; Uetani and Yano 2011; Pääkkö et al. 2007). However, the length of the fibers cannot be readily obtained from microscopy images, as a CNF is too long to be observed in its entirety under high magnification (Ishii et al. 2011). Furthermore, the high aspect ratio fibers tend to become entangled with each other, which makes it difficult to determine the ends of a single fiber (Ishii et al. 2011). Fukuzumi et al. (2013) measured the length and length distribution of TEMPO-

oxidized CNF (TOCN) using TEM images and investigated the effect of CNF length on film properties. They found that films prepared with a longer average length TOCN had high tensile strength and elongation at break. However, it was not easy to determine the fibril length using electron microscopes (TEM or SEM), even though these techniques offer clear and instant understanding of the structural features of CNF, because numerous observations are required for statistically reliable size evaluations. Understanding and controlling the characteristics of CNF would be useful to predict the properties of final product. Therefore, to use CNF, it is necessary to understand how pretreatment conditions affects the characteristics of CNF.

2. Objectives

The objective of this study is to optimize the carboxymethylation process as pretreatment for the production of CNF. Carboxymethylation process commonly uses several kinds of alcohol including ethanol, methanol and isopropanol to solvent-exchange water or as reaction mediums, it is imperative to simplify the process while increasing carboxymethylation efficiency. Some reaction conditions on the carboxymethylation were controlled to find main factor on carboxymethylation. Reaction sequence and solvent type for carboxymethylation were also investigated to optimize reaction. The solvent recycling is important for the environmental and economic aspects of the process. Thus, the compositions of the waste reaction medium were examined to understand crucial factor for solvent recycling and 4 Å molecular sieve treatment was conducted to dehydrate water in reaction medium. Fibrillation degree of carboxymethylated pulp, degree of polymerization, crystallinity, and width of CNF were examined as factors to understand CNF characteristics produced under different carboxymethylation conditions. In addition, aspect ratio of carboxymethylated CNF (CM CNF) depending on mechanical treatment intensity and carboxyl content were investigated by using sedimentation experiments. This study mainly consists of three parts:

- In the first part, the reaction efficiency of carboxymethylation depending on reaction conditions including solvent system, water content, and pulp consistency were investigated to optimize the pretreatment conditions. The characteristics of CM CNF produced under different reaction conditions were also evaluated.

2) In the second part, a way to recycle waste solvent from the carboxymethylation process was investigated. Solvent medium was recovered after carboxymethylation reaction and recycled in the next carboxymethylation reaction. Solvent medium properties including conductivity, pH, and water content were measured to investigate the composition of the waste solvent.

3) In the last part, characteristics of CM CNF in terms of morphology, suspension network strength, and film strength were investigated. To understand how reaction conditions affect the characteristics of CM CNF, various reaction conditions were controlled.

Chapter 2

Literature Reviews

1. Pretreatment for the production of CNF

The first successful isolation of cellulose to microfibrils was reported in 1983 (Turbak et al. 1983; Herrick et al. 1983). The fibrils ranging from 10 to a few hundred nanometers was disintegrated by intensive shear force and pressure. Strong entanglement and stable network properties of this material provide an opportunity to use thickeners, additives in coating, food, cosmetics, as well as reinforcement in composites (Oh et al. 2017; Suryanegara et al. 2009). Mechanical, enzymatic, and chemical pretreatments have been tested as methods to facilitate nanofibrillation (Wang et al. 2015; Ko et al. 2011, Suflet et al. 2006), which made the CNF a more attractive material for commercial applications (Nechyporchuk et al. 2016).

Enzymatic pretreatment were classified as two class. First, cellulose can be degraded by cellulase, which hydrolyze cellulose amorphous regions. Liu et al. (2015) studied the effect of cellulase treatment on bleached hardwood kraft pulp. It was found that amorphous region of cellulose is easily accessed by enzyme, which decreased the degree of polymerization (DP) of cellulose (Fig. 2-1). Qing et al. (2013) reported that enzyme pretreatment produced shortened fibrils due to preferential hydrolysis of amorphous regime of cellulose and the films prepared from highly crystalline enzyme pretreated CNF had the high tensile stiffness and low strain at break than chemical pre-treated CNF films. Second, the hemicellulase primarily catalyzes the hydrolysis of hemicellulose composition. Meng et al. (2014) investigated the effect of xylan removal, which most abundant composition in hemicellulose, on chemical reaction efficiency on pulp fiber. It was found that xylanase treatment for removing xylan was advantageous in saving the reaction time and chemical reactivity because the presence of xylan on the pulp prevents chemical accessibility.

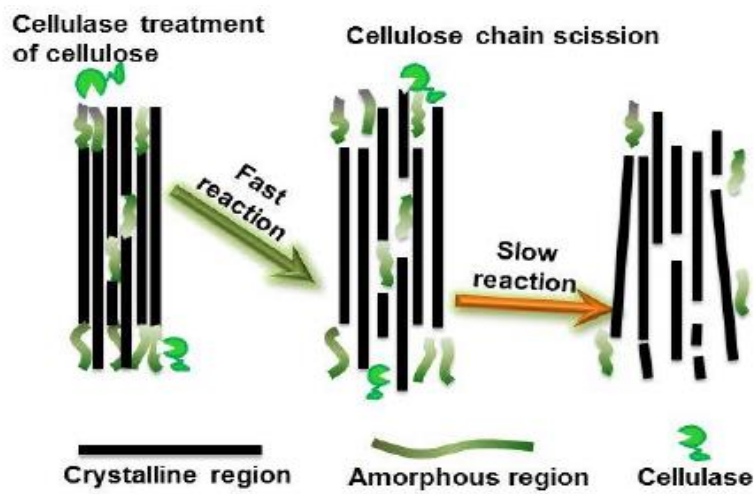


Fig. 2-1. Hypothesis of cellulose chain scission due to enzyme treatment (Liu et al. 2015).

CNF can be also prepared by chemical pretreatment including TEMPO (2,2,6,6-tetramethyl-1-piperidinyloxy)-mediated oxidation (Fig. 2-2a), and carboxymethylation (Fig. 2-2b).

There are two TEMPO-mediated oxidation systems have been reported. The TEMPO-mediated oxidation is conducted by the addition of NaClO to pulp suspension in the presence of catalytic TEMPO and NaBr at pH 10-11 under room temperature (de Nooy et al. 1995; Saito et al. 2013). This chemical reaction can also occur under acidic condition (Hirota et al. 2010; Saito et al. 2009). In the acidic condition, TEMPO, NaClO, and NaClO₂ are used under pH 4.8-6.8. However, relatively higher reaction temperature around 40-60 °C and longer oxidation times of 1-3 days are required. The C-6 hydroxyl groups of cellulose are converted to carboxylate group by TEMPO-oxidation (Isogai et al. 2011; Fan et al. 2009).

For the cost efficiency of this reaction, recycling and recovery of chemicals have been investigated due to TEMPO and NaClO represent the major costs. Casson and Bess (2006) reported that hypochlorite recycling can be achieved by electrolysis of sodium chloride, which generated by by-product of NaClO derived from TEMPO-oxidation filtrates. Kuutti et al. (2016) used octadecyl silane sorbent having porosity of 60 Å to adsorb TEMPO molecules.

The degree of substitution (DS) of commercially available carboxymethyl cellulose (CMC) is usually between 0.5 and 1.0. Such highly substituted CMC is soluble in water. However, carboxymethylated pulp with below a DS of 0.3 is insoluble in water and maintain their fiber structure (Eyholzer et al. 2010).

Carboxymethylation to produce CNF as pre-treatment was firstly introduced by Wågberg et al. (2008). Briefly, pulp was firstly solvent exchanged by ethanol

several time. The pulp fibers were then impregnated with isopropanol dissolved monochloroacetic acid. The reaction was then carried out under alkaline condition to methanol and isopropanol mixture solvent. This method has been used for typical carboxymethylation method as chemical pre-treatment even until now (Naderi et al. 2017). The combined pretreatment of beating and carboxymethylation was investigated to make the fibrillation more easy and to reduce energy consumption by Im et al. (2017). It was found that the sequence of carboxymethylation and beating was more effective in terms of energy saving than the single carboxymethylation treatment. Dried powder of CNF has advantage in terms of the low shipping cost and storage convenience. The ability of re-dispersion stability of carboxymethylated CNF after drying was compared to CNF produced by only mechanical treatment (Eyholzer et al. 2010). The results demonstrated that the carboxymethylated CNF can overcome hornification during drying process due to carboxyl groups.

In case of carboxymethylation, recycling of reaction solvents should be considered for the environmental impact and cost efficiency. However, mixture solvent has similar boiling point and forms azeotropes with water, it make separation through normal distillation difficult (Arvidsson et al. 2015).

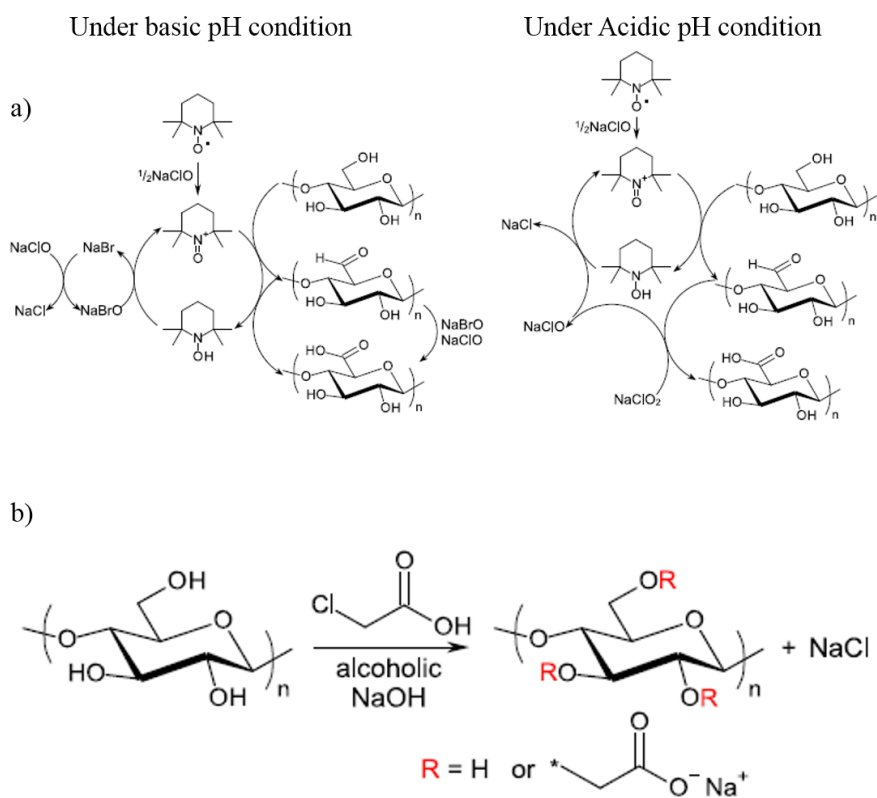


Fig. 2-2. Schematic diagrams of chemical pretreatment; (a) TEMPO-mediated oxidation, (b) Carboxymethylation (Nechyporchuk et al. 2016).

2. Reactivity of carboxymethylation

The first step in the carboxymethylation of CNF is an equilibrium reaction between sodium hydroxide and the hydroxyl groups of the pulp fiber (i.e., alkalization) [1].



where R is backbone of the pulp fiber.

Mansikkamäki et al. (2005) investigated the change in the crystalline region of cellulose from cellulose I to cellulose II during alkalization. The structural changes of cellulose crystallites in different solvent systems depend mainly on the soluble alkali concentration. The cellulose alkalization with sodium hydroxide in an alcohol/water solution is normally used to produce Na-cellulose. Ambjörnsson et al. (2013) studied how the reactivity of carboxymethylation depended on the sodium hydroxide concentration using near-infrared (NIR) Fourier transform (FT) Raman spectroscopy and concluded that the sodium hydroxide concentration in an alkalization stage had a distinct influence on the etherification reaction. Yokota (1985) also studied the alkalization of cotton linters in an isopropanol/water solution. It was found that after the addition of sodium hydroxide, the liquid mixture separated into two layers: a lower-layer solution (LLS) that mainly consisted of water and sodium hydroxide and an upper-layer solution (ULS) that mainly consisted of isopropanol and water with a very small amount of sodium hydroxide (Fig. 2-3). Bhattacharyya et al. (1995), who studied the effect of the water content in the organic reaction medium, showed that water aids the swelling of starch granules and thus facilitates the entry of the etherifying agent into the starch granules (Fig. 2-4).

The alkali cellulose, which is accessible and reactive towards MCA, reacts with MCA in the etherification [2] and finally hydroxyl groups are substituted by carboxymethyl groups.



The presence of an organic solvent during carboxymethylation promotes an even distribution of the NaOH and MCA during the reaction. Numerous studies have examined the solvent systems for carboxymethylation of pulp (Jie et al. 2004; Ramos et al. 2005; Qi et al. 2009). The effects of the solvent system are dependent on the solvent polarity and ability to dissolve ions (Stigsson et al. 2006). Isopropanol has been reported to be the most suitable organic solvent, with high efficiency and quality. Other organic media such as ethanol and methanol, however, are still used commercially due to their economic advantages (Mann et al. 1998; Tijssen et al. 2001). Qui et al. (1999) reported the synthesis of carboxymethyl cassava starch in ethanol. Among the experimental studies reported on the production of carboxymethylated CNF, only a limited number of studies dealt with the effect of the reaction conditions on carboxymethylation of CNF (Fall et al. 2011; Chen et al. 2013).

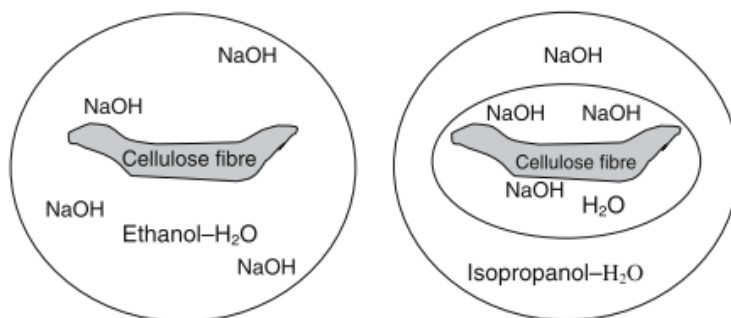


Fig. 2-3. Solvent effect depending on solvent polarity during alkalization (Stigsson et al. 2006).

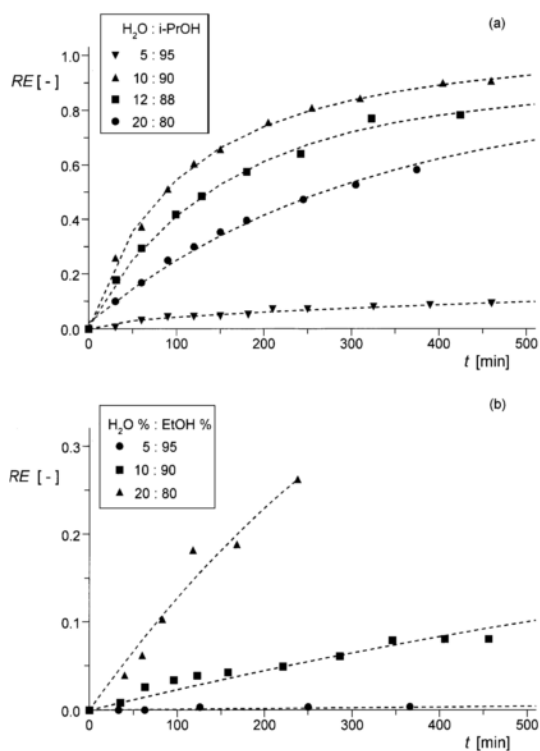


Fig. 2-4. Effect of the water content on the reaction efficiency (Tijen et al. 2001).

3. Quality assessment of CNF

3.1 Morphological properties of CNF

A number of research have been studied for the quality assessment of obtained CNF. The morphological properties of CNF is one of the most important quality control parameters. It is depends on mechanical treatment, pretreatment routes, and even starting materials (Jonoobi et al. 2015). Spence et al. (2011) showed that the MFC produced by homogenization resulted in large increases in specific surface area compared to microfluidization and grinding due to additional fiber shortening by impact forces against value. Generally, CNF produced by only mechanical treatment or with enzymatic pretreatment have thicker average width compared to chemically pretreated CNF (Henriksson et al. 2007; Suflet et al. 2006). Aulin et al. (2009) reported that the CNF produced by mechanical treatment and carboxymethylation pretreatment has a width of 10-30 nm and 10-15 nm, respectively.

Microscopic techniques including SEM and TEM can accurately measure the diameter of the fibers (Abe et al. 2007; Uetani and Yano. 2011; Pääkkö et al. 2007). Atomic force microscopes (AFM) have also been used to measure morphological properties of CNF (Shinoda et al. 2012; Saito et al. 2013). Besbes et al (2011) investigated the effect on fibrillation degree of TEMPO-oxidized pulp depending on carboxyl content. FE-SEM image was concluded that the pulp with over 500 $\mu\text{mol/g}$ of carboxyl content was disintegrated by CNF with width being in the range of 5-20 nm after five homogenizing passes at 600 bar. The microscopic measurements must be made at different magnifications, as CNF have broad fiber diameter distribution (Zhang et al. 2012). However, it is time consuming to perform nanoscale analysis as well as

hard to carry out the repetitive measurement.

The water retention value (WRV) and viscosity of the CNF suspension usually measured as indirectly assessment for the degree of fibrillation (Carrillo et al. 2014; Im et al. 2017). Im et al. (2017) studied about relationship between grinding number of passes and low shear viscosity depending on introduced carboxyl group content. It was found that low shear viscosity of diluted pulp or CNF suspension increased with increased the number of grinding passes. However, the viscosity reached a plateau when fibers were completely nanofibrillated. The pulp with higher carboxyl contents reached a plateau viscosity more quickly. Lassuyguette et al. (2008) reported similar tendency as well.

The light transmittance by ultraviolet-visible (UV) spectroscopy can also give an insight into the fibrillation degree. When the light passes through a suspension containing randomly dispersed particles, transparency or transmittance was decreased due to increased light scattering. Alila et al. (2013), who estimated the transmittance of CNF suspension depending on homogenization condition, reported that transmittance curve from 400 to 800 nm means an approximately extent of the nanofibrillation of pulp fiber. The light scattering encompass Rayleigh and Tyndall scattering. The former applied to the case when scattering particle is very small being lower than $1/10$ wavelength (about 40 nm). Therefore, the CNF with width lower than 40 nm will be involved in Rayleigh scattering. On the other hand, the later scattering accounts for particle sizes larger than a wavelength of light.

3.2 Rheological properties of CNF

CNF forms 3-dimensional percolated networks at very low suspension consistency due to their high aspect ratio. The rheological properties have been investigated to evaluate the network properties of CNF. The understanding and controlling the rheological properties of CNF are essential because it can reflect a behavior of this material in different industrial process including casting, mat formation, and drying (Sim et al. 2015). CNF suspension shows shear thinning and thixotropic behavior (Klemm et al. 2011). The storage modulus is strongly dependent on the suspension consistency. An increase suspension consistency from 0.125 to 5.9 % resulted in an increase of storage modulus by five orders of magnitude (Pääkkö et al. 2007). Ishii et al. (2011) measured the rheological properties of TEMPO-oxidized CNF by using stress-controlled rheometer. The results showed that when CNF suspension consistency above 0.03 w/v%, storage moduli and loss moduli were almost independent of frequency of oscillatory shear, which indicated that fibril forms the gel-like network structure due to entanglement.

The rheological properties of CNF can be affected by many factor including charge properties, degree of fibrillation, ionic strength of suspension, and pH. Benhamou et al. (2014) measured the elastic modulus of TEMPO-oxidized CNF as a function of the oxidation time for the 1 wt% CNF dispersion. The results showed that when oxidation time increased, the modulus was decreased due to the reduction of the CNF length. Tanaka et al. (2014), who evaluated the lengths of TEMPO-oxidized CNF by shear viscosity measurement of its dilute dispersion, showed that length weighted average length, L_w , measured by microscopic observation has linear relationship with the viscosity-average lengths, L_{visc} , calculated by shear viscosity measurement.

The viscosity of CNF depending on pH and ionic strength was also investigated by Jowkarderis and van de Ven (2014). They showed that when the pH of suspension decreased, the intrinsic viscosity was decreased because carboxyl groups were protonated and electrical double layer thickness was decreased.

The CNF is a potential materials to use rheology modifier in diverse industry. The addition of this material to bentonite-water based drilling fluids enhanced rheological properties including viscosity, shear stress, and yield point (Li et al. 2015). Hoeng et al. (2017) evaluated the suitability of CNF as a thickening agent on silver nanowire screen printing ink. They also modified CNF visco-elastic properties by combining hydroxypropylmethyl cellulose to obtain process compatibility. Oh et al. (2017) investigated the effect of CNF and CMC as pigment coating additives and found that CNF caused a less flocculated coating color than CMC because it does not significantly affect particle interaction and produced a porous coating layer with low addition level.

4. Application fields using CNF

4.1 Packaging

The packaging industry looks forward to sustainable materials. Currently, the packaging materials are mainly based on glass, aluminum and synthetic plastics (Nair et al. 2014). Increased environmental concerns about challenges of sustainability and renewable resources have been strongly advocated. The use of packaging materials should provide sufficient barrier against oxygen, water vapor, grease etc. CNF has vast possibilities of utilizing for packaging material. The ability to form hydrogen bonds resulting in strong network and make it very difficult for the molecules to pass through (Ferrer et al. 2017). Wu et al. (2012) produced multilayered organic/inorganic hybrid composite film from CNF and montmorillonite with a weight ratio of 50:50. Composite film has excellent mechanical and oxygen-barrier properties, despite of low densities. Chaabouni et al. (2017) studied about the effect of the addition of CNF on the properties of waterborne polyvinyl-acetate (PVA) for dispersion coating materials. It was found that CNF has strongly influence on physical properties of PVA matrix. The highly hydrophilic nature of CNF film may lead to low resistance to water. The chemical modification provides the means of permanently altering the nature of fiber cell wall (Hill. 2000). Acetylation of CNF by acetic anhydride is one of modification reaction, which changed the characteristics of cellulose surface from hydrophilic to hydrophobic. The oxygen permeability for pure MFC films of 44 μm average thickness is 17/18.5 $\text{mL m}^{-2}\text{day}^{-1}$, according to Syvered and Stenius (2009). In case of the acetylated CNF film, oxygen permeability was reported about 4.1/4.2 $\text{mL m}^{-2}\text{day}^{-1}$ (Rodionova et al. 2011). The recommended values of oxygen permeability for atmosphere packaging are below 10-20 $\text{mL m}^{-2}\text{day}^{-1}$ (Blakiston 2012).

Silane-based chemicals, such as octadecyldimethyl (3-trimethoxysilylpropyl) ammonium chloride (Andresen et al. 2007), 3-methacryloxypropyl-trimethoxysilane (Qu et al, 2012), and 3-glycidoxypopyltri-methoxysilane (Lu et al. 2008) has been studied to modify surface characteristic of CNF.

4.2 Composite reinforcement

The composite comprise two or more distinct components with different physical and chemical properties. The composite materials show enhanced mechanical properties and new functionality (Miao et al. 2013). For instance, glass fiber have high tensile strength, but no resistance to compression while the plastic resin show high compressive properties and relatively weak in tensile strength. Thus, glass-reinforces plastics (GRP) has superior properties in both compressive and tensile strength.

Numerous studies have been carried out to use CNF as composite reinforcement (Cheng et al. 2009; Siqueira et al. 2009; Wu et al. 2012). The results of those study indicated that fibrils with smaller diameters and longer lengths exhibit stronger reinforcing effect. Xu et al. (2009) compared the effect of cellulose nanocrystal (CNC) and CNF on the mechanical properties of polyethylene oxide (PEO) matrix. It was found that at CNF led to higher strength and modulus than CNC, at the same nanocellulose concentration, due to larger aspect ratio and entanglement of fibrils (Fig. 2-2). Fujisawa et al. (2012) prepared polystyrene (PS) composite reinforced with TEMPO-oxidized CNF with various weight ratios and reported that the storage modulus of the composites films increased significantly with TEMPO-oxidized CNF contents above the glass-transition temperature of PS due to the formation of network structure of TEMPO-oxidized CNF in the PS matrix.

To increase efficient reinforcement effect of CNF, it is necessary to disperse as individual fibrils. However, most synthetic polymers are hydrophobic, and thus it is difficult to disperse homogeneously hydrophilic CNF in synthetic polymer matrices without aggregation. Okita et al. (2011) investigated dispersion stability of TEMPO-oxidized CNF in polar organic solvents such as N,N-dimethylacetamide (DMAc), 1,3-dimethyl-2-imidazolidinon(DMI), N,N-dimethylformamide (DMF), and dimethylsulfoxide (DMSO), because most synthetic polymer used for molding process are soluble in organic solvent. It was concluded that dielectric constant and viscosity of organic solvents influence the nanodispersibility of TEMPO-oxidized CNF and only DMSO formed stable dispersion to individual fibrils.

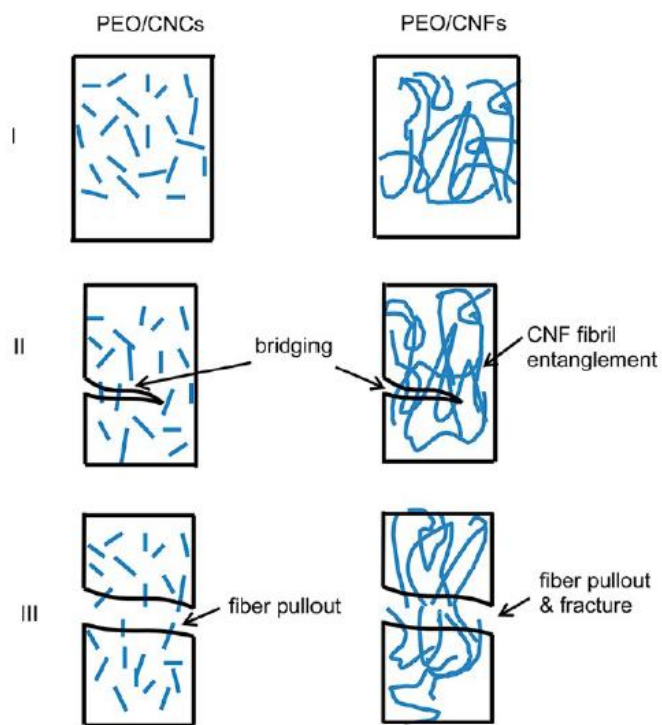


Fig. 2-2. Illustrations of fracture mechanism of nanocomposites (Xu, et al. (2009)).

4.3 Other case

CNF suspensions forms highly networked structure at a low concentration, which can hold a large amount of water while maintaining their structure. Dong et al. (2013) prepared TEMPO-oxidized CNF hydrogels by adding silver salt on the CNF suspension. The strong association of carboxylate group on TEMPO-oxidized CNF with Ag^+ led to entanglement of fibrils due to reduced electrostatic repulsion. High porous cellulose aerogel can be prepared by drying from CNF hydrogel. They entangled mechanically in aqueous suspension and form a homogenous gel structure at a low consistency (Missoum et al. 2013). Kim et al. (2015) produced good network stability foam in aqueous system by cross-linking with maleic acid and sodium hypophosphite. Korhonen et al. (2011) reported the CNF aerogel with a small density of 20-30 mg/cm^3 and porosity of >98% by vacuum freeze-drying. This aerogel absorbed a variety of organic solvents and prevents water absorption, simultaneously. Hydrogel and aerogel has a great potential for application in such fields as tissue engineering, drug delivery, sorbents, sensor, etc (Nechyporchuk et al. 2016).

The use of CNF as additive in paper making process gave the opportunity to decrease basis weight and increase filler content with maintaining paper strength. The mechanical properties of paper can be controlled by the fiber strength, the number of bonds between fiber, and the strength of the bonds (Petroudy et al. 2014). The paper strength can be increased by refining or beating, which improve flexibility and swelling ability of pulp fiber. However, the excess refining can lead to densification of paper structure. The high specific surface area of CNF improve the bond between fibers with cationic polyelectrolytes. Hii et al. (2012) investigated the optimal MFC quality and ground calcium carbonate (GCC) contents on strength properties of paper. They found that the MFC produced though higher homogenizer pass number improved the z-direction strength of paper even at 30 % filler loading.

Chapter 3

Effect of reaction variable on reactivity of carboxymethylation
and CNF production

1. Introduction

Numerous studies discussed the influence of the ionic group content of chemical modified pulp fiber on energy consumption in the mechanical step (Besbes et al. 2011; Liimatainen et al. 2013). However, the decrease in energy consumption by chemical pretreatment was generally regarded to reach industrially acceptable level (Naderi et al. 2015). Thus, the finding new ways to further reduce manufacturing cost are still required.

Development of new machinery can be an option for reduction of mechanical energy consumption. Aqueous counter collision, steam explosion, and extrusion have been introduced as new methods for producing CNF (Kondo et al. 2014; Manhas et al. 2015; Ho et al. 2015). Kondo et al. (2014) reported that aqueous counter collision treatment provides rapid disintegration of pulp without chemical modification. However, it is difficult to find examples of these technologies applied to mill scale production.

In the carboxymethylation process for the production of CNF, excessive usage of solvents such as ethanol, methanol, and isopropanol would cause a significant increase in production cost. Tijssen et al. (2001) investigated the effect of solvent condition in terms of the degree of substitution (DS). Different alcohols including methanol, three isomers of butanol, and acetone were compared as reaction mediums. Jie et al. (2004) evaluated the effect of the water content in the organic reaction medium on carboxymethylation. It was found that water is essential for the carboxymethylation reaction and the optimal water mass percentage is in the range of 7-13%. However, the main purpose of these studies was the preparation of carboxymethyl cellulose (CMC). It is difficult to find an optimized carboxymethylation process depending on reaction variable,

even though, a study on the carboxymethylation efficiency in terms of reactivity and chemical consumption is important to produce CNF at a low cost.

This chapter is aimed to investigate the effects of some reaction conditions including chemical concentration, solvent systems, water content, and pulp consistency on the carboxymethylation of pulp as a pretreatment method for the CNF production. The optimized reaction conditions would be advantageous for improving the reaction efficiency and for reducing the chemical cost to produce CNF. In addition, the properties of CNF manufactured under different reaction conditions were investigated.

2. Materials and Methods

2.1 Materials

To investigate the effect of chemical pretreatment on CNF production, the once-dried and never-dried bleached eucalyptus kraft pulp were used as a raw materials, which were supplied by Moorim P&P, Korea. The solids content of the pulp was 24%. In case of once-dried pulp, the pulp was disintegrated by using laboratory Valley beater without weight for 15 min. In case of never-dried pulp, the pulp was washed with deionized water and disintegrated using a stirrer at the stirring speed of 1,000 rpm. And then the pulp fibers were filtered using a vacuum filtration system to a consistency of 22% before carboxymethylation. The chemical composition of the pulp fiber was measured according to a TAPPI method (T 203 om-93). The pulp consisted of $79.4\% \pm 0.6\%$ cellulose, $18.8\% \pm 0.2\%$ hemicelluloses and small amounts of lignin and ash. For carboxymethylation, monochloroacetic acid (Sigma-Aldrich, 99.0%, MCA), ethanol (Duksan Reagents, 99.9%), sodium hydroxide (Samchun chemical, 98.0%), isopropanol (Duksan Reagents, 99.5%), and methanol (Duksan Reagents, 99.8%) were used without further purification.

2.2 Carboxymethylation as a pre-treatment

The carboxymethylation of pulp was conducted by two different way. First, to find out major factor affecting reactivity of carboxymethylation, the reaction was carried out according to the typically used method with reaction variables (Wågberg et al. 2008). Second, to optimize the reaction conditions, reaction sequence and solvent type was controlled. The detail description of each carboxymethylation process is as follows.

2.2.1 Effect of reaction variables on carboxymethylation

The reaction conditions such as chemicals amount, reaction temperature, and time were controlled to find out major factor affecting reactivity of carboxymethylation (Table 3-1).

The disintegrated pulp fibers were solvent exchanged to ethanol by washing 2 g of pulp three times in 200 mL of ethanol. The pulp was filtered using a vacuum filtration system to a consistency of 18 wt% after each solvent exchange step. The fiber was then impregnated with MCA dissolved in 200 mL of isopropanol for 30 min at 35 °C. In this reaction chamber, NaOH dissolved in 300 mL of methanol and isopropanol mixture (volume ratio of methanol to isopropanol was 1:4) was added for the second reaction. After the reaction, the carboxymethylated (CM) pulp fiber was washed with deionized water until the pH reached 7 ± 0.5 and the conductivity reached ≤ 20 $\mu\text{S/cm}$.

Table 3-1. Carboxymethylation reaction conditions depending on variable

Conditions	Variable
Pulp, g	2
Monochloroacetic acid, mmol/g	1 - 3
Sodium hydroxide, mmol/g	1 - 20
Reaction time, min	40 - 70
Reaction temperature, °C	45 - 65

2.2.2 Effect of reaction sequence and solvent type

To investigate reactivity of carboxymethylation reaction depending on reaction sequence and solvent type, four experiments were carried out (Table 3-2). In experiment 1, the disintegrated pulp fiber was solvent exchanged same as previous. 1 g of pulp was placed in 20 ml of IPA containing 0.96 mmol/g of MCA for 30 min at 35°C. And then, 3.68 mmol/g of NaOH dissolved in 300 mL of solvent mixture was added, which was carried out for 60 min at 65°C according to the method described by Wågberg et al. (2008). Experiment 1 is known as a typical method for preparing carboxymethylated CNF (Naderi et al. 2017; Siró et al. 2011; Aulin et al. 2010). Experiment 2 was carried out without a solvent exchange treatment for the pulp. In experiment 3, the influence of the reaction sequence was investigated. Alkalization with a solvent mixture was conducted before etherification. Experiment 4 consisted of the alkalization in isopropanol followed by the carboxymethylation.

To evaluate the effect of water on carboxymethylation, we controlled the amounts of pulp fiber and water in solvent. We used isopropanol and the pulp that was not solvent-exchanged at a consistency of 22 wt%. Pre-alkalization was followed by etherification.

Table 3-2. Reaction conditions tested for the carboxymethylation of pulp

Experiment	Solvent exchange of pulp	1 st reaction (30 min, 35°C)	2 nd reaction (60 min, 65°C)
		Chemical and solvent	
Exp 1-1	Yes	MCA in 200 mL IPA	NaOH in 300 mL MeOH & IPA
Exp 1-2	No	MCA in 200 mL IPA	NaOH in 300 mL MeOH & IPA
Exp 1-3	No	NaOH in 300 mL MeOH & IPA	MCA in 200 mL IPA
Exp 1-4	No	NaOH in 300 mL IPA	MCA in 200 mL IPA

2.3 Carboxyl group content

The carboxyl group content of the CM pulp was determined using a conductometric titration method in accordance with SCAN-CM 65:02 (Fig. 3-1). This method describes the analysis of total acidic content of pulp fiber, which was the sum of carboxyl group and sulphonic acid group. However, bleached kraft pulp used as a starting materials has negligible sulphonic acid group. Thus, the term of total acid group was replaced by carboxyl group content in this study. Briefly, 1 g of CM pulp in sodium form was converted to the proton form until all acid groups received H^+ as counter-ions and then titrated with 0.05 mol/L NaOH. The total amount of the carboxyl group was calculated according to Equation (1):

$$\text{Carboxyl group content} = (C_{NaOH} \times V_{NaOH}) / w \quad \text{Eq. (1)}$$

where C_{NaOH} , V_{NaOH} , and w are the concentration of the NaOH solution, the volume of the NaOH solution consumed at phase 2, and the oven-dry weight of the sample, respectively.

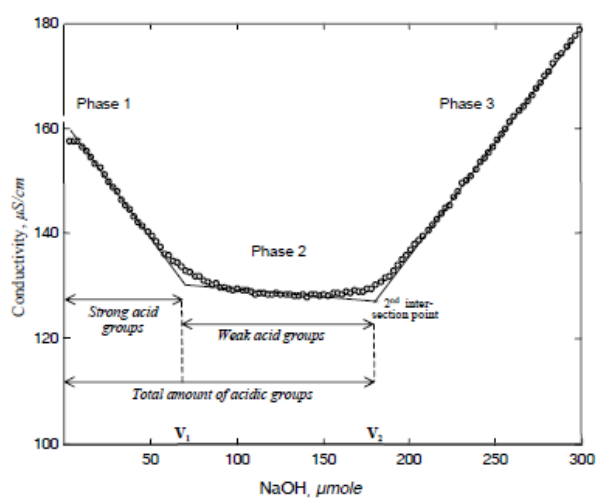


Fig. 3-1. Conductometric titration curve (SCAN-CM 65:02).

2.4 Preparation and characterization of CNF

The CM pulp fibers were used to prepare the CNF suspension. The consistency of the pulp suspension was adjusted to 1.0 wt%, and a sample of 1800 mL of the slurry was taken for CNF production. The pulp suspension was passed through a grinder (Fig. 3-2, Super Masscolloider, Masuko Sangyo Co., Ltd, Japan). The operation speed was 1500 rpm, and the gap distance was - 80 μm . The samples of CNF suspensions were collected for further study after grinding a certain number of passes.



Fig. 3-2. Grinder for preparation of CNF suspension.

To compare the fibrillation degree of pulp fiber produced under different reaction conditions, the low shear viscosity was measured (Brookfield DV2T-LV). Generally, as the number of grinder passes increased, the viscosity increased until it reached a plateau when the pulp fiber was completely nanofibrillated (Im et al. 2017). To evaluate the structural change of cellulose after carboxymethylation under different reaction conditions, the cupriethylenediamine (CED) viscosity (T 230 om-08) and crystallinity of CNF

(or pulp) were also determined. The measurement of crystallinity in CNF (or pulp) was carried out using an X-ray diffractometer with a Cu K α X-ray source (XRD, Bruker, D8 Advance, Germany). For crystallinity measurement of CNF films prepared by vacuum drying were scanned from 5 - 40 degree at a scanning speed of 0.5 sec/step.

The morphological characteristics of the fibrillated CNF were investigated using a field emission scanning electron microscope (FE-SEM, Carl Zeiss, SIGMA, UK) and transmission electron microscopy (TEM, Carl Zeiss, LIBRA 120, Germany). To prepare the CNF specimens for FE-SEM, the surface of a silicon wafer was modified by UV treatment, which changed its surface characteristic from hydrophobic to hydrophilic. Cationic poly-diallyldimethylammonium chloride (P-DADMAC) was applied onto the silicon wafer surface as an anchoring polymer. Then a dilute CNF (0.01%) suspension was applied using a spin coater (ACE-200, Korea). Finally, the specimen was sputtered with platinum for 100 seconds at 20 mA using a sputter coater (BAL-TEC SCD 005) for FE-SEM observation. For TEM analysis, a highly diluted CNF suspension (0.002 wt%) was deposited on a glow-discharged carbon Gu grid (Carbon type-B, Tedpella Inc.) and then negative staining was conducted. CNF sample was observed at an accelerating voltage of 160 kV.

The coalescence kinetics of CNF were investigated using a Turbiscan Ageing Station (Fig. 3-3, Formulaction Inc., France), which measures the light transmittance of near-infrared light ($\lambda_{\text{air}} = 880 \text{ nm}$) through a sample vial. The total analysis duration and analysis interval were 60 min and 5 min, respectively (Fig. 3-4). The transmission and backscattering results were converted to destabilization kinetics (Turbiscan stability index, TSI) as a function of time, according to Equation (2).

$$\text{Turbiscan stability index (TSI)} = \sqrt{\frac{\sum_{i=1}^n (xi - xBS)^2}{n-1}} \quad \text{Eq. (2)}$$

where xi is the average backscattering for each minute of measurement, xBS is the average value of xi and n is the number of scans.

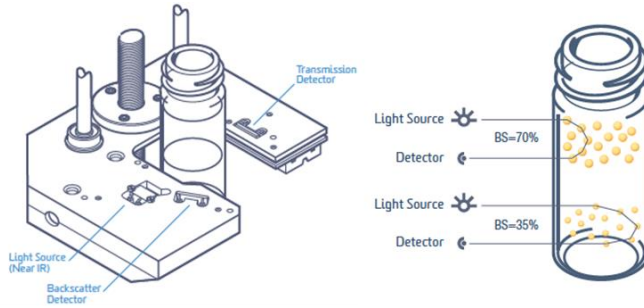


Fig. 3-3. Measurement principle of the Turbiscan Ageing Station.

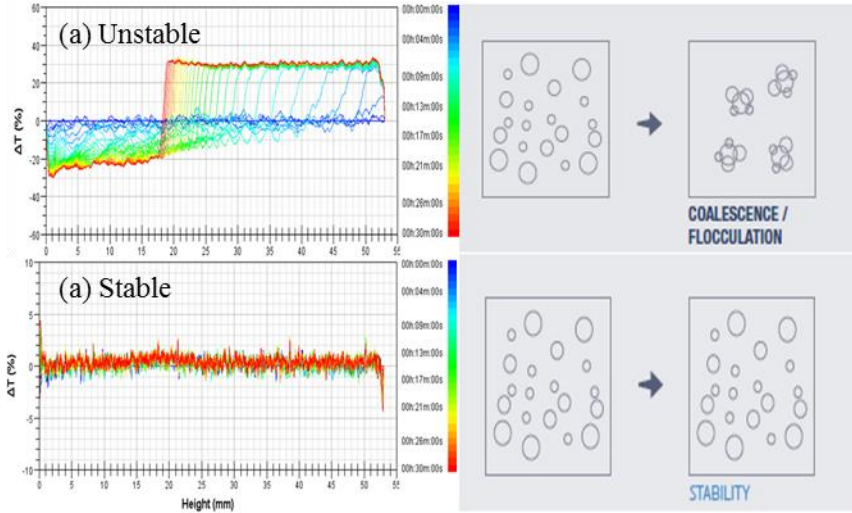


Fig. 3-4. Light transmission results obtained from Turbiscan Ageing station;
(a) Unstable suspension, (b) stable suspension.

3. Results & discussion

3.1 Reactivity of carboxymethylation depending on reaction conditions

3.1.1 Effect of reaction variables on carboxymethylation

The reactivity of carboxymethylation was examined by reaction variables including pulp types, addition level of chemical, reaction temperature, and time as shown Figs. 3-5 to 3-8. The increased concentration of MCA and reaction temperature had impacts on the carboxyl group content of pulp fiber (Figs. 3-5 and 3-6). Higher carboxyl group content facilitates the nanofibrillation process of pulp more easily and prevents clogging problem of the homogenizer (Besbes et al. 2011). A significant increase in the reactivity of carboxymethylation reaction was obtained when reaction temperature was increased, even though, the same level of concentration of chemicals were used. This finding suggests that the addition level of chemical can be reduced by controlling reaction temperature, economically. In case of reaction time (Fig. 3-7), the highest carboxyl group content was attained after 60 min of second reaction (i.e., etherification) and then reaction efficiency was maintained. Fig. 3-8 shows that the effect of NaOH amount on carboxymethylation reaction. It was clearly seen that an increase in concentration of NaOH over 4mmol/g did not give improvement of reactivity.

In addition, the carboxyl group content of once-dried pulp was compared to never-dried pulp at the same reaction conditions. The never-dried pulp shows higher reactivity than once-dried pulp at whole reaction condition. The irreversible agglomeration of the amorphous parts of the cellulose is occurred during drying. Johansson et al. (2011) reported that water cannot break the

hydrogen bonds during the rewetting of horrified cellulose (i.e., once-dried pulp condition). Thus, the reaction site of once-dried pulp was likely limited than never- dried conditions.

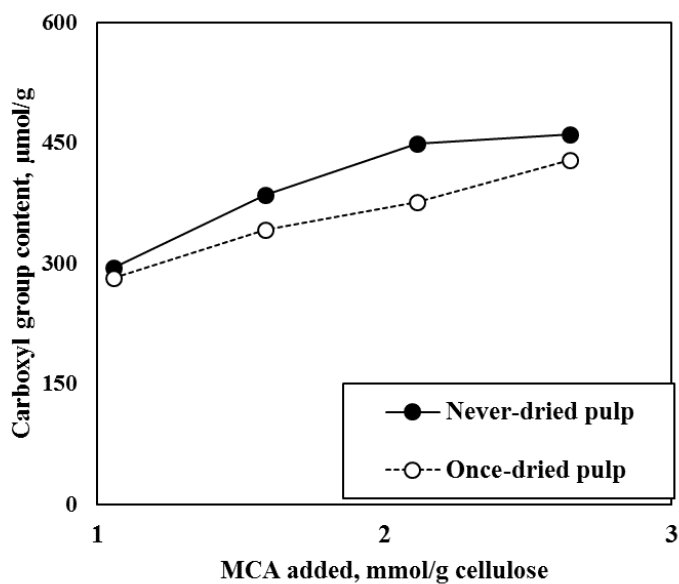


Fig. 3-5. Carboxyl group content of pulp fibers as a function of MCA amounts.

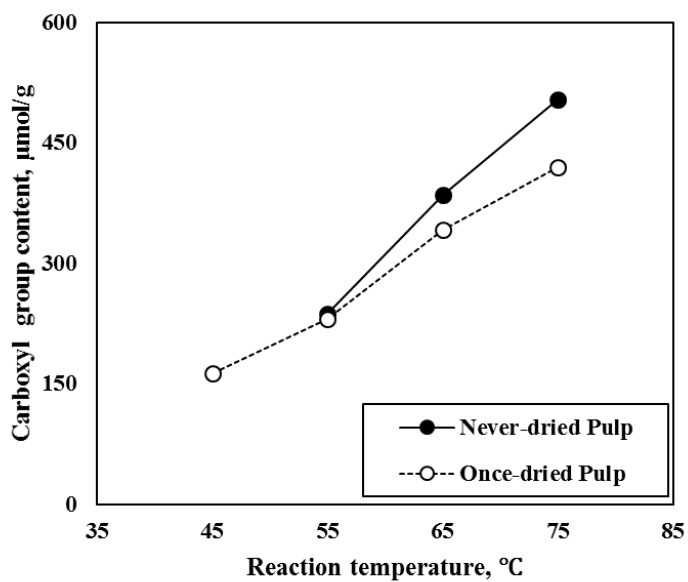


Fig. 3-6. Carboxyl group content of pulp fibers as a function of reaction temperature.

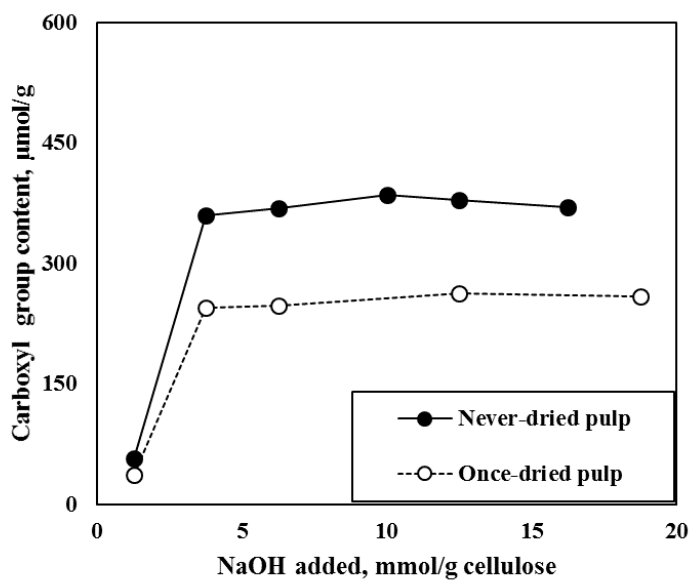


Fig. 3-7. Carboxyl group content of pulp fibers as a function of NaOH amounts.

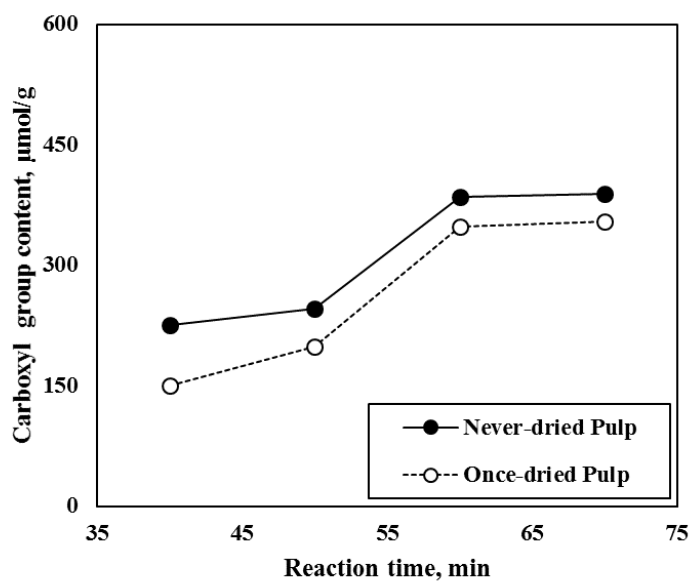


Fig. 3-8. Carboxyl group content of pulp fibers as a function of reaction temperature.

3.1.2 Preparation of CM pulp with different carboxyl content.

To investigate the effect of carboxyl group content on the fibrillation degree of CM pulp three carboxymethylation reaction were carried out (Table 3-3). The 50 g of solvent exchanged pulp fibers, same NaOH amounts, and reaction temperature was applied for the carboxymethylation. However, the pulp type, MCA amounts, and reaction temperature were controlled to produce CM pulp with different carboxyl group content. The untreated pulp condition was estimated to have carboxyl group contents of 50 $\mu\text{mol/g}$ (Table 3-3; Fig. 3-9a), which is attributed to hemicellulose contained in the pulp itself (Benhamou et al. 2014). The highest carboxyl group content was obtained with an increase in both MCA amount and reaction temperature (Table 3-3; Fig. 3-9b).

Table 3-3. Carboxymethylation conditions and carboxyl content of carboxymethylated pulp

Experiment	Pulp type	MCA, mmol/g	NaOH, mmol/g	Reaction temperature, °C	Reaction time, min	Carboxyl contents, $\mu\text{mol/g}$
Control	Once-dried	-	-	-	-	50
Exp 2-1		0.96	3.68	65	60	250
Exp 2-2	Never			75		330
Exp 2-3	-dried	1.85				530

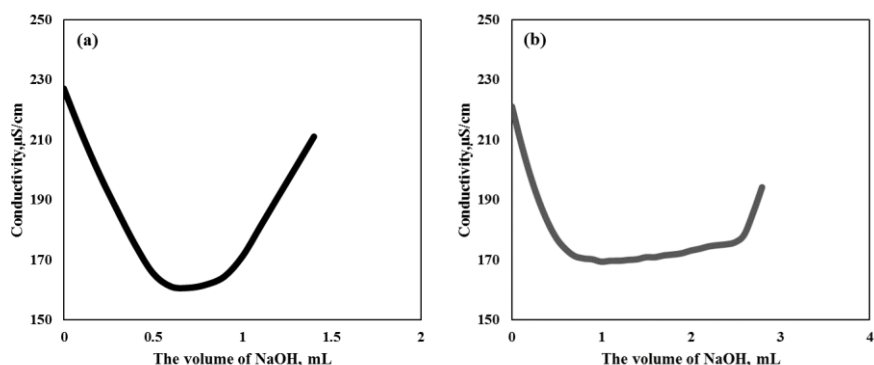


Fig. 3-9. Results on conductometric titration; (a) untreated pulp, (b) CM pulp (Exp 2-3).

3.1.3 Fibrillation degree of CM pulp with different carboxyl content

The low shear viscosity of the pulp ground in the Masscolloider was evaluated to estimate the fibrillation level as a function of the grinding pass number (Fig. 3-10). Obviously, the low shear viscosity increased with the pass number for all samples and reached a plateau, which indicated the complete fibrillation of the pulp to CNF. The results indicated that the fibrillation of the pulp was strongly influenced by the amount of carboxyl groups introduced in carboxymethylation because the carboxyl content eventually changed the interfibrillar electrostatic repulsion force. In case of untreated once-dried pulp, the thirty times of grinding pass was necessary to reach the plateau. Once-dried fiber requires more energy consumption to isolate individual fibrils than never-dried pulp condition, according to the result from Ryu (2013). The CM pulp with the highest carboxyl group content of 530 $\mu\text{mol/g}$, only four times grind pass was needed to complete fibrillation (Exp 2-3), which indicated that about 75 % of energy consumption was saved by carboxymethylation pre-treatment.

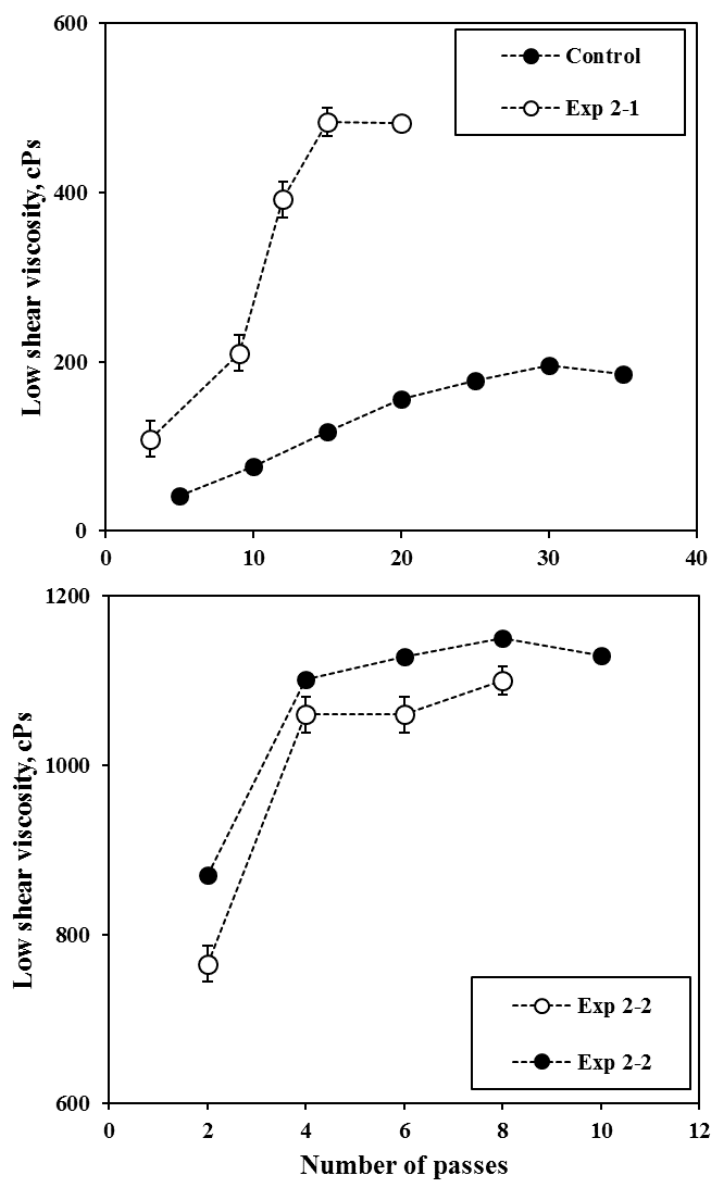


Fig. 3-10. Low shear viscosity of the untreated and CM CNF depended on the carboxyl content.

3.2 Effect of reaction sequence and solvent type

3.2.1 Reactivity of carboxymethylation

As mention in the introduction section, the decrease of energy consumption by chemical pretreatment was achieved industrial acceptable level through various researches. It became more important issue to find new ways for reducing manufacturing cost.

Fig. 3-11 shows the carboxyl group content of the carboxymethylated pulps prepared under the four experimental conditions listed in Table 3-2. A higher carboxyl group content was obtained when pulp was not solvent exchanged. The solvent-exchange process was carried out using a large amount of ethanol, which would cause a significant increase in the production cost of CNF. It is evident that solvent exchange does not provide an advantage for both the carboxymethylation reaction and cost saving. The carboxyl content was increased to 150 $\mu\text{mol/g}$ when alkalization was conducted first without the solvent exchange treatment (Exp 1-3). The highest carboxyl content of 310 $\mu\text{mol/g}$ was obtained when isopropanol was used as the sole solvent for the etherification after the alkalization of non-solvent exchanged pulp. This result indicates that isopropanol gave substantially better reactivity than the solvent mixture of methanol and isopropanol (Exp 1-4).

When the never-dried pulp was added to the isopropanol solution containing sodium hydroxide, some water contained in the pulp would mix with the isopropanol. It was shown that the liquid phase surrounding the cellulose fibers contained concentrated sodium hydroxide and water (Yokata 1985; Mansikkamäki et al. 2005). On the other hand, the bulk isopropanol has less

water and sodium hydroxide than the liquid phase surrounding the fiber surface. Thus, a highly concentrated alkali solution is present around the fiber, which increases the alkalization and carboxymethylation. Furthermore, the use of isopropanol for carboxymethylation is known to generate less side reaction between sodium hydroxide and MCA which forms sodium glycolate because the lower hydroxyl group activity of the non-polar solvent provides a tolerant environment for MCA (Ren et al. 2008; Klemm et al. 1998).

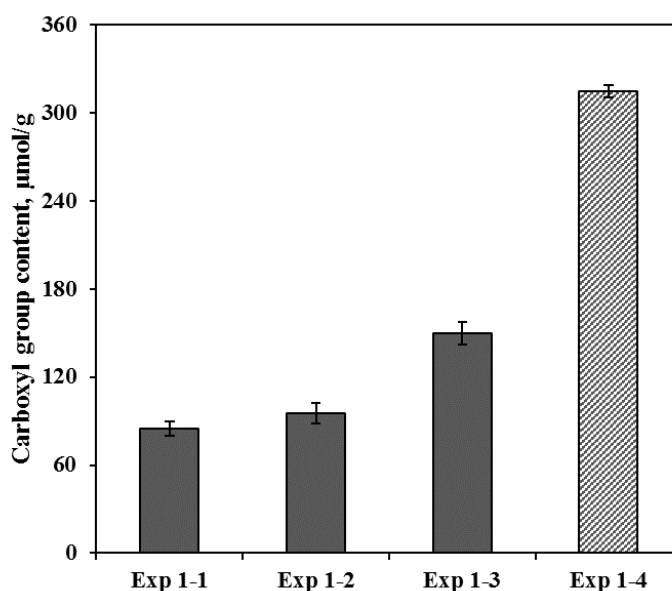


Fig.3-11. Carboxyl group content of carboxymethylated pulp prepared under four reaction conditions.

3.2.2 Effect of water content and pulp consistency

When non-solvent exchanged pulp is used as starting material for carboxymethylation, the pulp consistency and water contained in the pulp can influence the reaction rate (Tijssen et al. 2001). To determine the effect of pulp consistency and water content on the carboxymethylation reaction, the amount of pulp was increased from 1 to 4 g while keeping the total volume constant at 500 mL. This increase in the amounts of pulp corresponded to an increase in the pulp consistency from 0.2 to 0.8 w/v%. With this increase in the amount of pulp, the water content in the solvent increased to 2.85 w/v%. Fig. 3-12 shows that the amount of carboxyl groups increased continuously with the pulp consistency. An increase in pulp consistency accompanied the increase of the concentration of MCA and NaOH, which might have influenced the reaction rate. Not only the chemical concentration but also the water content increased with the pulp consistency.

To further evaluate the influence of the water content on the reaction, the amount of pulp was held constant at 1 g, and water was added to the solvent up to 7.5 w/v%. Fig. 3-13 shows that the carboxyl group remained around 300 $\mu\text{mol/g}$ when the water content in the isopropyl alcohol (IPA) was increased to 4.0 w/v% and decreased with further addition of water. Jie et al. (2004) also studied on the effect of the water content on carboxymethylation using cassava starch as a starting material and concluded that optimum water content in the reaction solvent is present. This finding suggests that an increase in the water content along with the pulp does not show any significant effect up to 4 w/v%, but eventually more water would decrease the carboxymethylation.

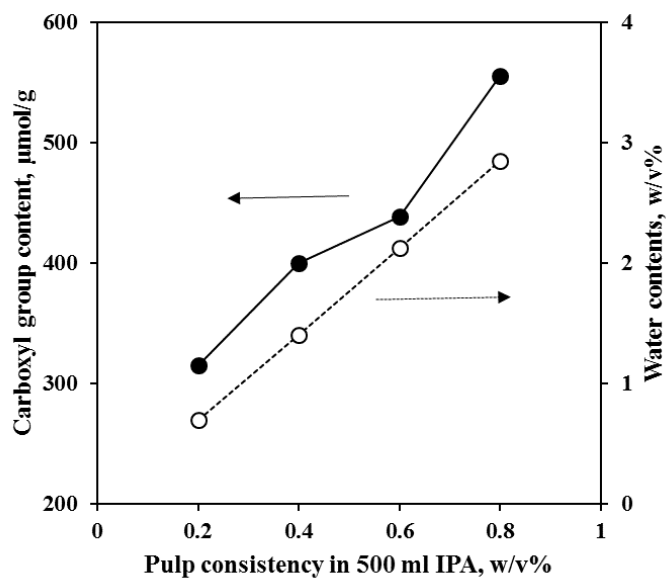


Fig. 3-12. Carboxyl content and water content increased with an increase in pulp consistency.

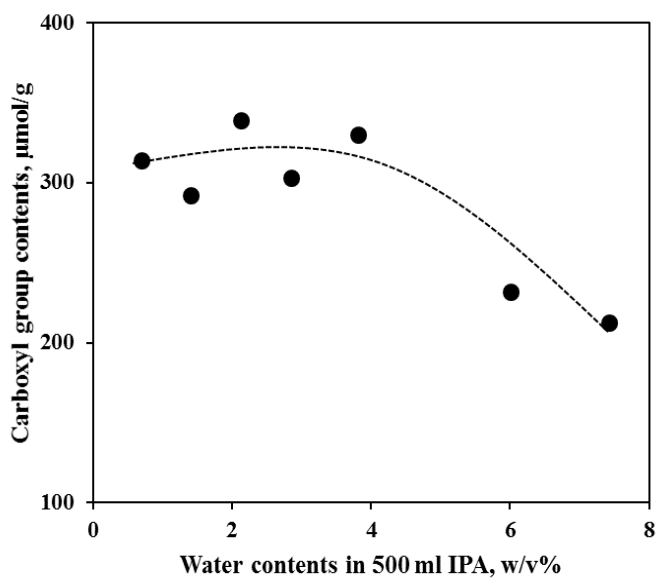


Fig. 3-13. Effect of water content in 500 mL IPA on the carboxyl group content.

To determine what effect the amount of isopropanol and pulp had on the carboxymethylation reaction, a second set of experiments was carried out (Table 3-4). The pulp consistency ranged from 0.2 to 1.33 w/v%, and the water content ranged from 0.70 to 4.84 w/v%.

Table 3-4. Experimental conditions for the investigation of the effect of pulp consistency and water

Experiment	Total volume of IPA, mL	Pulp consistency, w/v%		Water contents, w/v%	
		Pulp, 1 g	Pulp, 4 g	Pulp, 1 g	Pulp, 4 g
Exp 2-1	500	0.20	0.80	0.70	2.85
Exp 2-2	400	0.25	1.00	0.87	3.60
Exp 2-3	350	0.28	1.14	1.00	4.12
Exp 2-4	300	0.33	1.33	1.54	4.84

When 1 g of pulp was used, the reactivity of carboxymethylation decreased as the total isopropanol volume increased (Figure 3-14). The pulp consistency increased with a reduction of reaction medium, and the water content was less than 1.54 w/v%. When 4 g of pulp was used, however, the carboxyl content decreased with a reduction of isopropanol volume, especially when 350 or 300 mL of isopropanol were used. These two conditions resulted in a water content of greater than 4.0 w/v%.

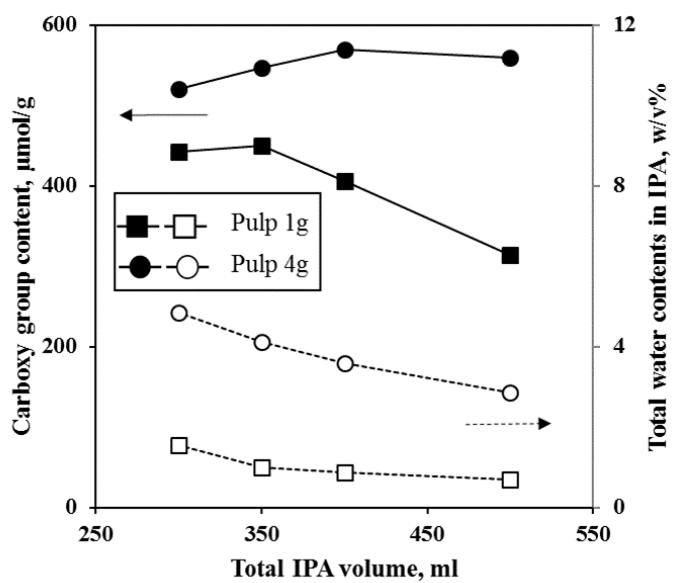


Fig. 3-14. Carboxyl group content and total water content as a function of IPA volume.

3.3 Reaction conditions for CNF production

To evaluate the characteristics of CNF with different carboxyl group contents, three carboxylation reactions were carried out (Table 3-5). The first and second reactions were carried out using solvent exchanged pulp in a solvent mixture medium, which contained two or three time more MCA and NaOH than the third experiment. In the third experiment, a sample of 50 g of non-solvent exchanged pulp was used for the reaction, and isopropanol was used as the only reaction solvent. The pulp consistency for this reaction was 1.0 w/v%, and the water content was 3.6 w/v%. Table 3-5 also shows the amounts of the carboxyl group contents for three pulps after carboxymethylation. We found that carboxymethylation in IPA without solvent exchange was as effective as experiment 1, which used three times more MCA and NaOH.

Table 3-5. Carboxymethylation conditions and carboxyl content of the carboxymethylated pulp

Experiment	Solvent exchange	Reaction solvent	MCA, mmol/g	NaOH, mmol/g	Carboxyl content, $\mu\text{mol/g}$
Exp 4-1	Yes	MeOH & IPA	2.88	11.04	607
Exp 4-2	Yes	MeOH& IPA	1.92	7.36	370
Exp 4-3	No	IPA	0.96	3.68	570

3.4 Properties of carboxymethylated CNF produced by different reaction conditions

The low shear viscosity of carboxymethylated pulp with different carboxyl content was depicted as a function of grinding pass number in Fig 3-15. The pulps with 570 and 607 $\mu\text{mol/g}$ of carboxyl content reached the plateau after the fifth grinding pass. For the pulp with a low carboxyl content of 370 $\mu\text{mol/g}$, it was necessary to grind 11 times to reach the plateau for low shear viscosity.

Figure 3-16 shows the CED viscosity of untreated pulp and CNFs prepared with or without carboxymethylation. Untreated CNF was made by grinding the pulp slurry at 1.0 wt% consistency thirty times through the grinder. CED viscosity of the untreated CNF was substantially decreased by the grinding treatment for nanofibrillation indicating that the mechanical treatment had an impact on cellulose DP, which is consistent with previous results (Syverud et al. 2011). In the case of carboxymethylated CNF, there was no significant change in CED viscosity even though different reaction conditions and grinding pass number were employed to obtain carboxymethylated CNFs with different carboxyl contents ranged from 370-607 $\mu\text{mol/g}$.

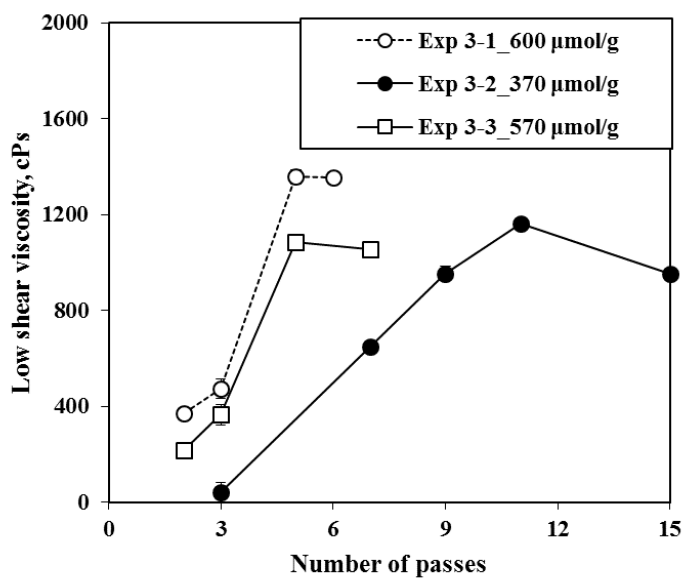


Fig. 3-15. Low shear viscosity of the carboxymethylated CNF depended on the carboxyl content.

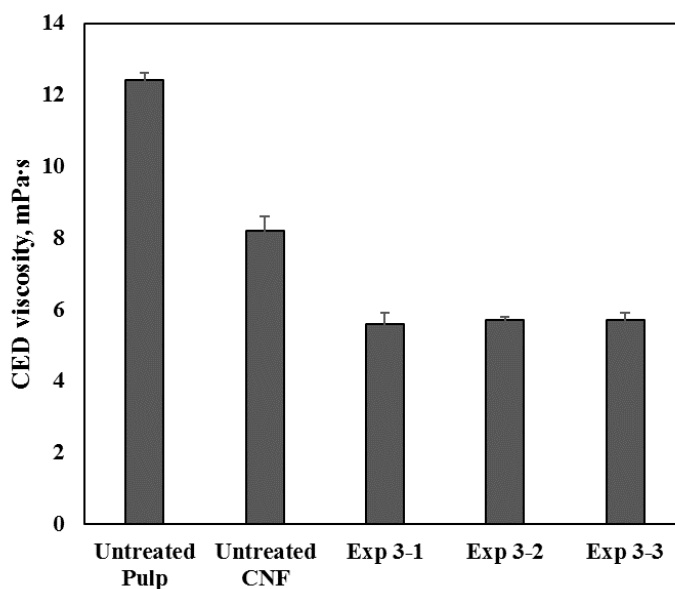


Fig. 3-16. CED viscosity of pulp and CNF depending on the reaction conditions.

The results of XRD analysis showed that carboxymethylation decreased the crystallinity of CNF (Fig. 3-17). This indicates that breakage of hydrogen bonds in the crystalline region of cellulose chains was resulted by carboxymethylation (Mohkami and Talaeipour. 2011). However, no difference in the crystallinity was observed between Exp 3-1 and Exp 3-3, which indicated that the carboxymethylation conditions employed in this study did not have any significant effect on crystallinity.

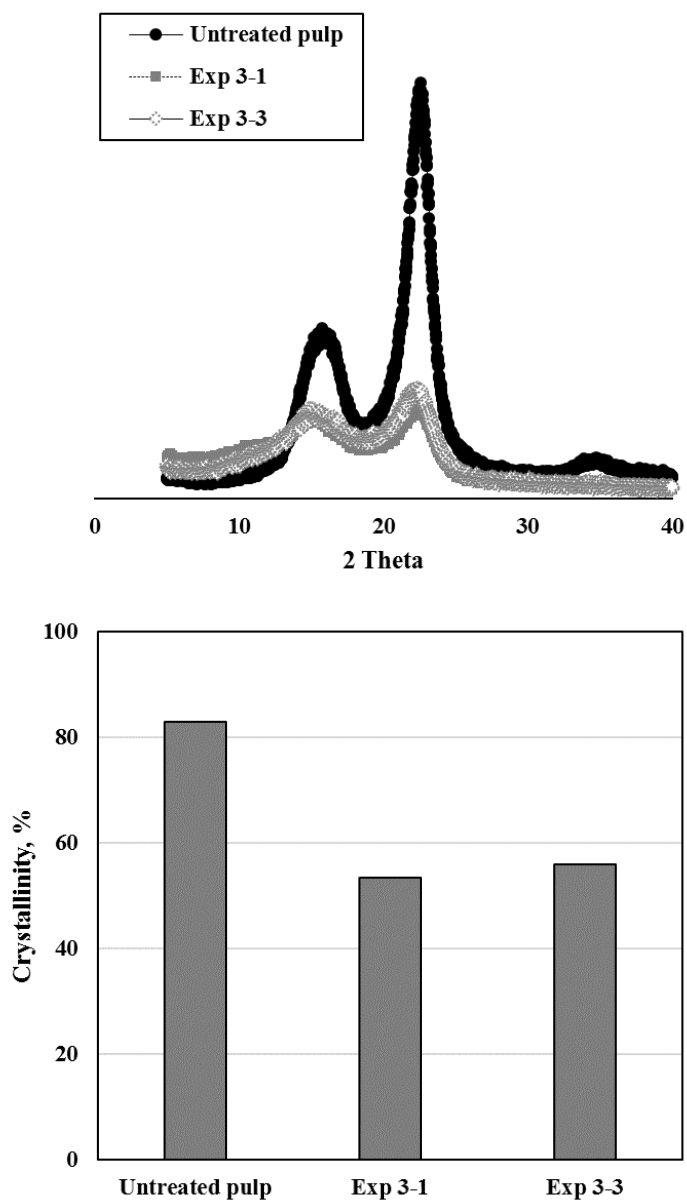


Fig. 3-17. XRD pattern and crystallinity of untreated pulp and two CNFs.

The morphology and width of CNF were examined using FE-SEM, TEM and image analysis methods (Fig. 3-18; Table 3-6). The widths of three CNF samples were very similar even though they were prepared under different reaction conditions and their carboxyl contents ranged from 370 $\mu\text{mol/g}$ to 607 $\mu\text{mol/g}$. Fall et al. (2011) have measured the widths of carboxymethylated CNF with different carboxyl contents using cryo-TEM image and concluded that the individual fibrils had similar widths from 5.5nm to 4.3nm regardless of surface charge. The widths of CNFs obtained from the FE-SEM were greater than those from TEM. Wang et al. (2012) pointed out that TEM imaging can resolve nanofibrils and even elemental fibrils while SEM imaging is only able to resolve large fibrils. This difference in the resolution of the two instruments is the generally accepted reason for the difference in width measurement (Onyianta et al. 2018). The platinum coating required for SEM imaging was likely to be another reason of the width difference.

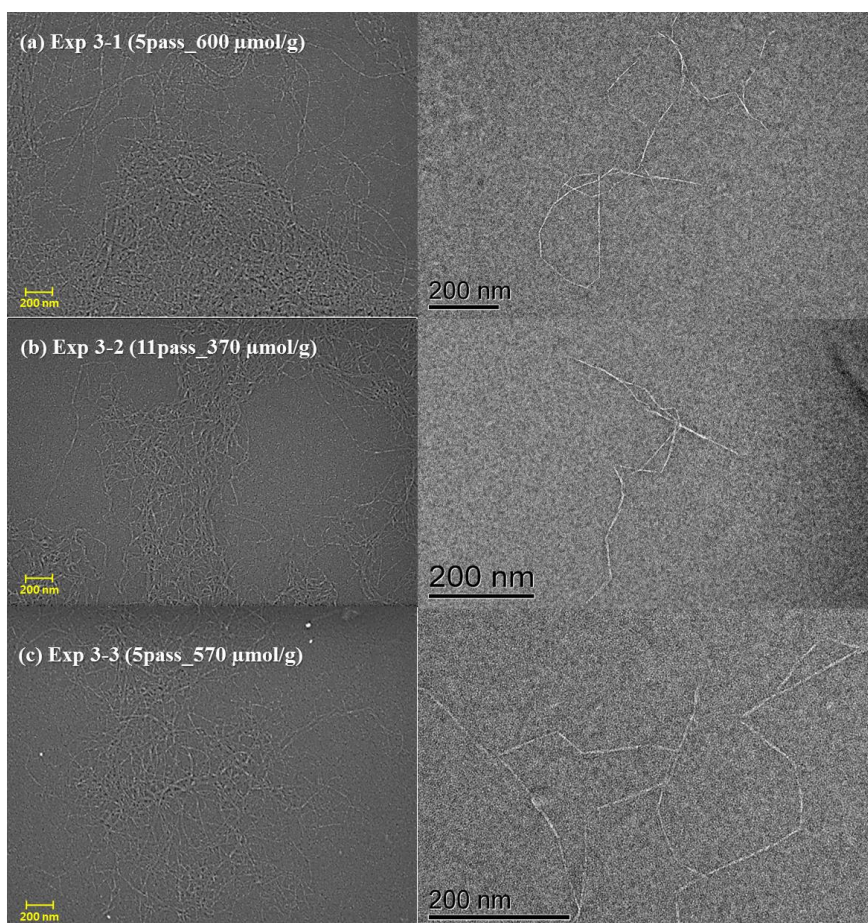


Fig. 3-18. FE-SEM (left) and TEM images (right) of the carboxymethylated CNFs with different amounts of carboxyl contents; (a) 607 $\mu\text{mol/g}$, (b) 370 $\mu\text{mol/g}$, (c) 570 $\mu\text{mol/g}$.

Table 3-6. Average and standard deviation of CNF widths

	Exp 3-1	Exp 3-2	Exp 3-3
FE-SEM image	$13.1 \pm 3.3 \text{ nm}$	$14.4 \pm 3.1 \text{ nm}$	$12.4 \pm 2.8 \text{ nm}$
TEM image	$5.2 \pm 1.2 \text{ nm}$	$5.7 \pm 1.4 \text{ nm}$	$5.2 \pm 1.7 \text{ nm}$

To evaluate the suspension stability of CNF depending on the carboxyl group content, CNF suspension was diluted to 0.03% with deionized water. An increase in TSI indicates that the sedimentation of the dispersed phase to the bottom of the vial occurs more quickly (Wiśniewska. 2010). Well-dispersed fibrils that remain stable in the suspension indicate that the width of CNF is finer and the quality of CNF is more uniform, which are two basic property required for the production of high quality CNF-based products (Fall et al. 2011). In Fig. 3-19, the TSI value of the dilute CNF is plotted against aging time. As expected, the dispersion stability depended on the width and carboxyl content; the CNF with the lowest carboxyl content and thicker in width settled faster than other two CNFs. These results indicated that the carboxyl content and width was the critical factor for CNF stability.

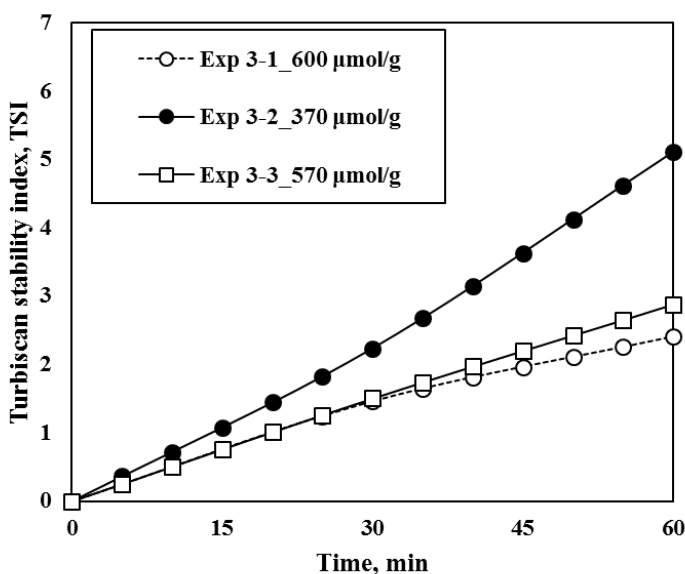


Fig. 3-19. Destabilization kinetics of the CNF suspension determined with TSI.

4. Summary

The optimal reaction conditions for carboxymethylation as a pretreatment method for CNF preparation were investigated. The characteristics of CNF produced by different solvent conditions were also examined.

The carboxyl group content of carboxymethylated pulp was strongly influenced by reaction temperature and MCA concentration. An increase in reaction temperature can improve reactivity at the same level of chemical, indicating that chemicals consumption can be reduced more economically.

Solvent exchange of pulp by ethanol, which has been generally conducted before carboxymethylation, prevented a cost-effective preparation of CNF. High reactivity can be achieved without the solvent exchange step of the pulp. Highly effective carboxymethylation was achieved using only an isopropanol medium without the solvent exchange step of the pulp.

The optimum reaction condition used only one third of MCA and NaOH for the same level of carboxymethylation. The presence of water did not hamper the reaction if the amount was less than 4 w/v%. The number of mechanical treatment steps required to produce CNF in Masscolloider substantially decreased as carboxyl content increased. Pulp with a high carboxyl content resulted in a more stable suspension due to the increased electrostatic repulsion between the fibrils. Even though, the widths of CNF samples prepared under different reaction conditions were very similar.

Chapter 4

Recycling of isopropanol for cost-effective, environmentally friendly carboxymethylation process

1. Introduction

As mentioned before, the carboxymethylation is one of the most widely used as a pretreatment for the production of CNF. However, carboxymethylation step uses alcohols to solvent-exchange water or as reaction mediums for carboxymethylation, it is imperative to recycle solvent for cost-saving and to minimize environmental impact.

In the chapter 3, optimization of reaction conditions for carboxymethylation as a pretreatment was investigated. The results showed that high reaction efficiency can be achieved using isopropanol (IPA) as a sole reaction medium, and the solvent exchange step of the pulp and the presence of water in the reaction medium decrease the carboxymethylation reaction of pulp fiber. It was also shown that solvent waste from the carboxymethylation reaction is likely to contain water deriving from non-solvent-exchanged wet pulp.

IPA and water form an azeotropic mixture at 87.4% IPA concentration. An azeotrope is a mixture of liquids that maintains its composition and boiling point during distillation (Fig. 4-1, Cho and Jeon 2006). The separation of water from this mixture by conventional methods such as solvent extraction and distillation is difficult and uneconomical (Rachipudi et al. 2011; Mao et al. 2010). Thus a new, inexpensive, environmentally friendly separation method for the azeotropic mixture is needed to achieve high reaction efficiency in carboxymethylation. Tijssen et al. (2001) proposed a method to produce highly substituted carboxymethyl starch using aqueous IPA as a sole reaction medium. The purification of IPA for the next reaction was conducted using normal distillation with a pervaporation method, and highly substituted carboxymethyl starch (DS of 1.5) was obtained. However, the retentate leaving the

pervaporation system had a specified H₂O/IPA composition, and the water content was usually greater than 5%.

Adsorptive distillation, which uses adsorbents such as molecular sieves, biobased desiccants, or silica gels, is a method that can be used to remove water from azeotropic mixtures. The molecular sieves are environmentally friendly crystalline alumino-silicate materials, and are able to selectively separate molecules depending on molecular size (Jain and Gupta. 1994; Martucci et al. 2012). Mjalli et al. (2005) conducted a separation experiment on an azeotropic isopropanol/water solution using type 3 Å and 4 Å molecular sieves and found that the molecular sieves adsorbed water while excluding the adsorption of isopropanol.

Recycling solvent is an essential step in the carboxymethylation of pulp fiber, because it is important for the environmental and economic aspects of the process (Arvidsson et al. 2015). Unfortunately, however, no studies to date have examined how to handle or recycle waste solvent from the carboxymethylation process of pulp fiber, except for the use of incineration (Chen et al. 2013; Naderi et al. 2017; Arvidsson et al. 2015).

In this chapter, a way to recycle the solvent medium used in the carboxymethylation reaction was investigated. Several solvent medium properties, including conductivity, pH, and water content, were evaluated to investigate the composition of the waste solvent. A type 4 Å molecular sieve was tested as a material to separate water in the reaction medium. In addition, the properties of CM CNF produced using the recycled solvent as a reaction medium were investigated.

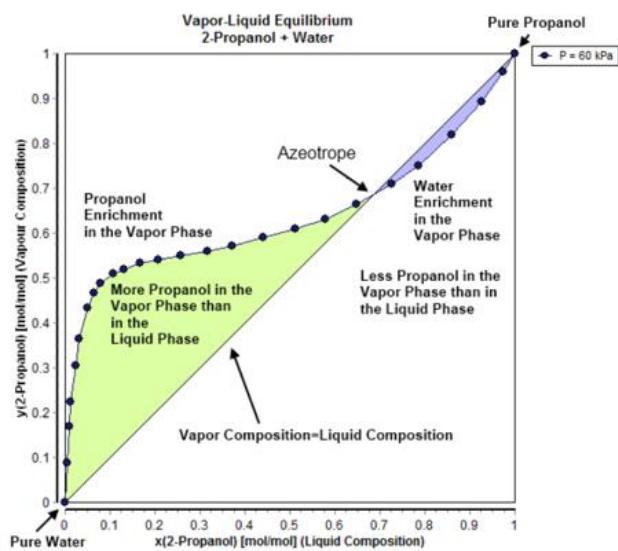


Fig. 4-1. Vapor-liquid equilibrium of isopropanol /water mixture
(Marzal et al. 1996).

2. Materials and Methods

2.1 Materials

To investigate the effect of solvent recycling on carboxymethylation, A molecular sieve 4 Å (Sigma Aldrich, Beads type, 8-12 mesh) crystalline metal aluminosilicates having a three-dimensional interconnecting network of silica and alumina tetrahedra was used as a drying agent to dehydrate waste solvent (Fig. 4-2). Monochloroacetic acid (MCA, Sigma-Aldrich, 99.0%) and sodium hydroxide (NaOH, Samchun Chemicals, 98.0%) were used as chemical reagents, and isopropanol (IPA, Duksan Reagents, 99.5%) was used as the sole solvent medium for carboxymethylation.

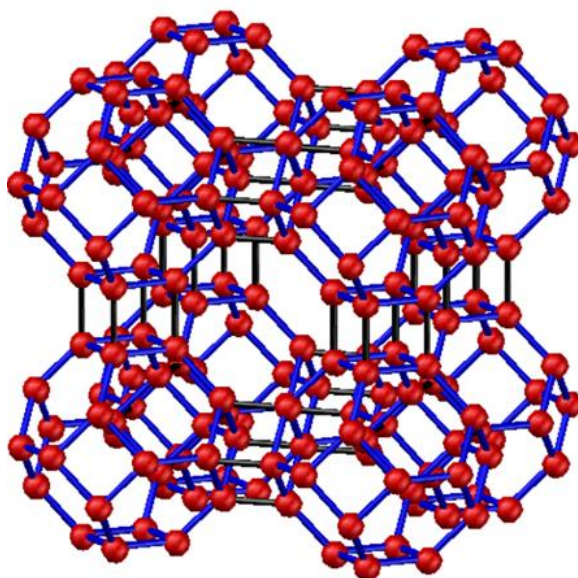


Fig. 4-2. Intra-structure of molecular sieve.

2.2 Carboxymethylation conditions as a pretreatment

As mentioned in previous study, optimized carboxymethylation reaction was conducted . Briefly, 5 g of pulp fiber was placed in 500 mL of IPA containing 4 mmol/g of NaOH for 30 min at 35 °C for alkalization. Next, 1 mmol/g of MCA was added to this reaction chamber for esterification, which was carried out for 60 min at 65°C. The pulp consistency of this reaction chamber was 1.0 w/v% and water content was 3.1 w/v% . After carboxymethylation, reacted IPA filtrate was obtained by filtering using 400 mesh for reuse in the next carboxymethylation stage. All other reaction conditions were the same as in the first reaction, except that filtered IPA was used as the reaction medium. The carboxyl group content of the CM pulp, which indicates the reaction rate of carboxymethylation, was evaluated using a conductometric titration method in accordance with SCAN-CM 65:02.

2.3 Recycling of isopropanol

IPA recycling is desirable for economic and environmental reasons. However, IPA recycled from carboxymethylation inevitably contains a small amount of water deriving from the wet pulp. Because water content in the reaction medium is a critical factor in the carboxymethylation reaction (Im et al. 2018; Tijssen et al. 2001), its content should be controlled to obtain CM pulp with the required amount of carboxyl content. To dehydrate IPA, 50 wt% of a molecular sieve was added to the recovered IPA and kept for 24 hr at 25 °C. The water content in the recovered IPA was evaluated using the Karl Fischer titration method (870 KF titrino plus, Metrohm, Swiss). The molecular sieve that absorbed water from the recovered IPA was dried using a microwave oven for 10 min to ensure that all moisture within the crystal was evaporated. The dried molecular sieve

was then reused for water absorption. The pH and conductivity of IPA were also determined to investigate the presence of by-products after carboxymethylation.

2.4 Preparation and characterization of CNF

A high pressure homogenizer (Fig. 4-3, GEA, Niro Soavi Panda Plus, Italy) was used to produce CM CNF. The consistency and total volume of CM pulp, which were produced using recycled IPA, were adjusted to 0.5 wt% and 1 L, respectively. The pulp suspension was then passed through the homogenizer at a pressure of 500 bar. Suspension samples were collected after each step of homogenization to evaluate the degree of fibrillation. To evaluate the effect of solvent condition on the CM pulp, the cupriethylenediamine (CED) viscosity (T 230 om-08), which indicates the degree of polymerization of the pulp fiber, was determined.

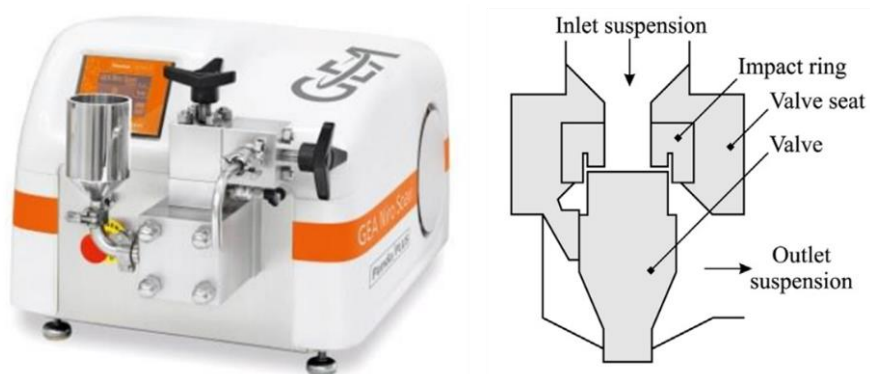


Fig. 4-3. Homogenizer for preparation of CNF suspension.

The morphological properties of the pulp and CNF depending on the pass number were investigated using a field emission scanning electron microscope (FE-SEM, Carl Zeiss, Sigma, UK). To prepare the CNF specimens for FE-SEM, a highly diluted suspension (0.003 wt%) was deposited on the glow-discharged carbon grid (Carbon type-B, Tedpella Inc.). After natural drying, the specimen was sputtered with platinum for 100 s at 20 mA using a sputter coater (BAL-TEC SCD 005) for observation. The width of the specimen, depending on the pass number, was calculated using Image-J software.

3. Results and discussion

3.1 Reactivity of carboxymethylation

Carboxymethylation was carried out four times to estimate the effect of recovered IPA on reaction efficiency. First, carboxymethylation was carried out using fresh IPA as the reaction medium. After the first carboxymethylation reaction, the used IPA was recovered and reused again as a reaction medium without any treatment for the second carboxymethylation reaction. The use of recycled IPA was repeated two more times. At all carboxymethylation reaction steps, never-dried bleached eucalyptus kraft pulp was used.

Fig. 4-4 shows the carboxyl group content of the pulps after carboxymethylation reaction as a function of the IPA recycling number. Recycling number zero means that fresh IPA was used as the reaction medium. Recycling numbers 1, 2, and 3 indicate that the IPA was recovered and reused for carboxymethylation after being used one, two, or three times before, respectively. All of the other reaction conditions, such as the amount of chemicals, temperature, and time, remained the same. The highest carboxyl group content of 430 $\mu\text{mol/g}$ was obtained when fresh IPA was used as the reaction medium. As the IPA recycling number increased, the carboxyl group content decreased, which indicates that the repeated use of IPA substantially decreased reaction efficiency. Thus, it is desirable to find a way to keep the carboxymethylation reaction efficiency high while recycling IPA, because an increase of the charged group content in pulp by chemical pretreatment facilitates nanofibrillation of pulp fiber, which reduces mechanical energy consumption in CNF production (Besbes et al. 2011; Tejado et al. 2012).

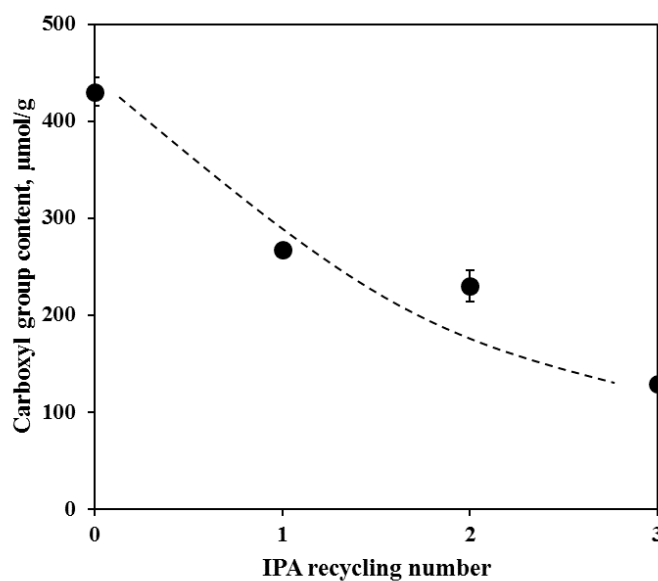


Fig. 4-4. Carboxyl group content of CM pulp as a function of the IPA recycling number.

Fig. 4-5 shows the conductivity of IPA just after dissolving NaOH in the IPA and after completion of the carboxymethylation reaction. The conductivity of the fresh IPA was 0.01 $\mu\text{S}/\text{cm}$. When NaOH was dissolved in the fresh IPA, the conductivity of IPA increased to 50 $\mu\text{S}/\text{cm}$ because of the increase of hydroxyl ions in the reaction medium. The conductivity increased constantly with the IPA recycling number, which was attributed to the accumulation of NaOH in the reaction medium. By-products of the carboxymethylation reaction such as sodium chloride are another likely reason for an increase in conductivity, according to [2] (Ambjörnsson et al. 2013).



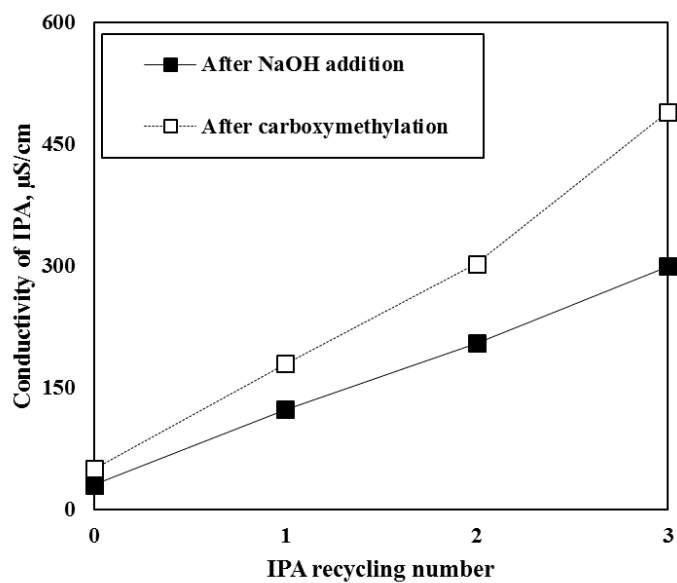


Fig. 4-5. Conductivity of IPA before alkalization and after carboxymethylation.

The water content in recycled IPA was determined using the Karl Fisher titration method, as shown in Fig. 4-6. As the IPA recycling number increased, water content in the IPA increased linearly. It has been shown that water content in the reaction medium influences the carboxymethylation reaction rate (Tijssen et al. 2001; Bhattacharyya et al. 1995). It is worth noting, however, that after a certain threshold level of water content the reaction rate decreases significantly. For instance, Im et al. (2018) have shown that water content in the IPA does not have any significant effect when it is less than 4 w/v%. They also have shown that the presence of more water in the IPA medium tends to decrease carboxymethylation reactivity (Im et al. 2018). Therefore, water content in the recycled IPA, which increases with the IPA recycling number, should be reduced to keep the reaction efficiency of carboxymethylation high.

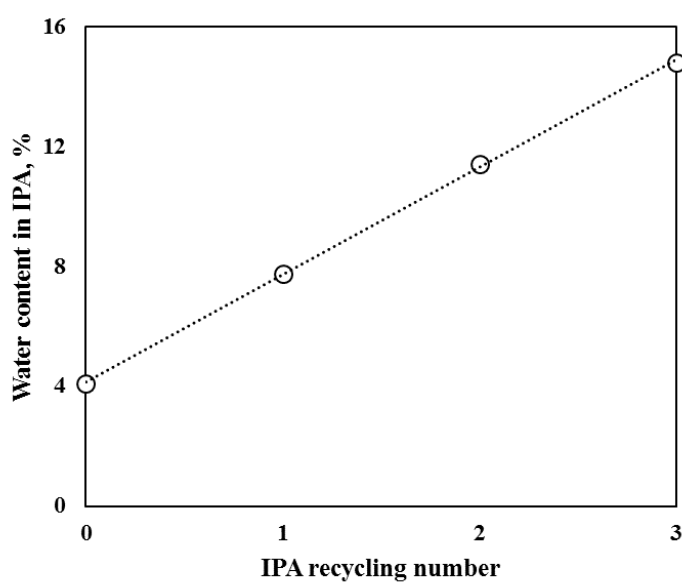


Fig. 4-6. Water content in the recycled IPA.

A model experiment was conducted to evaluate the effect of water content in the alkalization stage of carboxymethylation reaction. The IPA water content was adjusted from 4 to 16 wt%, which covers the whole range of water content in the IPA at all recycling stages, as shown in Fig. 4-5. Next, 5 g of pulp fiber was impregnated with 4 mmol/g of NaOH dissolved in 500 mL of IPA, which contained different amounts of water, for 30 min at 35 °C. The IPA was then filtered using 400 mesh wire after alkalization, and acid-base titration was conducted to evaluate the amount of unreacted NaOH in the IPA (Fig. 4-7). For the acid-base titration experiment, 100 mL of filtered IPA with different water content was titrated with 0.1 M of hydrochloric acid.

Three distinct regions appeared in the titration curve. First, the presence of excess OH⁻ in the IPA before the equivalence point gave high pH values. Then the pH dropped abruptly when H⁺ was sufficient to react with all OH⁻ at the equivalence point. Finally, the pH changed to acidic conditions when excess H⁺ was added to the IPA (Fig. 4-8, Harris. 2007). Fig. 4-9 shows the amount of hydrochloric acid required for the equivalence point, which indicates the amount of unreacted NaOH in the IPA. As can be seen in Fig. 4-9, the amount of unreacted NaOH increased as water content in IPA increased, which shows that an increase of water content in the IPA prevents the reaction of NaOH with hydroxyl groups of the pulp fiber, i.e., alkalization. Unreacted NaOH in IPA can also react with MCA during etherification, which causes an undesirable side-reaction to form sodium glycolate [3] (Kooijman et al. 2003).



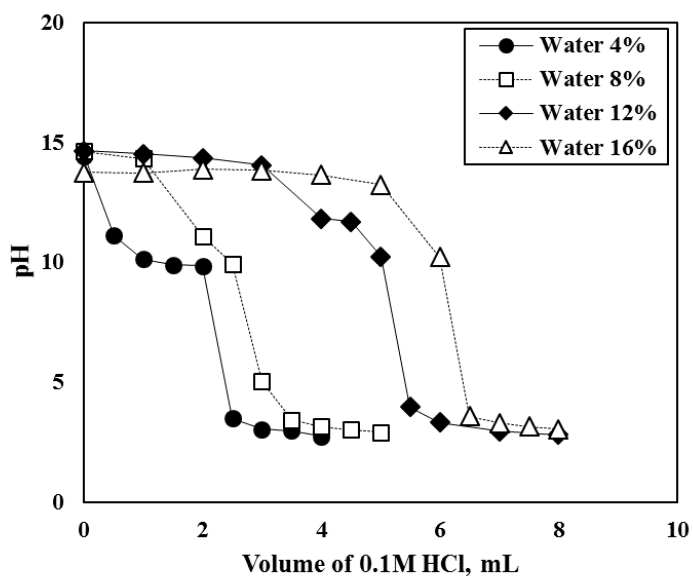


Fig. 4-7. Titration curves of IPA containing different amounts of water.

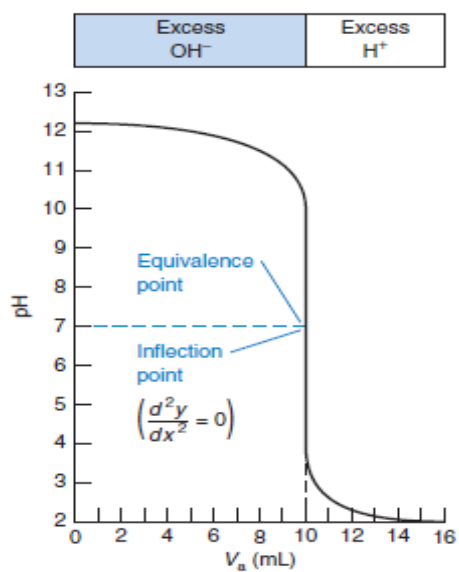


Fig. 4-8. Titration curve by acid-base titration (Harris. 2007).

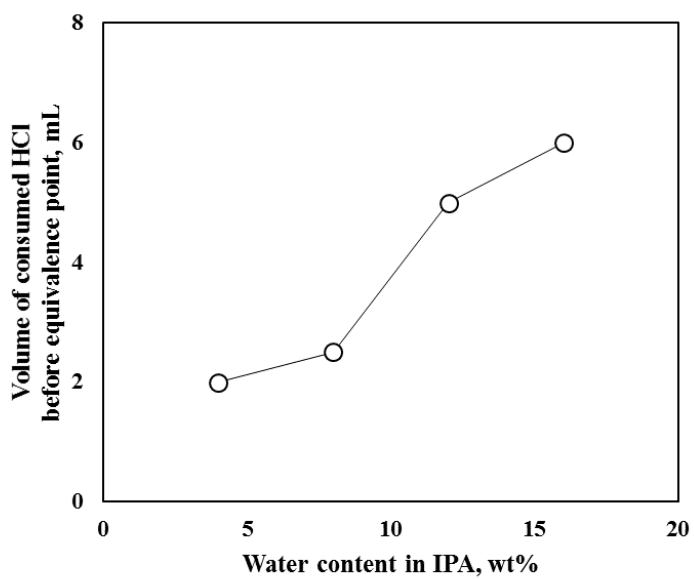


Fig. 4-9. Amount of HCl consumed before the equivalence point.

3.2 Dehydration of recovered IPA

The 4 Å molecular sieve was used as a drying material to dehydrate recovered IPA. The unique micro-pore or cage structure of the molecular sieve has a high affinity for polar water molecules, but excludes IPA molecules from penetrating into the pore structure (Teo and Ruthven 1986). To investigate the effect of the molecular sieve on the dehydration of recovered IPA, the molecular sieve was added to the recovered IPA after the first carboxymethylation reaction up to 50 wt% of the IPA and left for 24 hr at 25°C.

Fig. 4-10 shows the water content in the recovered IPA as a function of the soaking time of the molecular sieve. As can be clearly seen, the water content in IPA decreased with soaking time and reached a minimal plateau after 16 hr. Both the conductivity and pH of the IPA decreased and were restored to the original values with an increase in dehydration time (Fig. 4-11). Hydroxide ions interact very strongly with water molecules because the local polarity of OH⁻ attracts water molecules and forms hydroxide ion-water clusters (i.e., (H₂O)_nOH⁻, n=1 - 5) (Tuckerman et al. 2002; Xantheas. 1995; Guha et al. 2014). Therefore, these results suggest that the hydroxide-water clusters were removed during the treatment with the molecular sieve. To investigate what effect the temperature of IPA had on the dehydration efficiency, temperature of IPA was adjusted from 25 °C to 55 °C and molecular sieve soaked for 8 hr. Fig. 4-12 shows the conductivity of recovered IPA depending on temperature. The result suggests that an increase in the temperature does not any significant effect on IPA dehydration.

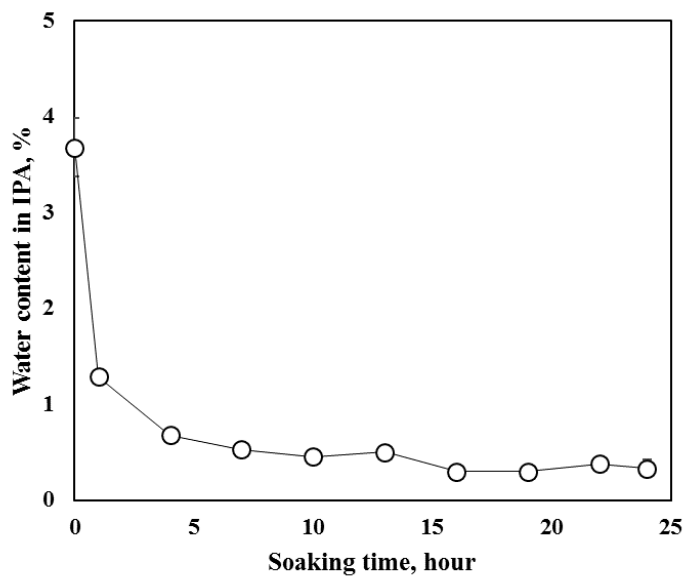


Fig. 4-10. Water content of IPA as a function of soaking time of the molecular sieve.

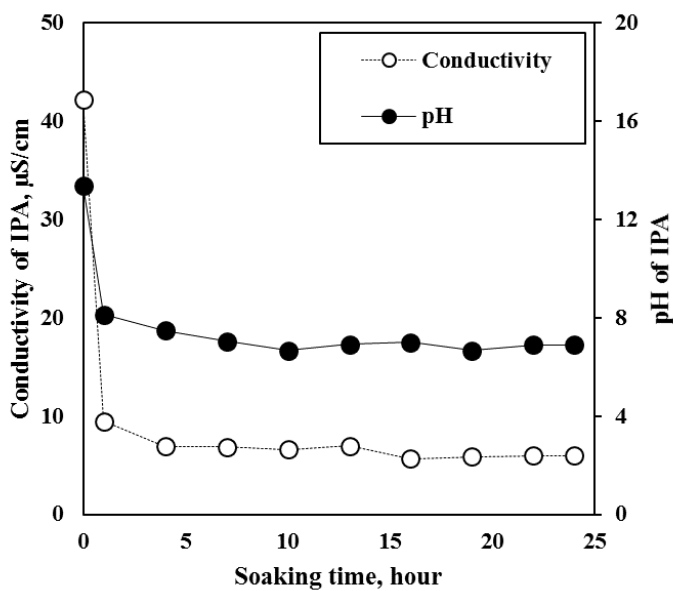


Fig. 4-11. Conductivity and pH of IPA as a function of soaking time of the molecular sieve.

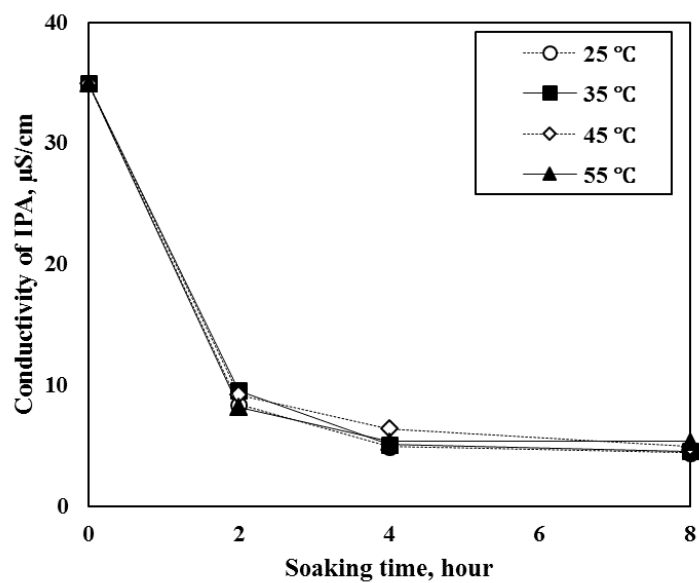


Fig. 4-12. Conductivity of IPA depending on temperature.

Carboxymethylation of CNF was carried out under the same reaction conditions using IPA dehydrated with the molecular sieve. Fig. 4-13 shows the conductivity of the IPA after the carboxymethylation reaction and after treatment with the molecular sieve. Molecular sieve treatment decreased IPA conductivity to the same level irrespective of the recycling number, which indicates that almost complete dehydration of the water derived from the pulp fiber was achieved. Thus, the same level of carboxyl group contents was obtained irrespective of the IPA recycling number (Fig. 4-14).

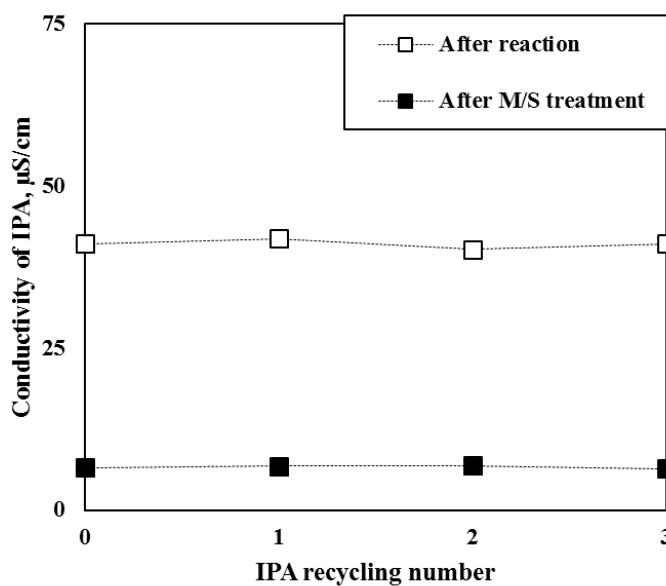


Fig. 4-13. Conductivity of IPA after the carboxymethylation and after the dehydration treatment with molecular sieve.

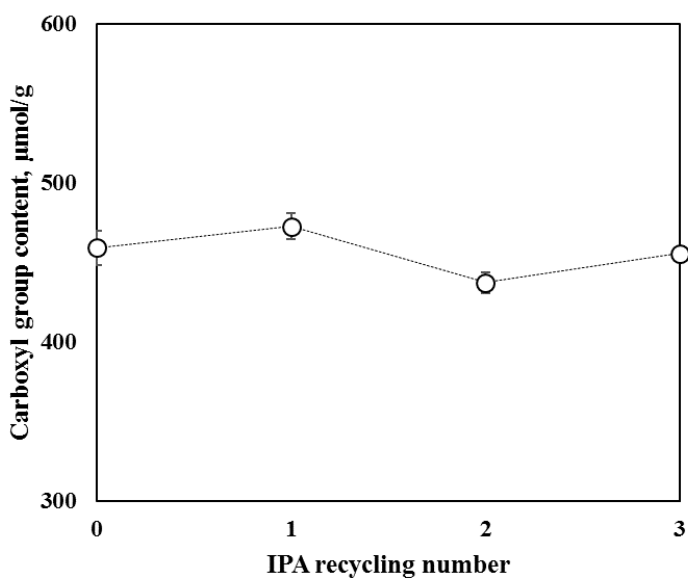


Fig. 4-14. Carboxyl group content of carboxymethylated pulps.

3.3 Properties of CM pulp and CNF

To investigate the characteristics of CM pulp and CNF produced using recycled and dehydrated IPA, the amount of carboxyl groups and CED viscosity of the CM pulp were determined. A 50 g sample of pulp fiber was used for carboxymethylation reaction under the same reaction conditions.

Figs. 4-15 and 4-16 show conductivity and pH of IPA before and after molecular treatment for 16 hr at 25 °C, respectively. Same as previous results (Fig. 4-12), Conditions of IPA were almost restored as fresh IPA. Carboxyl group content and CED viscosity remained almost constant irrespective of the use of recycled dehydrated IPA, as shown in Fig. 4-17. Thus, the carboxymethylation efficiency remained the same. Fig. 4-18 shows the low shear viscosity as a function of homogenizing pass number. As mentioned before, viscosity value did not increase after complete isolation of pulp fiber. The same level of fibrillation tendency was measured for three CM pulp condition, regardless of the use of recycled IPA.

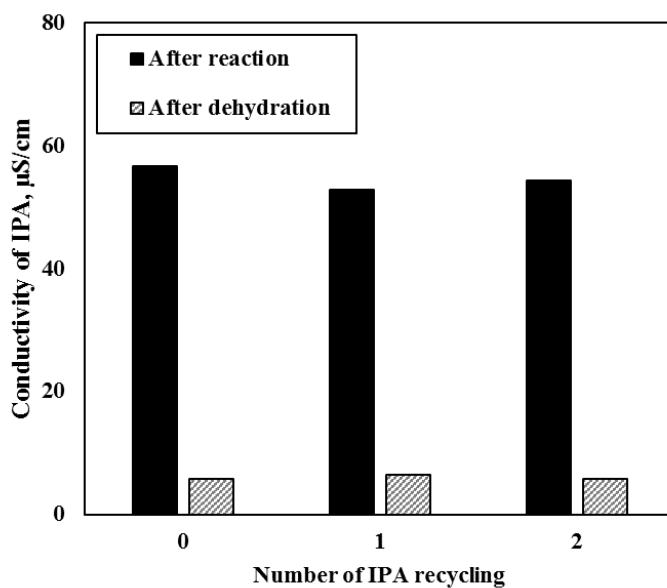


Fig. 4-15. Conductivity of IPA before and after molecular sieve treatment.

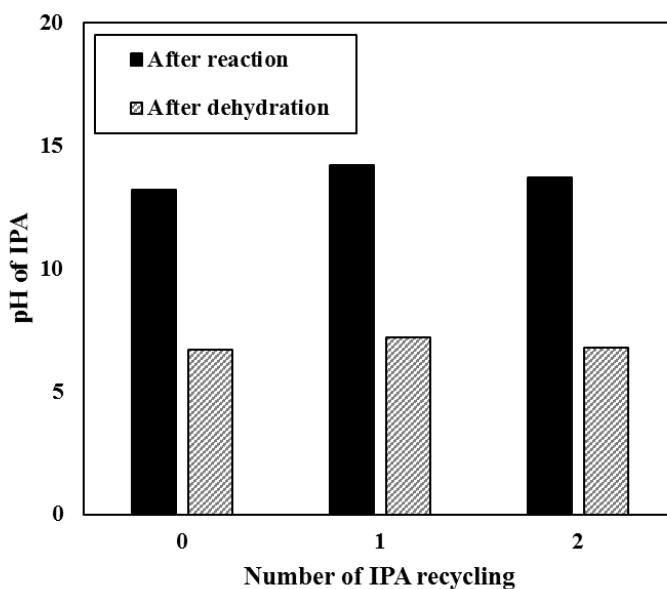


Fig. 4-16. pH of IPA before and after molecular sieve treatment.

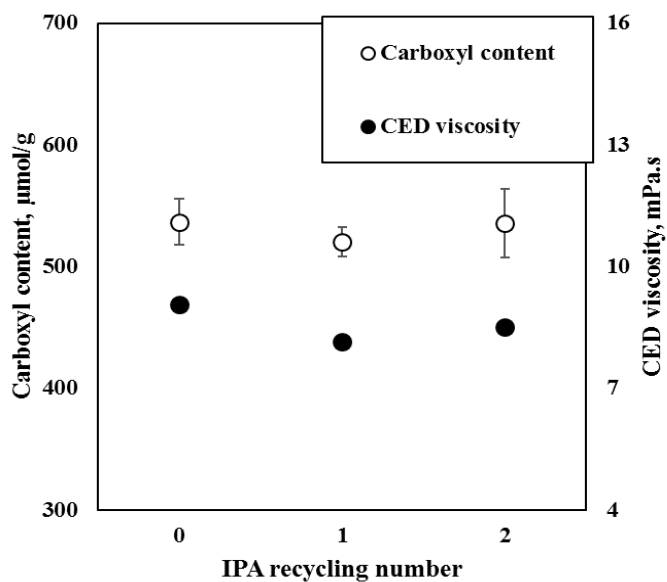


Fig. 4-17. Carboxyl group content and CED viscosity of CM pulp.

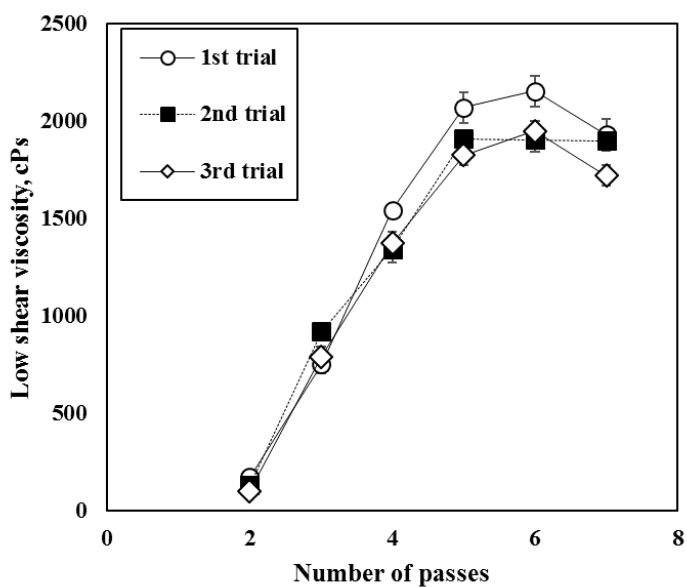


Fig. 4-18. Fibrillation degree of CM pulp prepared by fresh and recycled IPA.

Figs. 4-19 and 4-20 show the morphological properties of CM pulps, which were produced using the fresh IPA and the second recycled IPA, after passing 2, 3, 5 and 6 times through the homogenizer, respectively. Widths of carboxymethylated pulp decreased, and the distribution of widths became more uniform irrespective of the use of recycled IPA as the pass number of the homogenizing process increased (Figs. 4-21 and 4-22). Complete nanofibrillation was achieved after five passes for all three pulps. Spence et al. (2011) reported that 20 passes through the homogenizer was required to manufacture microfibrillated cellulose under a pressure condition similar to that applied in this experiment. Thus, the carboxyl groups introduced by carboxymethylation facilitated the nanofibrillation of pulp by increasing the electrostatic repulsion between fibrils. The average widths of the three CM CNFs were very similar and ranged from 12.1 nm to 12.8 nm (Fig. 4-21), which showed that the use of recycled IPA did not have any negative effect on the properties of CM CNF. The recycling of IPA after dehydration using the molecular sieve has the economic advantage of saving solvent while maintaining the same quality of cellulose nanofibrils.

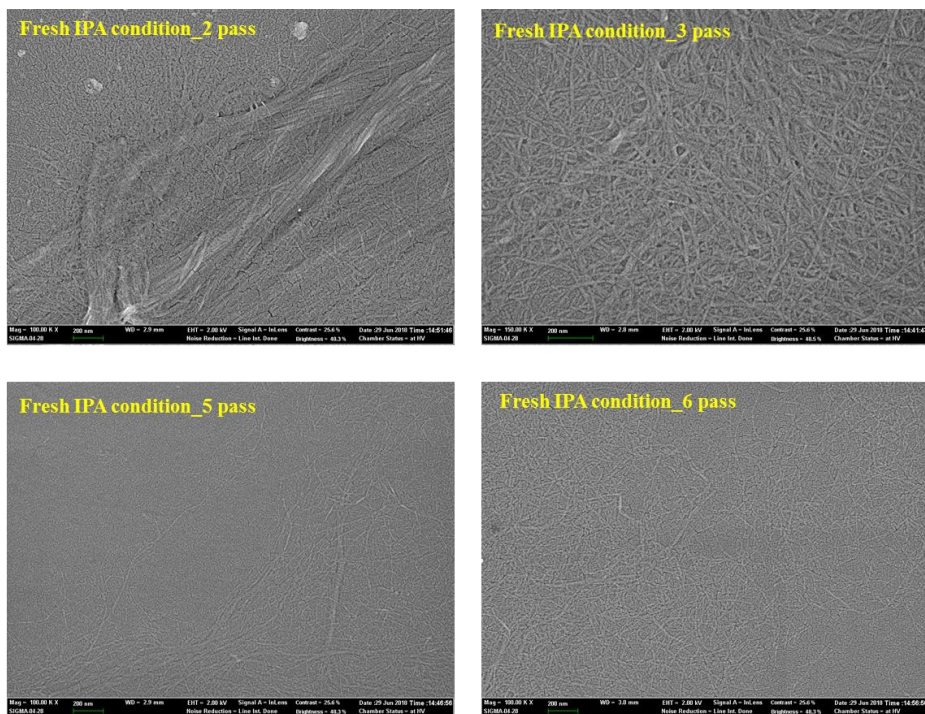


Fig. 4-19. Morphological properties of carboxymethylated pulp produced by fresh IPA as a function of pass number.

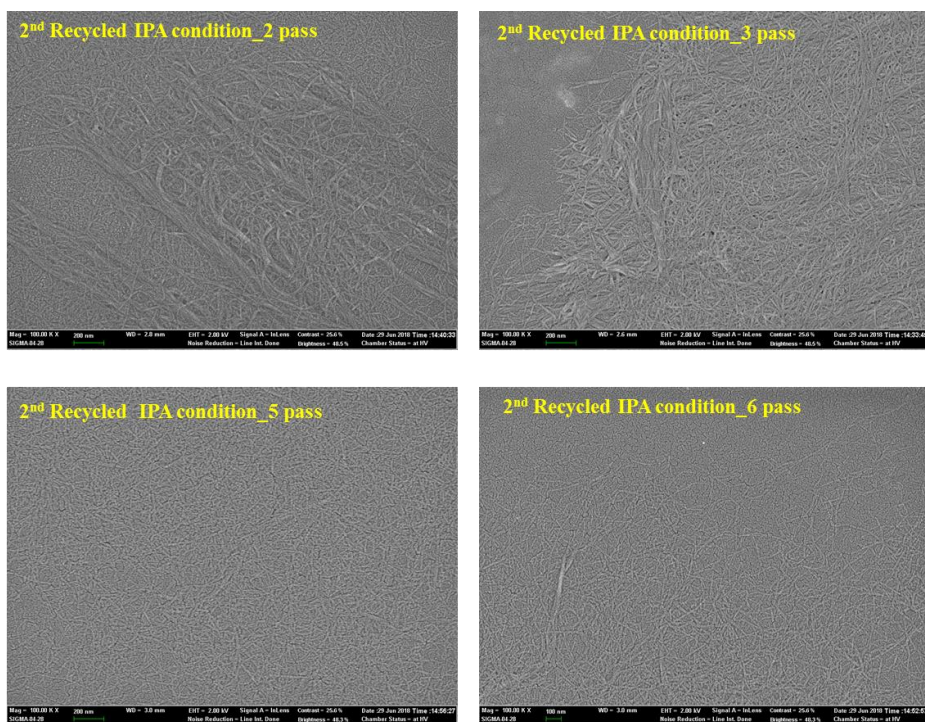


Fig. 4-20. Morphological properties of carboxymethylated pulp after 2, 3, 5 and 6 passes. The second recycled IPA was used in carboxymethylation.

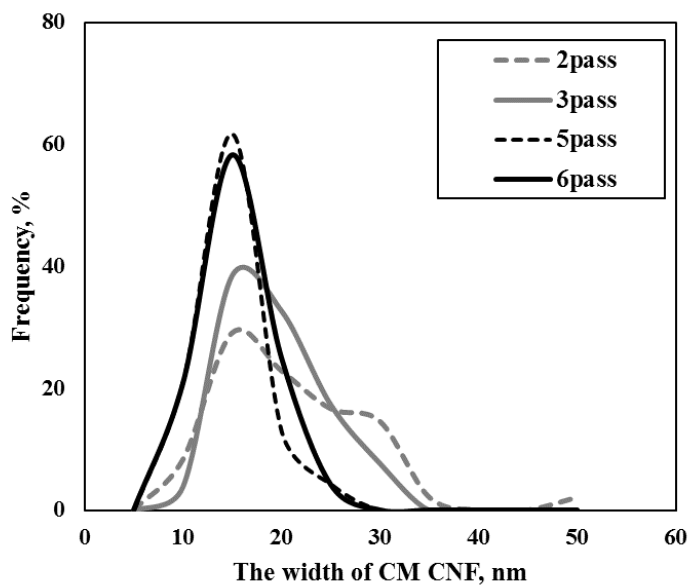


Fig. 4-21. Width distribution curves of carboxymethylated pulp prepared using the fresh IPA.

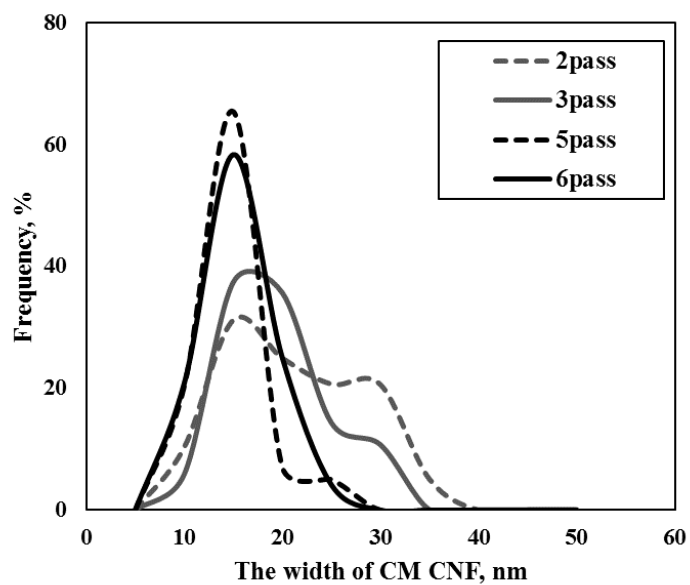


Fig. 4-22. Width distribution curves of carboxymethylated pulp prepared using the second recycled IPA.

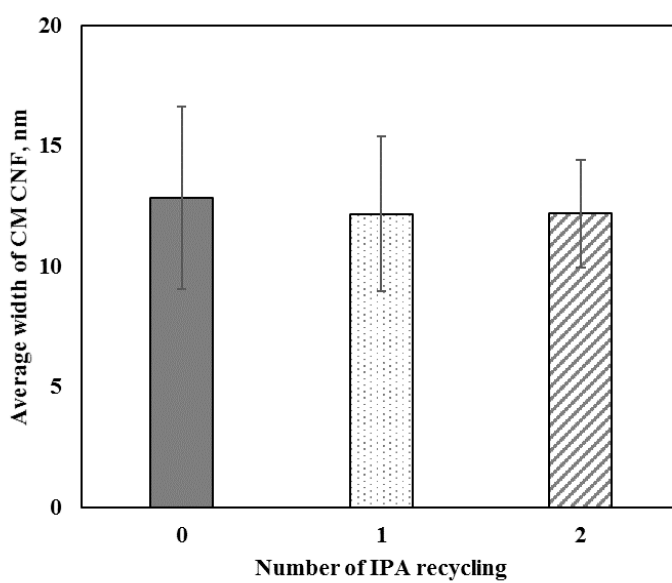


Fig. 4-23. Average widths of CM CNF.

4. Summary

An approach to recycling IPA used in the carboxymethylation of pulp fiber was investigated as a cost-effective and environmentally friendly method of production CNF. Carboxymethylation reaction of pulp fiber was carried out using IPA as the sole solvent and non-solvent exchanged pulp. IPA was recovered after carboxymethylation reaction and recycled in the next carboxymethylation reaction.

Simple recycling of IPA decreased the reaction efficiency of carboxymethylation due to the increase of water content in IPA deriving from wet-pulp fiber. As water content in the IPA increased, reaction efficiency substantially decreased, and the amount of untreated NaOH increased.

To dehydrate the recovered IPA, a 4Å molecular sieve was used as a drying material. It was shown that dehydration restored carboxymethylation efficiency to the same level as when fresh IPA was used. The molecular sieve can be reused after evaporating the adsorbed moisture.

The characteristics of the CM pulp and CNF produced using the recycled IPA were also evaluated, including fibrillation tendency, average width, and width distribution. Use of recycled and dehydrated IPA did not reveal any differences in the CED viscosity of the pulp and the width of CM CNFs. Three of CM CNF was prepared using a homogenizer, and five passes were required for complete nanofibrillation of the CM pulp fiber.

Chapter 5

Characteristics of CM CNF depending on preparation conditions

1. Introduction

CNFs are suitable reinforcing materials for nanocomposites because of their inherent characteristics such as biodegradability, renewability, very high tensile strength, low thermal coefficient, etc. (Fujisawa et al. 2013; Saito et al. 2013). A low CNF loading (<10 wt.%) is enough to brought reinforcing effect (Boufi et al. 2014). Sim et al. (2016) prepared high-strength porous sheets mixed with pulp fiber/CNF or PET/CNF combination. The results showed that the addition of CNF was beneficial in improving the filtration efficiency of particles due to increased specific area.

The morphological properties of CNFs are essential parameters for controlling the mechanical properties of CNF-based materials. As mentioned in literature review chapter, Microscopic techniques such as, SEM, TEM, and AFM can accurately measure the width of the fibers (Iwamoto et al. 2014; Pääkkö et al. 2007; Shinoda et al. 2012; Saito et al. 2013; Uetani and Yano, 2011). However, it is difficult to measure the length of the fibrils from the microscopy image due to entanglement between fibrils (Ishii et al. 2011).

Dynamic viscoelastic or shear viscosity measurements of CNF suspension of measured as indirectly methods to estimate the average length of CNF (Tanaka et al. 2014; Ishii et al. 2011). The average lengths determined by rheological measurement have been one order of magnitude higher than those measured by microscopy. This discrepancy has been attributed to the fact that the nanofibrils used in the dynamic viscoelastic measurements were not completely isolated, but partially aggregated in water (Tanaka et al. 2014).

Sedimentation experiments could also be used to assess the aspect ratio of CNFs. Raj et al. (2016) evaluated aspect ratios using the sedimentation method proposed by Zhang et al. (2012). Theoretically, the sedimentation method is based on a gel point (or critical concentration) that is defined as the lowest volume fraction where the fiber forms a continuous network. Kerekes and Schell (1992) defined the crowding factor, N , as the number of fibers in a spherical volume with a diameter equal to the length of a fiber.

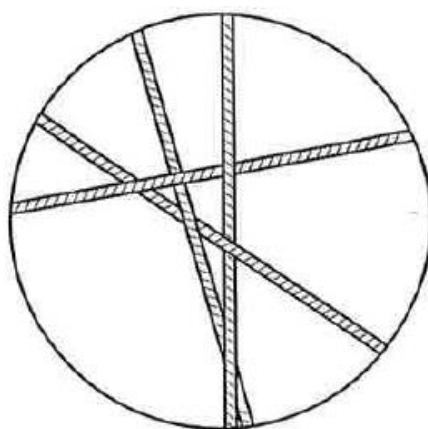


TABLE I
FIBRE SUSPENSION REGIMES

Regimes	Type of Fibre Contact	N
Dilute	Chance Collision	$N < 1$
Semi-Concentrated	Forced Collision	$1 < N < 60^*$
Concentrated	Continuous Contact	$N > 60^*$

* Value assigned in this study

Fig. 5-1. Crowding factor, N , depending on suspension consistency (Kerekes and Schell 1992).

The crowding factor can be expressed, according to Equation (3):

$$N = (2/3) \Phi A^2 \quad \text{Eq. (3)}$$

where Φ and A are the volumetric concentration and aspect ratio of fiber, respectively. Experimentally, the gel point occurs at a crowding number of approximately $16(\pm 4)$, as proposed by Martinez et al. (2001). Then, volumetric concentration for the gel point, Φ_c , can be simplified as follows:

$$\Phi_c = 24/A^2 \quad \text{Eq. (4)}$$

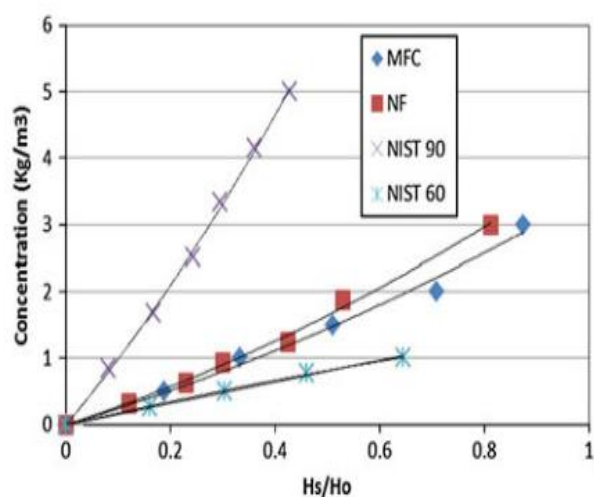
For fiber suspension, it is often convenient to use weight fraction, C . According to Varanasi et al. (2013), C can be written as follows:

$$C = \rho_f \Phi / (\rho_f \Phi + \rho_l (1 - \Phi)) \quad \text{Eq. (5)}$$

where ρ_f and ρ_l are the density of the fibers and liquid, respectively. Thus, if $\Phi \ll 1$, then Equation (5) may be re-expressed as follows:

$$\Phi_c = C_c (\rho_l / \rho_f) \quad \text{Eq. (6)}$$

where C_c is the weight fraction of the gel point. Then, combining Equations (4) and (6), the aspect ratio of the fiber can be calculated using the weight fraction of the gel point (Fig. 5-2). The assumed density of the CNF is 1.5 g/cm^3 (Svagan et al. 2008; Varanasi et al. 2013).



Sample	Fitting equation	Gel point solids concentration (kg/m ³)	Solids mass fraction
MFC	$y = 2.03x^2 + 1.78x, R^2 = 0.98$	1.78 (0.54)	0.00178
NF	$y = 1.98x^2 + 2.30x, R^2 = 0.99$	2.30 (0.27)	0.00230
NIST90	$y = 5.65x^2 + 9.35x, R^2 = 0.99$	9.35 (0.50)	0.00935
NIST60	$y = 1.59x, R^2 = 0.99$	1.59 (0.02)	0.00159

Fig. 5-2. Sedimentation data and weight fraction of gel point from sedimentation method (Varanasi et al. 2013).

Several studies have examined how the charge content of pulp fiber influences the mechanical energy that is required to completely isolate the pulp fiber (Tejado et al. 2012; Syverud et al. 2011). Besbes et al. (2011) found that pulp with higher carboxyl content reduced the mechanical energy consumption and that TOCN prepared with different levels of carboxyl content have almost homogeneous widths (3-4 nm), regardless of the mechanical treatment intensity. The fundamental properties of CNF-based products are influenced by the CNF morphologies. However, the effect of the mechanical intensity and carboxyl content on the morphological properties of CNF has not been studied in detail.

In this chapter, the effect of carboxyl content and mechanical intensity (i.e., number of grinding pass) on the morphological properties of carboxymethylated CNFs (CM CNFs) was investigated. In addition, the effect of preparation conditions on the rheological properties of CM CNF suspension and the mechanical properties of CM CNF film were investigated.

2. Materials and Methods

2.1 Carboxymethylation conditions as a pretreatment

The carboxymethylation reaction was carried out according to the method described in the chapter 3 and 4. During the carboxymethylation, the carboxyl content of the pulp fiber was controlled by changing the amounts of MCA (Table 5-1).

Table 5-1. Reaction conditions for the carboxymethylation of pulp

Pulp fiber, g	Condition	Total IPA, mL	NaOH, mmol/g dry pulp	MCA, mmol/g dry pulp
19	A	1,800	3.68	0.96
	B			0.80
	C			0.50

To produce CM CNFs, the consistency and total volume of the CM pulp suspension was adjusted to 0.5 wt.% and 3 L, respectively. The pulp suspension was passed through a grinder (Super Masscolloider, Masuko Sangyo Co., Ltd, Japan). The operation speed and gap distance were 1,500 rpm and -80 μm , respectively.

Transmission electron microscopy (TEM, Carl Zeiss, LIBRA 120, Germany) was used to evaluate the width of the CM CNFs with different carboxyl contents. For TEM analysis, the CM CNF suspension was diluted with deionized water to 0.002% and then deposited on a glow-discharged carbon grid (Carbon type-B, Ted Pella Inc.). The CM CNF samples were observed at an accelerating voltage of 160 kV after negative staining. The average width of the CM CNFs

was obtained using Image-J software. Furthermore, the cupriethylenediamine (CED) viscosity of the CM CNFs was measured to investigate the degree of polymerization according to the TAPPI Standard (T 230 om-08).

2.2 Estimation of the aspect ratios of CM CNFs

It is difficult to settle down the highly charged CNFs in water suspension because the repulsive forces make the charged CNFs stable (Iwamoto et al. 2014). Onyianta and Williams (2018) evaluated the gel point of carboxymethylated and TEMPO-oxidized CNFs by adding inorganic salts. In this study, the gel point analysis by sedimentation was employed to calculate the aspect ratios of the CM CNFs. To screen the surface charge before the sedimentation experiments, CM CNF samples with different carboxyl contents were diluted with deionized water to 0.3 wt.%, and then dispersed in NaCl solutions with concentrations ranging from 0.03 to 0.18 M at 0.1 w/v%. The zeta potentials of the CNFs at different salt concentrations were evaluated using Zetasizer (Nano Zs, Malvern Instruments, Ltd.) at 25°C. The sedimentation experiments were conducted with CM CNFs that had the same zeta potential, which was achieved by dispersing the CM CNF in salt solutions with different concentrations based on the carboxyl contents of the CM CNFs. CM CNF suspensions with 0.1 - 0.02 w/v% consistency were prepared and allowed to fully sediment in 50 mL glass cylinders for 5 days. The plot of the concentration against the relative sediment height (sediment height H_s to initial suspension height H_0) was fitted with a quadratic equation, where the linear fit shows the gel point/connectivity threshold. The aspect ratio was then calculated using Equations (4) and (6).

2.3 Rheological properties of CM CNFs

The rheological properties of the CM CNFs were studied using a Bohlin cone and plate rheometer (CVO, Malvern instrument, USA) with a gap angle between the cone and plate of 4° and a cone diameter of 4 cm. The rotational viscosity with an increase in shear rate was measured using CM CNF suspensions at 0.5 wt.%. An oscillatory rheometer was also used to find the network properties of the CM CNF suspensions. Two modes of amplitude sweeps were carried out to evaluate the rheological properties of the CM CNFs. One shear-stress-amplitude sweep was performed in the range of 0.5 to 100 Pa at a constant frequency of 1 Hz and a second shear-strain-amplitude sweep was carried out in the range of 1 to 100 Hz at a constant stress of 0.5 Pa.

2.4 Preparation and analysis of CM CNFs film

The CM CNF films were prepared by pouring the CM CNF suspensions onto polystyrene petri dishes after degassing under a 0.1 MPa vacuum for 1 hour and drying at 25°C and 55% humidity for 6 days. The mechanical properties of the CM CNF films, such as tensile property, elongation at break, and modulus of elasticity, were evaluated using a Universal Testing Machine (Instron Co., USA). The width of the specimen and the measurement span were 15 and 30 mm, respectively. The strain rate during measurement was 3 mm/min. The crystallinity of the CM CNF films was measured using an X-ray diffractometer with a Cu K α X-ray source (XRD, Bruker, D8 Advance, Germany) set at 5 to 40 degrees with a scanning speed of 0.5 sec/step. The crystallinity index was estimated from the diffraction patterns using the Segal method. The crystallinity was calculated from the height ratio between the intensity of the crystalline peak ($I_{200} - I_{AM}$) and total intensity (I_{200}) according to Equation (7).

$$\text{Crystallinity(\%)} = ((I_{200} - I_{AM}) / I_{200}) \times 100, \quad \text{Eq. (7)}$$

where I_{200} is the total intensity of the 200 peak at $2\Theta = 22.7^\circ$, and I_{AM} is the minimum intensity between the 200 and 110 peaks at $2\Theta = 18^\circ$, respectively (Thygesen et al. 2005).

3. Results and discussion

3.1 Characteristics of the CM pulp and CNF

Table 5-2 shows the characteristics of the CM pulp and CNFs manufactured under the different reaction conditions. The carboxyl content of the pulp fiber increased as the amount of MCA increased. The number of grinding passes required to obtain completely isolated CM CNFs decreased as the carboxyl content increased (Fig. 5-3), which is consistent with previous studies by Tejado et al. (2012) and Wågberg et al. (2008).

Table 5-2. Characteristics of CM CNFs produced under different reaction conditions

Classification	Carboxyl contents, $\mu\text{mol/g}$	Width, nm (st.dev)	CED viscosity, $\text{mPa}\cdot\text{s}$
CM CNF A	510	5.1 (0.98)	6.57
CM CNF B	330	5.1 (1.05)	6.26
CM CNF C	220	4.9 (0.87)	4.98

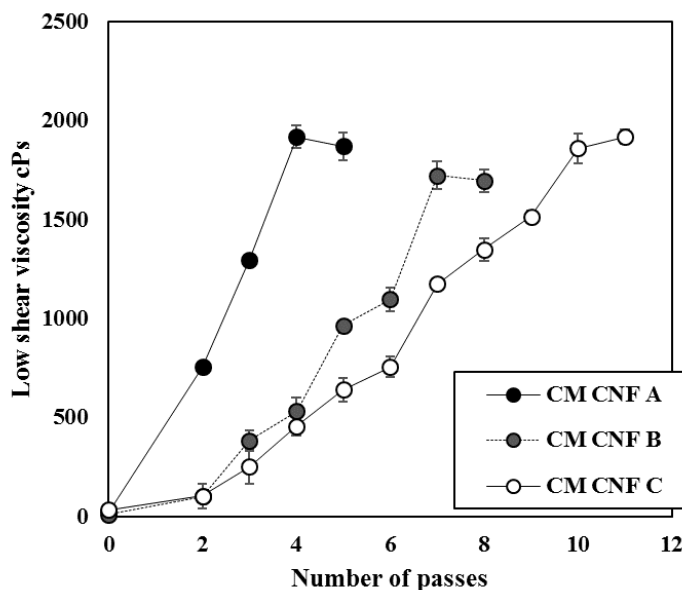


Fig. 5-3. Fibrillation degree of CM pulps produced by different reaction conditions.

The average widths of the three CM CNF samples were similar, ranging from 4.9 nm to 5.1 nm, as shown in Table 5-2. Figure 5-4 also shows that the shapes of the CM CNFs were very similar. However, the CED viscosity value, which indicates the degree of polymerization of cellulose, decreased as the number of grinding passes increased. Shinoda et al. (2012) investigated the relationship between the length and degree of polymerization (DP) of TOCNs and concluded that there is a linear relationship between the average fibril length and the DP of TOCNs. This implies that a reduction in CED viscosity accompanied by an increase in the number of grinding passes is associated with the reduction of the CM CNF length.

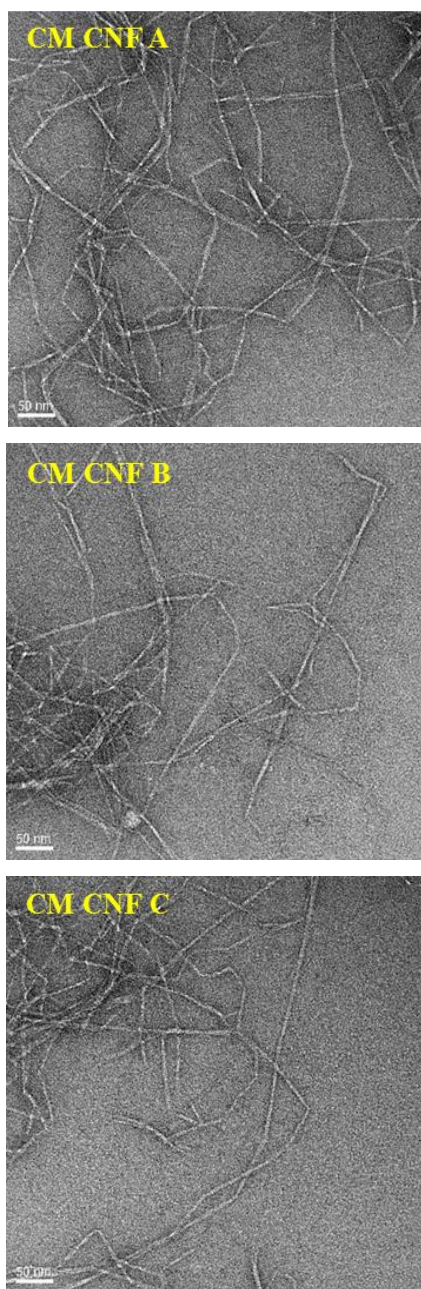


Fig. 5-4. TEM images of the CM CNFs with different carboxyl content and number of grinding passes.

3.2 Aspect ratios of CM CNF manufactured under different conditions

It is difficult to determine the ends of a single fiber in TEM images because many fibrils are entangled with each other and the image areas are not large enough to display whole fibrils from end to end (Fig. 5-4). Furthermore, as can be clearly seen in Fig. 5-5, the length distribution of CM CNFs, which was completely individualized, were very broad. This result indicates that the calculation of length difference of three CM CNFs though the TEM image analysis was not reliable. These problems, which associated with the microscopic analysis, can be resolved using a sedimentation experiment.

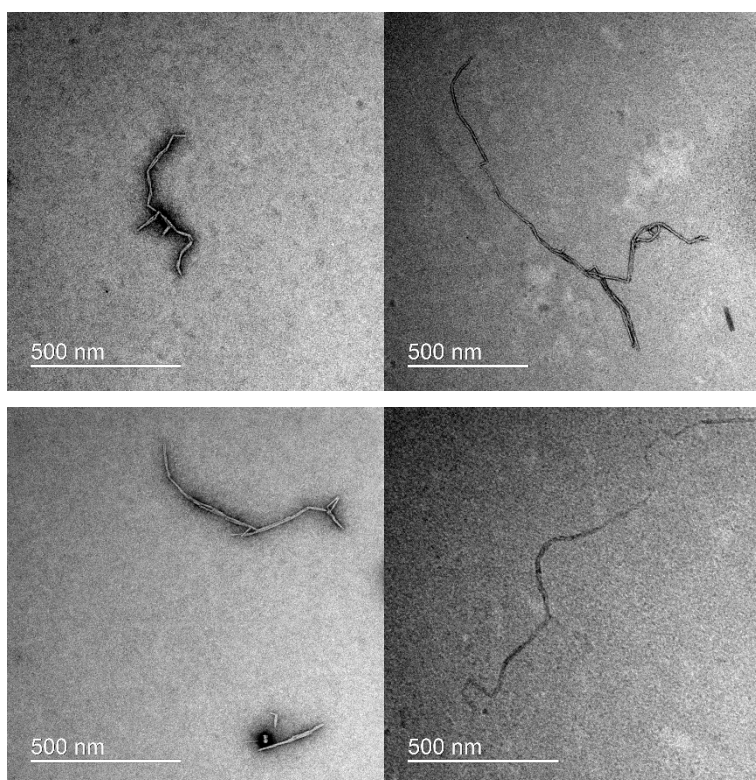


Fig. 5-5. TEM-image of CM CNFs with difference length.

Fig. 5-6 shows the sedimentation tendency of untreated CNF and CM CNF A under different consistency ranging from 0.05 to 0.5 wt.% of CNF for 24 hr. Untreated CNF was produced by grinding thirty times through grinder, which has -25.6 mV of zeta potential. As can be clearly seen, different sedimentation behavior of between untreated and CM CNF was observed. The sedimentation of untreated CNF with lower consistency occurred more rapidly while CM CNF, which had the highest carboxyl content and showed a zeta-potential of -53 mV in deionized water, did not settle down for 24 hr due to high electrostatic repulsion force between the fibrils. This implies that the zeta potentials of high charged CNF for the sedimentation experiment must be controlled.

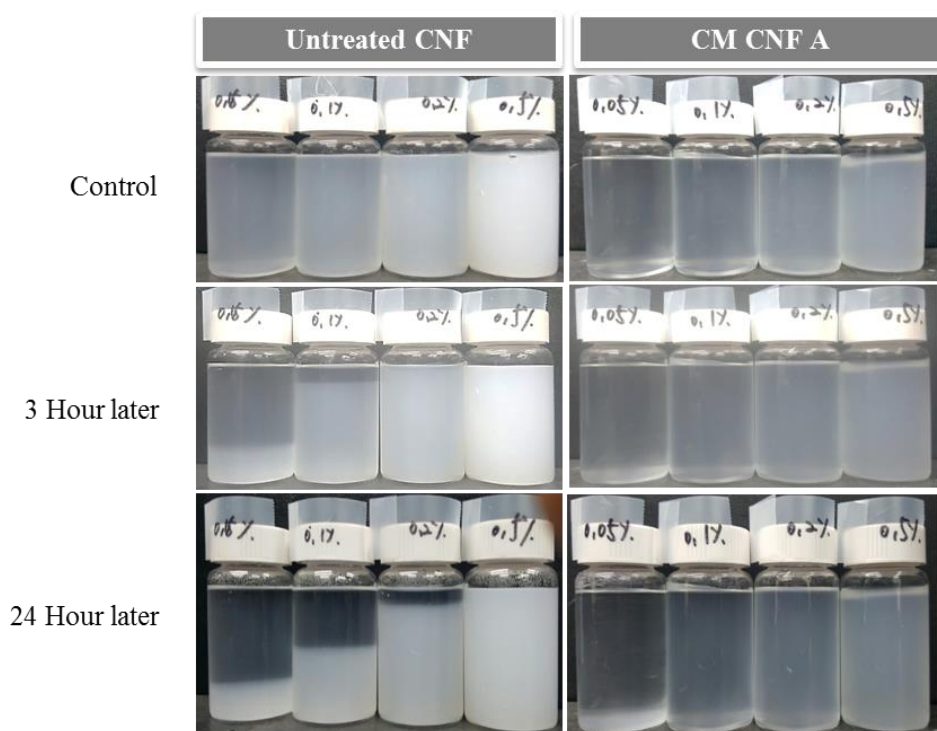


Fig. 5-6. Sedimentation tendency of untreated CNF and CM CNF A under different consistency.

Thus, before carrying out the sedimentation experiment, the zeta-potential of the CM CNF suspensions at 0.1 w/v% was determined using NaCl concentration (Fig. 5-7). Increases in the NaCl concentration led to more rapid changes in the zeta potential of CM CNF A. The zeta potentials of CM CNF B and C also changed with the increase in salt concentration. CM CNF C, which had the lowest carboxyl content, had the smallest change in zeta potential with salt concentration. The zeta potentials of the three CM CNF samples were adjusted to -25 mV, which was the zeta potential of untreated CNF, by adjusting the concentrations of salt solutions. The zeta potentials of -25 mV for CM CNF A, CM CNF B, and CM CNF C were obtained by adjusting the concentration of salt solutions to 0.1 M, 0.13M, and 0.18 M, respectively. These salt concentrations were used to dilute the three CM CNF samples to 0.2 - 1.0 w/v% for the sedimentation experiments (Fig. 5-8).

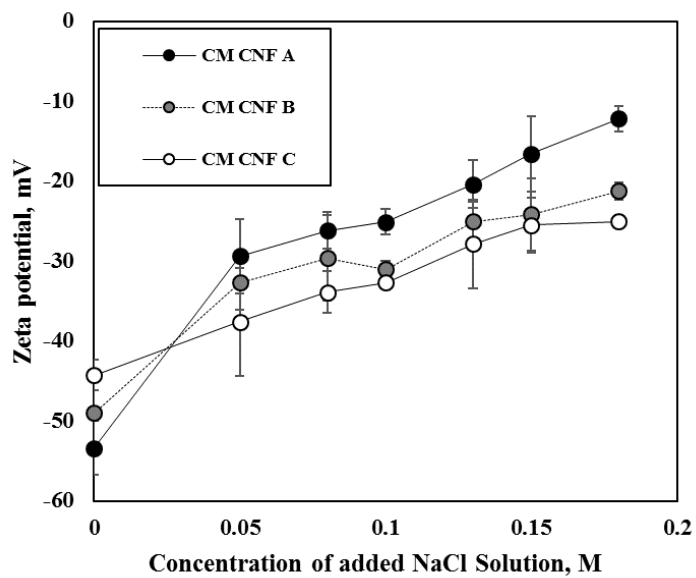


Fig. 5-7. Zeta potential of CM CNFs at different salt concentration.

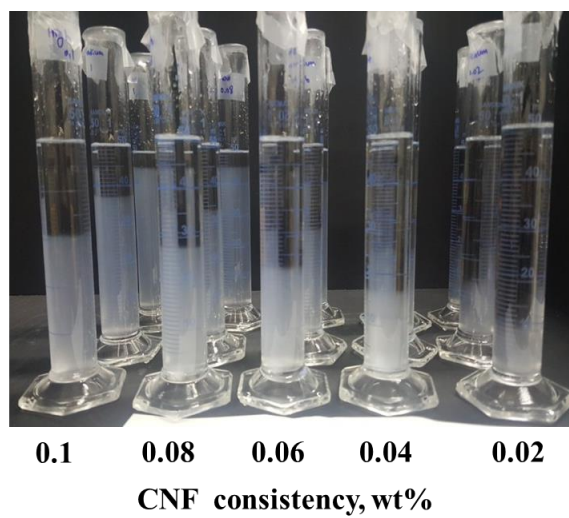


Fig. 5-8. Sedimentation behavior of CM CNFs neutralized by NaCl.

Fig. 5-9 shows the quadratic fit of the plot of the concentration of CM CNFs against the relative sediment height. Table 5-3 displays the results of the sedimentation experiment including the quadratic regression, gel point, and calculated aspect ratio. The width, zeta potential, and length of the CM CNFs might influence the sedimentation tendency. The width and zeta potential of the three CM CNFs were very similar to each other. Therefore, the aspect ratio is the only one of the three factors that affects sedimentation tendency. Table 5-3 shows that the CM CNFs prepared under different conditions had different aspect ratios. CM CNF A, which had the highest carboxyl content and underwent the mildest mechanical treatment, had the highest aspect ratio of 171. This indicates that the carboxyl content of CM CNFs influences both the mechanical energy needed to produce the CNF and the aspect ratio of the fibrils. Wågberg et al. (2008) reported that the length (L) and width (d) of CM CNF was $L \leq 1 \mu\text{m}$ and $d \approx 5 - 15\text{nm}$, respectively. This result agrees with the results calculated from sedimentation. Onyianta and Williams (2018) also calculated the aspect ratio of charged CNF using sedimentation. It was reported that the aspect ratio of CM CNF with carboxyl content of $550 \mu\text{mol/g}$ was 229 ± 18 . This difference was likely attributed to different salt concentration to dilute CNF, which influenced charge properties of CNF.

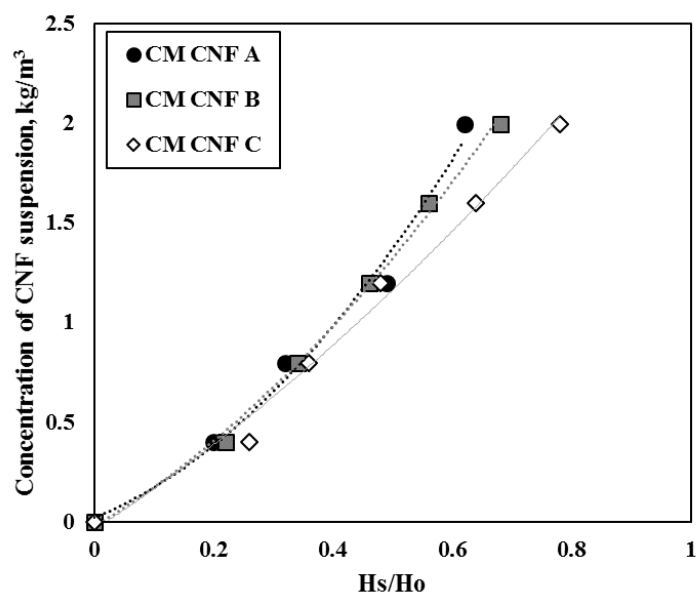


Fig. 5-9. Sedimentation tendency of CM CNFs.

Table 5-3. Quadratic regression, gel point, and aspect ratio

Classification	Quadratic regression (R^2)	Gel point (weight fraction)	Aspect ratio
CM CNF A	$y = 2.95x^2 + 1.227x$ (0.988)	0.0012	171
CM CNF B	$y = 1.85x^2 + 1.767x$ (0.997)	0.0018	142
CM CNF C	$y = 0.91x^2 + 1.952x$ (0.989)	0.0020	135

3.3 Rheological properties of CM CNF

Fig. 5-10 to 12 show the rheological properties of the CM CNFs at 0.5 wt.%. Shear thinning was clearly observed (Fig. 5-9), which was caused by the interactions between fibrils orientated along the shear direction. CM CNF A had a higher shear viscosity than the other two CNFs. The shear viscosities of CM CNF B and C were the same, irrespective of the carboxyl content and mechanical treatment level.

The amplitude and frequency sweep mode measurements were performed to find the network properties of the CM CNFs. Fig. 5-11 plots the storage modulus of CM CNFs against shear stress. The storage modulus had a plateau region in the low shear stress range. When the shear stress increased beyond the yield stress, the storage modulus decreased significantly. Yield stress is generally accepted as an indication of network strength. The network associated with the fibrils began to break down at the yield point. In a CNF system, yield stress depends on the aspect ratio (Müller et al. 2017; Li et al. 2015). Obviously, CM CNF A had a higher yield stress than CNF-B and CNF-C, which is consistent with CM CNF A's high aspect ratio, as measured in the sedimentation experiment (Fig. 5-12). Onyianta et al. (2018) also evaluated the aspect ratio and rheological properties of TEMPO-oxidized CNF and carboxymethylated CNF. They concluded that the CNF with higher aspect ratio showed higher storage modulus and critical strain.

Fig.5-13 shows the storage modulus as a function of frequency. The storage modulus increased as the aspect ratio increased, indicating that the CM CNF with the highest aspect ratio had the strongest network properties.

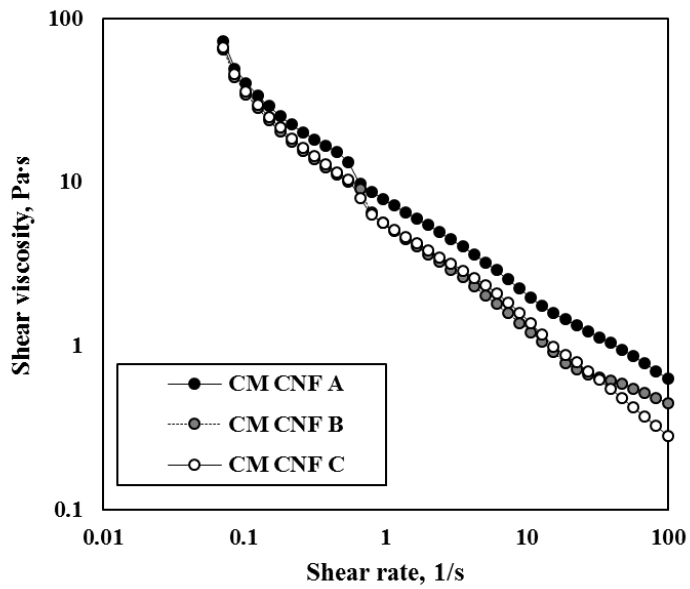


Fig. 5-10. Rotation viscosity of CM CNF suspensions produced by different conditions.

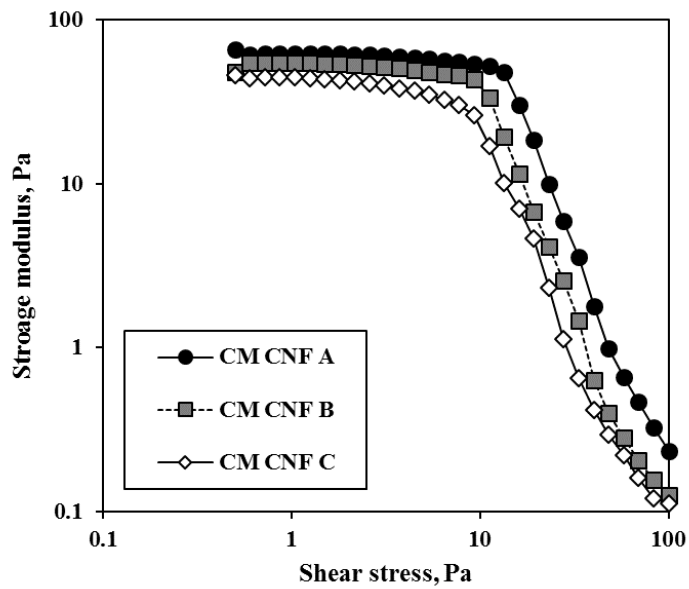


Fig. 5-11. Storage modulus of CM CNFs as a function of stress.

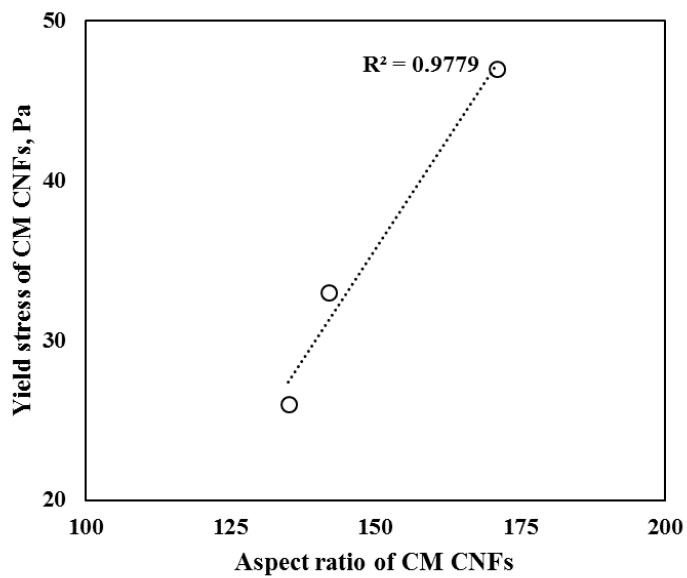


Fig. 5-12. Yield stress of CM CNFs depending on aspect ratio.

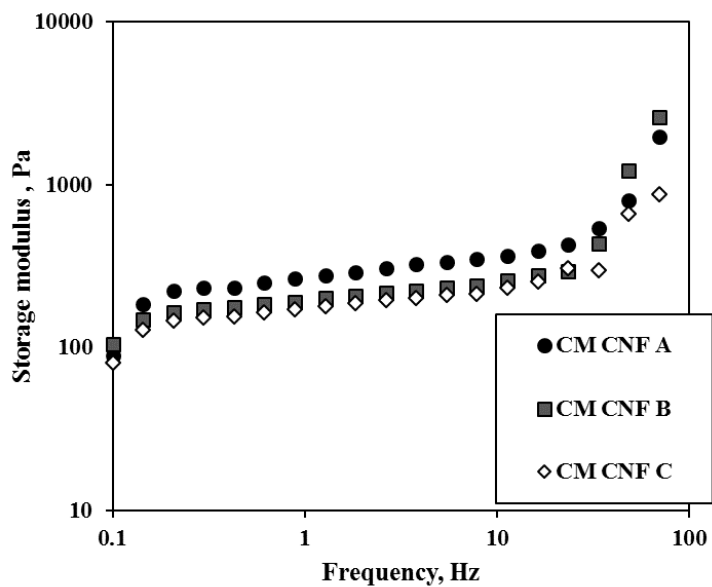


Fig. 5-13. Storage modulus of CM CNFs with frequency sweep.

3.4 Mechanical properties of CM CNF film

The transparent CM CNF films with different aspect ratio were prepared by casting method for 6 day (Fig. 5-14). Sim. (2016) also made the untreated CNF and CM CNF film. They reported that the light transmittance of those film was 78.4% and 87.9%, respectively.



Fig. 5-14. CM CNF film produced by casting method.

Fig. 5-15 and Table 5-4 show the XRD patterns and crystallinities of CNF samples, respectively. The crystallinities of the three CM CNF samples were around 60%, suggesting that carboxymethylation and mechanical treatment had no significant effects on crystallinity. Similar results have been reported by Siró et al. (2010) and Aulin et al. (2009). The densities of the CM CNFs films prepared using three CNFs are also listed in Table 5-4. The density of the film made of CM CNF C was higher than those of two other films, presumably because of its low aspect ratio as mentioned by Zhao et al. (2015).

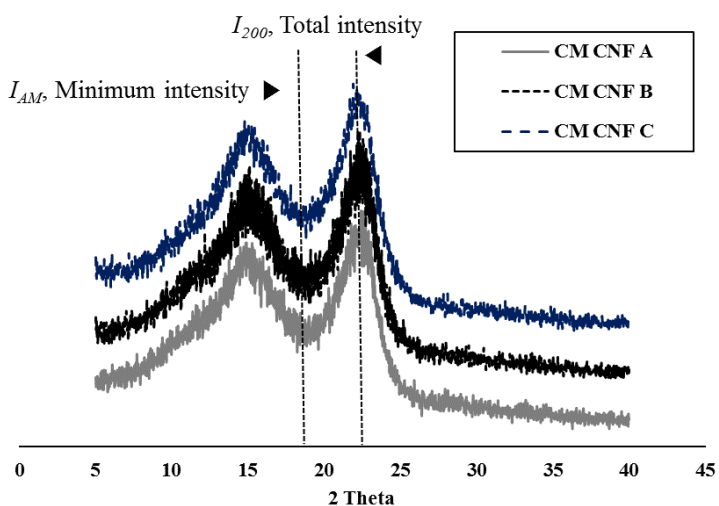


Fig. 5-15. XRD pattern of CM CNFs.

Table 5-4 Properties of the CM CNF films

Sample	Crystallinity, %	Density, g/ cm ³
CM CNF A	60.4	1.03
CM CNF B	64.8	1.04
CM CNF C	58.6	1.19

Figs 5-16 and 17 show the mechanical properties of the CM CNF films. There are clear correlations between the morphological properties of the CNF and the mechanical properties of the CNF films. There was a linear relationship between the tensile index and tensile strength of CNFs (Fig. 5-16). This indicated that the tensile property of film at the same basis weight is proportional to the aspect ratio. The film produced using CM CNF with a high aspect ratio also showed a high elongation at the break but a low modulus of elasticity due to the interconnection between fibrils. Fukuzumi et al. (2013) have shown that an increase in fibril length improves tensile strength and elongation at break. Lower tensile index of CM CNF film was attained compare with the results by Naderi et al. (2015). And this was attributed to the fact that the grinder gave lower specific area of CNF than homogenizer as pointed out by Spence et al. (2011).

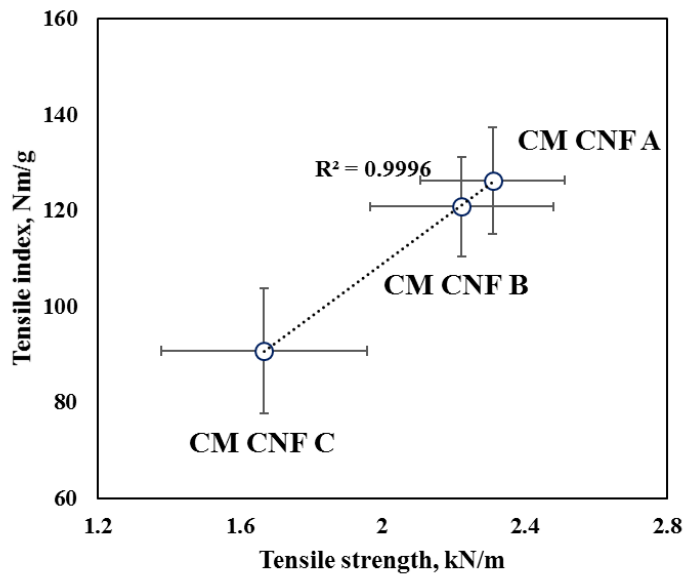


Fig. 5-16. Relationship between tensile index and tensile strength of CM CNFs films.

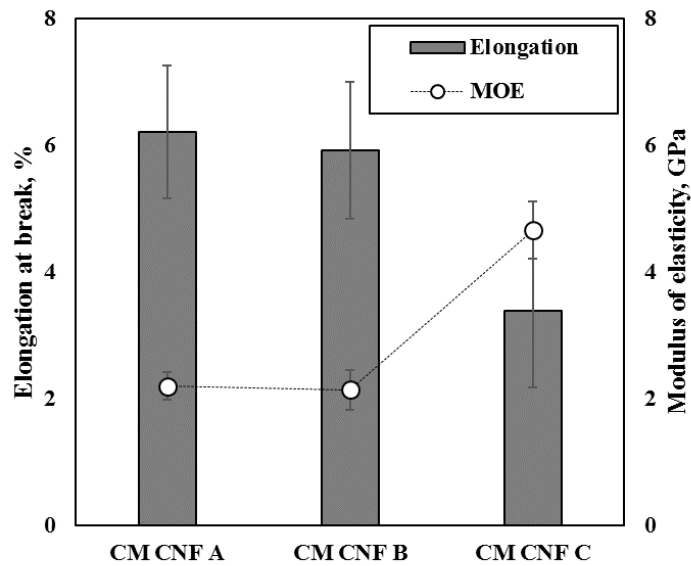


Fig. 5-17. Elongation at break and modulus of elasticity for three CM CNF films.

4. Summary

In this chapter, the influence of carboxyl content and mechanical treatment on the morphological properties of CM CNF was investigated. The carboxyl content of the pulp fiber was controlled by controlling the amount of MCA in the carboxymethylation reaction. The network properties of CM CNF suspensions and the mechanical properties of CM CNF films were also evaluated.

The width was measured using TEM image analysis. However, it is difficult to measure length of fibrils because many fibrils are entangled with each other and the image area are not large enough to display whole fibrils. To solve this weakness, the aspect ratio of the CM CNF was investigated using sedimentation experiments.

High charged CM CNF by introduced carboxyl group cannot settle down due to electrostatic repulsion force between fibrils. To settle down the fibrils under the same condition, the zeta potential of the CM CNFs with different carboxyl content was controlled by adding salt solutions. The aspect ratio was decreased as the number of grinding passes increased, which was dependent on the carboxyl content of the pulp fiber.

The rheological properties and the tensile properties of CM CNF films were all strongly influenced by the aspect ratio of CM CNFs. The CM CNF with the highest aspect ratio had the greatest network strength in suspension and produced the film with the strongest mechanical properties.

Chapter 6

Overall Conclusions

This study was aimed to optimize the carboxymethylation process for the production of CNF. Because higher carboxyl content can reduce the mechanical energy consumption, it is important to increase reaction activity at the same level of chemical consumption. To find out main factors of carboxymethylation efficiency, various reaction conditions were controlled. The recycling solvent is an essential step in carboxymethylation in terms of environmental and economic aspects of the process. Thus a new, inexpensive, environmentally friendly way for recycling of solvent was investigated. Finally, the morphological properties of CM CNF depending on carboxyl content and mechanical intensity was also estimated because the fundamental properties of CNF-based products are influenced by the CNF morphologies.

The effect of reaction variable such as the amount of chemicals, reaction time, temperature, and pulp type were controlled to find out main factors of general carboxymethylation method as a pre-treatment. It was shown that the carboxyl group content, which indicates degree of reaction activity, was affected by MCA amount and reaction temperature. Never-dried pulp showed higher reaction efficiency than once-dried pulp. To consider carboxymethylation efficiency in terms of reactivity and chemical consumption, the optimal carboxymethylation conditions were also investigated. The effect of solvent system, water content, and pulp consistency on carboxymethylation was assessed. It was found that high reaction activity can be achieved without the solvent exchange step of pulp and using only an IPA as reaction medium. The presence of water derived from wet-pulp affected reaction efficiency if the amount was over than 4 w/v%. The optimized reaction conditions used only one-third of chemicals for the same level of reaction efficiency, which indicated that chemical reagent and solvent for carboxymethylation can be reduced using optimized reaction conditions. Fibrillation degree, degree of polymerization,

and crystallinity of CM CNF produced under different reaction conditions were estimated. The number of mechanical treatment steps required to produce CNF substantially decreased as carboxyl content increased. The degree of polymerization and crystallinity of CM CNF having similar carboxyl content in spite of different reaction condition employed did not show significant difference. The optimum carboxymethylation reaction is expected for improving the reaction efficiency and for reducing the chemical cost.

Because carboxymethylation process uses huge amount of alcohols as reaction mediums, the recycling solvent should be consider for environmental and economic point of view. The waste IPA generated optimum carboxymethylation reaction contains water derived from wet-pulp. To recycling solvent water content should be adjusted because water content influenced carboxymethylation activity. However, IPA and water form an azeotropic mixture at 87.4 % IPA concentration, the separation of water from this mixture is difficult and uneconomical. In this study, adsorptive distillation using molecular sieve was adopted to separate water. The micro-pore or cage structure of the molecular sieve has a high affinity for polar water molecules while excluding IPA molecules. As the IPA recycling number increased, water content in the reaction medium increased linearly. An increased in water content in IPA prevented the reaction of NaOH with hydroxyl groups of the pulp fiber and increased unreacted NaOH in the waste IPA. The water content, pH, and conductivity of waste IPA was restored after molecular sieve treatment to the same level of fresh IPA. Moreover, the use of recycled dehydrated IPA maintained the carboxymethylation efficiency the same. The recycling of IPA after dehydration using the molecular sieve has the economic and environmental advantage of saving solvent while maintaining the same quality of CNF.

The characteristics of CNF are essential parameters for controlling the mechanical properties of CNF-based material. The chemical pre-treatment have made it possible to obtain CNF with narrow width distribution, which can be observed by microscopic techniques. However, the length of the fibers cannot be readily obtained from microscopy images due to entanglement of fibrils. The aspect ratio of CM CNF depending on mechanical intensity and carboxyl group content was investigated. Sedimentation experiment based on gel point analysis and the crowding number theory were conducted to evaluate aspect ratio of CM CNF samples. The carboxyl group content of CM CNF samples was controlled by controlling the amount of MCA in the carboxymethylation reaction. The higher carboxyl group content in the CM CNF reduced the amount of mechanical energy required and increased the aspect ratio. The dynamic rheological properties of CM CNF suspensions were also performed to find the network properties of CM CNF. The viscosity and storage modulus increased as the aspect ratio increased and The CM CNF with higher aspect ratio showed higher yield stress, which generally accepted as an indication of network strength. The mechanical properties of CM CNF films showed clear correlations with the morphological properties of the CNF. The CM CNF film prepared with high aspect ratio showed a high elongation at break and tensile properties due to the interconnection between fibrils.

Optimization of carboxymethylation as a pretreatment for the production of CNF were investigated in this study. Characteristics of CM CNF including electrostatic, morphological, and rheological properties were also evaluated. Based on these results, it is expected that carboxymethylation process can be used more economically and quality of CM CNF can be controlled to the desired purpose.

Reference

Abe, K., Iwamoto, S. and Yano, H., Obtaining cellulose nanofibers with a uniform width of 15 nm from wood, *Biomacromolecules* 8: 3276-3278 (2007).

Ahola, S., Österberg, M. and Laine, J., Cellulose nanofibrils-adsorption with poly (amideamine) epichlorohydrin studied by QCM-D and application as a paper strength additive, *Cellulose* 15:303-314 (2008).

Ahola, S., Salmi, J., Johansson, L. S., Laine, J. and Österberg, M., Model films from native cellulose nanofibrils. Preparation, swelling, and surface interactions. *Biomacromolecules* 9: 1273-1282 (2008).

Alila, S., Besbes, I., Vilar, M. R., Mutjé, P. and Boufi, S., Non-woody plants as raw materials for production of microfibrillated cellulose (MFC): A comparative study, *Industrial Crops and Productions* 41: 250-259 (2013).

Arvidsson, R., Nguyen, D. and Svanström, M., Life cycle assessment of cellulose nanofibrils production by mechanical treatment and two different pretreatment process, *Environ. Sci. Technol* 49: 6881-6890 (2015).

Andresen, M., Stenstad, P., Meretro, T., Landgsrud, S., Syverud, K., Johansson, L. S. and Stenius, P., Nonleaching antimicrobial films prepared from surface-modified microfibrillated cellulose, *Biomacromolecules* 8(7): 2149-2155 (2007).

Ambjörnsson, H. A., Schenzel, K. and Germgård, U., Carboxymethyl cellulose produced at different mercerization conditions and characterized by NIR FT Raman spectroscopy in combination with multivariate analytical methods, *BioResources* 8(2):1918-1932 (2013).

Aulin, C., Ahola, S., Josefsson, P., Nishino, T., Hirose, Y., Österberg, M. and Wågberg, L., Nanoscale cellulose films with different crystallinities and mesostructures - their surface properties and interaction with water, *Langmuir* 25(13): 7675-7685 (2009).

Aulin, C., Netrval, J., Wågberg, L. and Lindström T., Aerogels from nanofibrillated cellulose with tunable oleophobicity, *Soft Matter* 6:3298-3305 (2010).

Benhamou, L., Dufresne, A., Magnin, A., Mortha, G. and Kaddami, H., Control of size and viscoelastic properties of nanofibrillated cellulose from palm tree by varying the TEMPO-mediated oxidation time, *Carbohydrate Polymer* 99: 74-83 (2014).

Besbes, I., Alila, S. and Boufi, S., Nanofibrillated cellulose from TEMPO-oxidized eucalyptus fibres: effect of the carboxyl content. *Carbohydrate Polymer* 84: 975-983 (2011).

Bhattacharyya, D., Singhal, R. S. and Kulkarni, P. R., A comparative account of conditions for synthesis of sodium carboxymethyl starch from corn and amaranth starch, *Carbohydrate Polymers* 27:247-253 (1995).

Blakiston, B. A., Principles and application of modified atmosphere packaging of foods, Springer-Science+Business Media (2012).

Boufi, S., Kaddami, H. and Dufresne, A., Mechanical performance and transparency of nanocellulose reinforced polymer nanocomposite, *Macromol. Mater. Eng* 299:560-568 (2014).

Candanedo, S. B., Roman, M. and Gray, D. G., Effect of reaction conditions on the properties and behavior of wood cellulose nanocrystal suspensions, *Biomacromolecules* 6: 1048-1054 (2005).

Carrillo, C. A., Laine, J. and Rojas, O. J., Microemulsion systems for fiber deconstruction into cellulose nanofibrils, *ACS Appl. Mater. Interfaces* 6: 22622-22627 (2014).

Casson, L. W. and Bess, J. W., On-site sodium hypochlorite Generation, Water Environment Foundation, University of Pittsburgh, Pittsburgh, PA (2006).

Chaabouni, O. and Boufi, S., Cellulose nanofibrils/polyvinyl acetate nanocomposite adhesives with improved mechanical properties, *Carbohydrate Polymers* 152: 64-70 (2017).

Chen, Y., Wan, J., Dong, X. and Ma, Y., Fiber properties of eucalyptus kraft pulp with different carboxyl group contents, *Cellulose* 20:2839-2846 (2013).

Cheng, Q., Wang, S., Rials, T. G., Poly(vinyl alcohol) nanocomposites reinforced with cellulose fibrils isolated by high intensity ultrasonication, *Composites: Part A* 40: 218-224 (2009).

Cho, J. and Jeon, J., Optimization study on the azeotropic distillation process for isopropyl alcohol dehydration, *Korean J. Chem. Eng* 23(2): 1-7 (2006).

de Nooy, A. E. J., Besemer, A. C., van Bekkum, H., van Dijk, J. A. P. P. and Smit, J. A. M., TEMPO-mediated oxidation of pullulan and influence of ionic strength and linear charge density on the dimensions of the obtained polyelectrolyte chains, *Macromolecules* 29: 6541-6547 (1996).

Dong, H., Snyder, J. F., Tran, D. T. and Leadore, J. L., Hydrogel, aerogel and film of cellulose nanofibrils functionalized with silver nanoparticles, *Carbohydrate Polymers* 95: 760-767 (2013).

Espinosa, C. S., Kuhnt, T., Foster, E. J. and Weder, C., Isolation of thermally stable cellulose nanocrystals by phosphoric acid, *Biomacromolecules* 14:1223-1230 (2013).

Eyholzer, C., Bordeanu, N., Lopez-Suevos, F., Rentsch, D., Zimmermann, T. and Oksman, K., Preparation and characterization of water-redispersible nanofibrillated cellulose in powder form, *Cellulose* 17:19-30 (2010).

Fall, A. B., Lindström, S. B., Sundman, O., Ödberg, L. and Wågberg, L., Colloidal stability of aqueous nanofibrillated cellulose dispersions, *Langmuir* 27:11332-11338 (2011).

Fan, Y., Satio, T. and Isogai, A., TEMPO-mediated oxidation of β -chitin to prepare individual nanofibrils, *Carbohydrate Polymers* 77: 832-838 (2009).

Ferrer, A., Pal. L. and Hubbe, M., Nanocellulose in packaging: Advances in barrier layer technologies, *Industrial Crops and Product* 95: 574-582 (2017).

Fujisawa, S., Ikeuchi, T., Takeuchi, M., Satio, T. and Isogai, A., Superior reinforcement effect of TEMPO-oxidized cellulose nanofibrils in polystyrene matrix: optical, thermal, and mechanical studies. *Biomacromolecules* 13: 2188-2194 (2012).

Fukuzumi, H., Saito, T. and Isogai, A., Influence of TEMPO-oxidized cellulose nanofibril length on film properties, *Carbohydrate polymers* 93: 172-177 (2013).

Fujisawa, S., Saito, T., Kimura, S., Iwata, T. and Isogai, A., Surface engineering of ultrafine cellulose nanofibrils toward polymer nanocomposite materials. *Biomacromolecules* 14:1541-1546 (2013).

Ghanadpour, M., Carosio, F., Larsson, P. T. and Wågberg, L., Phosphorylated cellulose nanofibrils: A renewable nanomaterial for the preparation of intrinsically flame-retardant materials, *Biomacromolecules* 16: 3399-3410 (2015).

Guha, S., Neogi, S. G. and Chaudhury, P., Study of structure and spectroscopy of water-hydroxide ion cluster: A combined simulated annealing and DFT-based approach, *J. Chem. Sci* 126(3): 659-675 (2014).

Harris, D. C., *Quantitative chemical analysis*. (7th ed). New York: W. H. Freeman and Company, Chapter 11 (2007).

Henriksson, M., Henriksson, G., Berglund, L. and Lindström, T., An environmentally friendly method for enzyme-assisted preparation of microfibrillated cellulose (MFC) nanofibers, *European Polymer Journal* 43(8): 3434-3441 (2007).

Herrick, F. W., Casebier, R. L., Hamilton, J. K. and Sandberg, K. R., Microfibrillated cellulose: Morphology and accessibility, *J Appl Polym Sci: Appl Polym Symp* 37, 797-813 (1983).

Hil, C., Gregersen, Ø. W., Chinga-Carrasco, G. and Eriksen, Ø., The effect of MFC on the pressability and paper properties of TMP and GCC based sheet, *Nordic Pulp and Paper Journal* 27(2): 388-396.

Hill, C. A. S., Wood-plastic composites: strategies for compatibilising the Phases, *Journal of the Institute of Wood Science* 15(3): 140-146 (2000).

Hilmen, E., Separation of Azeotropic mixtures: tools for analysis and studies on batch distillation operation, PhD thesis, Norwegian University (2000).

Hirota, M., Tamura, N., Saito, T. and Isogai, A., Water dispersion of cellulose II nanocrystals prepared by TEMPO-oxidation of mercerized cellulose at pH 4.8, *Cellulose* 17: 279-288 (2010).

Ho, T. T. T., Abe, K., Zimmermann, T. and Yano, H., Nanofibrillation of pulp fibers by twin-screw extrusion, *Cellulose* 22: 421-433 (2015).

Hoeng, F., Denneulin, A., Reverdy-Bruas, N., Krosnicki, G. and Bras, J., Rheology of cellulose nanofibrils/silver nanowires suspension for the production of transparent and conductive electrodes by screen printing, *Applied Surface Science* 394: 160-168 (2017).

Im, W., Lee, S., Lee, H. L. and Youn, H. J., Effect of a combined pretreatment of beating and carboxymethylation on properties and nanofibrillation of pulp fibers, *Journal of Korea TAPPI* 49(5): 12-19 (2017).

Im, W., Lee, S., Rajabi Abhari, A., Youn, H. J. and Lee, H. L., Optimization of carboxymethylation reaction as a pretreatment for production of cellulose nanofibrils, *Cellulose* 25: 3873-3883 (2018).

Isogai, T., Satio, T. and Isogai, A., Wood cellulose nanofibrils prepared by TEMPO-electro-mediated oxidation, *Cellulose* 18(2): 421-431 (2011).

Ishii, D., Saito, T. and Isogai, A., Viscoelastic evaluation of average length of cellulose nanofibers prepared by TEMPO-mediated oxidation, *Biomacromolecules* 12: 548-550 (2011).

Iwamoto, S., Lee, S. H. and Endo, T., Relationship between aspect ratio and suspension viscosity of wood cellulose nanofibers, *Polymer Journal* 46: 73-76 (2014).

Jain, A. K. and Gupta, A. K., Adsorptive drying of isopropyl alcohol on 4A molecular sieves: Equilibrium and kinetic studies, *Separation Science and Technology* 29(11): 1461-1472 (1994).

Jie, Y., Wen-ren, C., Manurung, R. M., Ganzeveld, K. J. and Heeres, H. J., Exploratory studies on the carboxymethylation of cassava starch in water-miscible organic media, *Starch/Stärke* 56:100-107 (2004).

Jonoobi, M., Oladi, R., Davoudpour, Y., Oksman, K., Dufresne, A., Hamzeh, Y. and Davoodi, R., Different preparation methods and properties of nanostructured cellulose from various natural resources and residues: a review, *Cellulose* 22(2): 935-969 (2015).

Jowkarderis, L. and van de Ven, T. G. M., Intrinsic viscosity of aqueous suspensions of cellulose nanofibrils, *Cellulose* 21(4): 2511-2517 (2014).

Kerekes, R. J. and Schell, C. J., Characterization of fibre flocculation regimes by a crowding factor, *Journal of Pulp and paper Science* 18(1): J32-38 (1992).

Kim, C. H., Youn, H. J. and Lee, H. L., Preparation of cross-linked cellulose nanofibril aerogel with water absorbency and shape recovery, *Cellulose* 22: 3715-3724 (2015).

Klemm, D., Philipp, B., Heinze, T. and Hjeinze, U., *Comprehensive Cellulose Chemistry*. Wiley-VCH, New York (1998).

Ko, C. H., Chen, F. J., Lee, J. J. and Tzou, D. L. M., Effects of fiber physical and chemical characteristics on the interaction between endoglucanase and eucalypt fibers, *Cellulose* 18:1043-1054 (2011).

Kondo, T., Kose, R., Naito, H. and Kasai, W., Aqueous counter collision using paired water jets as a novel means of preparing bio-nanofibers, *Carbohydrate Polymer* 112: 284-290 (2014).

Kooijman, L. M., Ganzeveld, K., Manurung, R. M. and Heeres, H. J., Experimental studies on the carboxymethylation of arrowroot starch in isopropanol-water media, *Starch/Stärke* 55: 495-503 (2003).

Korhonen, J. T., Kettunen, M., Ras, R. H. A. and Ikkala, O., Hydrophobic nanocellulose aerogels as floating, sustainable, reusable, and recyclable oil absorbent, *Appl. Mater. Interfaces* 3: 1813-1816 (2011).

Kuuti, L., Pajari, H., Rovio, S., Kokkonen, J. and Nuopponen, M., Chemical recovery in TEMPO Oxidation, *BioResources* 11(3): 6050-6061 (2016).

Lasseguett, E., Roux, D. and Nishiyama, Y., Rheological properties of microfibrillar suspension of TEMPO-oxidized pulp, *Cellulose* 15: 425-433 (2008).

Li, M, C., Wu, Q., Song, K., Qing, Y. and Wu, Y., Cellulose nanoparticles as modifiers for rheology and fluid loss in bentonite water-based fluids, *ACS Appl. Mater. Interfaces* 7: 5006-5016 (2015).

Liu, S., Wang, Q., Yang, G., Chen, J., Ni, Y. and Ji, X., Kinetics of viscosity decrease by cellulose treatment of bleached hardwood kraft-based dissolving pulp, *Bioresources* 10(2): 2418-2424 (2015).

Mann, G., Kunze, J., Loth, F. and Fink, H. P., Cellulose ethers with a block-like distribution of the substituents by structure-selective derivatization of cellulose, *Polymer* 39(14):3155-3165 (1998).

Manhas, M., Balasubraanian, K., Prajith, P., Rule, P. and Nimje, S., PCL/PVA nanoencapsulated reinforcing fillers of steam exploded/autoclaved cellulose nanofibrils for tissue engineering application, *RSC Adv* 5: 23999-24008 (2015).

Mansikkamäki, P., Lahtinen, M. and Rissanen, K., Structural changes of cellulose crystallites induced by mercerization in different solvent system: determined by powder X-ray diffraction method, *Cellulose* 12:233-242 (2005).

Mao, Z., Cao, Y., Jie, X., Kang, G., Zhou, M. and Yuan, Q., Dehydration of isopropanol-water mixtures using a novel cellulose membrane prepared from cellulose/N-methylmorpholine-N-oxide/H₂O solution, *Separation and Purification Technology* 72: 28-33 (2010).

Martinez, D. M., Buckley, K., Jivan, S., Lindström, A., Triruvengadaswamy, R., Olson, J. A., Ruth, T. J. and Kerekes, R. J., Characterizing the mobility of papermaking fibres during sedimentation. 12th Fundamental Research Symposium, Oxford, pp 225-254 (2001).

Martucci, A., Pasti, L., Marchetti, N., Cavazzini, A., Dondi, F. and Alberti, A., Adsorption of pharmaceuticals from aqueous solutions on synthetic zeolites, *Microporous and Mesoporous Materials* 148: 174-183 (2012).

Marzal, P., Montón, J. B. and Rodrigo, M. A., Isobaric Vapor-Liquid Equilibria of the water + 2-propanol system at 30, 60, and 100 kPa, *J. Chem. Eng. Data* 41:608-611 (1996).

Meng, Q., Li, H., Fu, S. and Lucia, L., The non-trivial role of native xylans on the preparation of TEMPO-oxidized cellulose nanofibrils, *Reactive and Functional Polymers* 85:142-150 (2014).

Miao, C. and Hamad. W. Y., Cellulose reinforced polymer composites and nanocomposites: a critical review, *Cellulose* 20:2221-2262 (2013).

Missoum, L., Belgacem, M. N. and Bras, J., Nanofibrillated cellulose surface modification: a review, *Materials* 6(5): 1745-1766 (2013).

Mjalli, F., Al-Asheh, S., Banat, F. and Al-Lagtah, N., Representation of adsorption data for the isopropanol-water system using neural network techniques, *Chem. Eng. Technol* 28(12): 1529-1539 (2005).

Mohkami, M. and Talaeipour, M., Investigation of the chemical structure of carboxylated and carboxymethylated fibers from waste paper via XRD and FTIR analysis, *BioResources* 6(2): 1988-2003 (2011).

Müller, M., Öztürk, E., Arlov, Ø., Gatenholm, P. and Wong, M. Z., Alginate sulfate-nanocellulose bioinks for cartilage bioprinting applications, *Annals of Biomedical Engineering* 1: 210-223 (2017).

Naderi, A., Larsson, P. T., Stevanic, J. S., Lindström, T. and Erlandsson, J., Effect of the size of the charged group on the properties of alkoxyated NFCs, *Cellulose* 24(3):1307-1317 (2017).

Naderi, A., Lindström, T. and Sundström, J., Repeated homogenization, a route for decreasing the energy consumption in the manufacturing process of carboxymethylated nanofibrillated cellulose?, *Cellulose* 22: 1147-1157 (2015).

Nair, S. S., Zhu, J., Deng, Y. and Ragauskas, A. J., High performance green barriers based on nanocellulose, *Sustainable Chemical Processes* 2:23 (2014).

Nakagaito, A. N., and Yano, H., The effect of morphological changes from pulp fiber towards nano-scale fibrillated cellulose on the mechanical properties of high-strength plant fiber based composites, *Appl. Phys. A* 78: 547-552 (2004).

Nechyporchuk, O., Belgacem, M. N. and Bras, J. Production of cellulose nanofibrils: A review of recent advances, *Industrial Crops and Products* 93: 2-25 (2016).

Oh, K., Lee, J., Im, W., Rajabi Abhari, A. and Lee, H. L., Role of cellulose nanofibrils in structure formation of pigment coating layers, *Ind. Eng. Chem. Res* 56:9569-9577 (2017).

Okita, Y., Fujisawa, S., Saito, T. and Isogai, A., TEMPO-oxidized cellulose nanofibrils dispersed in organic solvents, *Biomacromolecules* 15: 518-522 (2011).

Onyianta, A. J., Dorris, M. and Williams, R. L., Aqueous morpholine pre-treatment in cellulose nanofibril(CNF) production: comparison with carboxymethylation and TEMPO oxidization pre-treatment methods, *Cellulose* 25: 1047-1064 (2018).

Onyianta, A. J. and Williams, R., The use of sedimentation for the estimation of aspect ratios of charged cellulose nanofibrils, *Advances in Natural Fibre Composites* 195-203 (2018).

Petroudy, S. R. D., Syverud, K., Chinga-Carrasco, G., Ghasemian, A. and Resalati, H., Effects of bagasse microfibrillated cellulose and cationic polyacrylamide on key properties of bagasse paper, *Carbohydrate Polymers* 99: 311-318 (2014).

Pääkkö, M., Ankerfors, M., Kosonen, H., Nykänen, S., Ahola, M., Österberg, M., Ruokolainen, J., Laine, J., Larsson, P. T., Ikkala, O. and Lindström, T., Enzymatic hydrolysis combined with mechanical shearing and high-pressure homogenization for nanoscale cellulose fibrils and strong gels, *Biromacromolecules* 8:1934-1941 (2007).

Qi, H., Liebert, T., Meister, F. and Heinze, T., Homogenous carboxymethylation of cellulose in the NaOH/urea aqueous solution, *Reactive & Functional Polymer* 69:779-784 (2009).

Qing, Y., Sabo, R., Zhu, J. U., Agarwal, U., Cai, Z. and Wu, Y., A comparative study of cellulose nanofibrils disintegrated via multiple processing approaches, *Carbohydrate Polymers* 97:226-234 (2013).

Qiu, H. and He, L., Synthesis and properties study of carboxymethyl cassava starch, *Polymers for Advanced Technologies* 10:468-472 (1999).

Qu, P., Zhou, Y., Zhang, X., Yao, S. and Zhang, L., Surface modification of cellulose nanofibrils for poly(lactic acid) composite application, *Journal of Applied Polymer Science* 125(4): 3084-3091 (2012).

Rachipudi, P. S., Kariduraganavar, M. Y., Kittur, A. A. and Sajjan, A. M., Synthesis and characterization of sulfonated-poly(vinyl alcohol) membranes for the pervaporation dehydration of isopropanol, *Journal of Membrane Science* 383: 224-234 (2011).

Ramos, L. A., Frollini, E. and Heinze, T., Carboxymethylation of cellulose in the new solvent dimethyl sulfoxide/tetrabutylammonium fluoride, *Carbohydrate Polymer* 60:259-267 (2005).

Raj, P., Mayahi, A., Lahtinen, P., Varanasi, S., Garnier, G., Martin, D. and Batchelor, W., Gel pint as a measure of cellulose nanofibre quality and feedstock development with mechanical energy, *Cellulose* 23:3051-3064 (2016).

Ren, J. L., Sun, R. C. and Peng, F., Carboxymethylation of hemicelluloses isolated from sugarcane bagasse, *Polymer Degradation and Stability* 93:786-793 (2008).

Rodionova, G., Lenes, M., Eriksen, Ø. and Gregersen, Ø., Surface chemical modification of microfibrillated cellulose: improvement of barrier properties for packaging applications, *Cellulose* 18: 127-134 (2011).

Ryu, J., Fundamental properties of nanofibrillated cellulose in suspension and mat states, PhD thesis, Seoul National University (2013).

Saito, T., Hirota, M, Tamura, N., Kimura, S., Fukuzumi, H., Heux, L., and Isogai, A., Individualization of nano-sized plant cellulose fibrils by direct surface carboxylation using TEMPO catalyst under neutral conditions, *Biomacromolecules* 10: 1992-1996 (2009).

Saito, T., Kuramae, R., Wohler, J., Berglund, L. A. and Isogai, A., An ultrastrong nanofibrillar biomaterial: the strength of single cellulose nanofibrils revealed via sonication-induced fragmentation. *Biomacromolecules* 14:248-253 (2013).

Saito, T., Okita, Y., Nge, T. T., Sugiyama, J. and Isogai, A., TEMPO-mediated oxidation of native cellulose: Microscopic analysis of fibrous fractions in the oxidized products. *Carbohydrate Polymers* 65:435-440 (2006).

Shinoda, R., Saito, T., Okita, Y. and Isogai, A., Relationship between length and degree of polymerization of TEMPO-oxidized cellulose nanofibrils. *Biomacromolecules* 13: 842-849 (2012).

Sim, K., Preparation and characterization of porous sheet with cellulose nanofibrils and its potential application, PhD thesis, Seoul National University (2016).

Sim, K. and Youn, H. J., Preparation of porous sheets with high mechanical strength by the addition of cellulose nanofibrils, *Cellulose* 23:1383-1392 (2016).

Siró, I., Plackett, D., Hedenqvist, M., Ankerfors, M. and Lindström, T., Highly transparent films from carboxymethylated microfibrillated cellulose: the effect of multiple homogenization steps on key properties, *Journal of Applied Polymer Science* 119:2652-2660 (2011).

Siqueira, G., Bras, J. and Dufresne, A., Cellulose whiskers versus microfibrils: influence of the nature of the nanoparticle and its surface functionalization on the thermal and mechanical properties of nanocomposites, *Biomacromolecules* 10(2): 425-432 (2009).

Spence, K. L., Venditti, R. A., Rojas, O. J., Habibi Y. and Pawlak, J. J., A comparative study of energy consumption and physical properties of microfibrillated cellulose produced by different processing methods, *Cellulose* 18:1097-1111 (2011).

Stigsson, V., Kloow, G. and Germgård, U., The influence of the solvent system used during manufacturing of CMC, *Cellulose* 13:705-712 (2006).

Suflet, D. M., Chitanu, G. C. and Popa, V. I., Phosphorylation of polysaccharides: New results on synthesis and characterization of phosphorylated cellulose, *Reactive & Functional Polymers* 66:1240-1249 (2006).

Suryanegara, L., Nakagaito, A. N. and Yano, H., The effect of crystallization of PLA on the thermal and mechanical properties of microfibrillated cellulose-reinforced PLA composites, *Composites Science and Technology* 69: 1187-1192 (2009).

Svagan, A. J., Azizi Samir, M. A. S. and Berglund, L. A., Biomimetic foams of high mechanical performance based on nanostructured cell wall reinforced by native cellulose nanofibrils, *Adv. Mater* 20: 1263-1269 (2008).

Syverud, K., Chinaga-Carraso, G., Toledo, J. and Toledo, P. G., A comparative study of Eucalyptus and Pinus radiata pulp fibres as raw materials for production of cellulose nanofibrils, *Carbohydrate Polymer* 84:1003-1038 (2011).

Syverud, K. and Stenius P., Strength and barrier properties of MFC films, *Cellulose* 16: 75-85 (2009).

Tanaka, R., Saito, T., Ishii, D. and Isogai, A., Determination of nanocellulose fibril length by shear viscosity measurement, *Cellulose* 21: 1581-1589 (2014).

Tejado, A., Alam, M. N., Antal, M., Yang, H. and van de Ven, T. G. M., Energy requirements for the disintegration of cellulose fibers into cellulose nanofibers, *Cellulose* 19: 831-842 (2012).

Teo, W. K. and Ruthven, D. M., Adsorption of water from aqueous ethanol using 3-Å molecular sieves, *Ind. Eng. Chem. Process Des. Dev.*, 25 (1): 17-21 (1986).

Thygesen, A., Oddershede, J., Lilholt, H., Thomsen, A. B. and Ståhl, K., On the determination of crystallinity and cellulose content in plant fibres, *Cellulose* 12: 563-576 (2005).

Tijssen, C. J., Kolk, H. J., Stamhuis, E. J. and Beenackers, A. A. C. M., An experimental study on the carboxymethylation of granular potato starch in non-aqueous media, *Carbohydrate Polymer* 45:219-226 (2001).

Tuckerman, M. E., Marx, D. and Parrinello, M., The nature and transport mechanism of hydrated hydroxide ions in aqueous solution, *Nature* 417(6892): 925-929 (2002).

Turbak, A. F., Snyder, F. W. and Sandberg, K. R., Microfibrillated cellulose, a new cellulose product: properties, uses, and commercial potential, *J Appl Polym Sci: Appl Polym Symp* 37:815-827 (1983).

Uetani, K. and Yano, H., Zeta potential time dependence reveals the swelling dynamics of wood cellulose nanofibrils. *Langmuir* 28:818–827 (2012).

Varanasi, S., He, R. and Batchelor, W., Estimation of cellulose nanofibre aspect ratio from measurements of fibre suspension gel point, *Cellulose* 20: 1885-1896 (2013).

Wang, M., Olszewska, A., Walther, A., Malho, J. M., Schacher, F. H., Ruokolainen, J., Ankerfors, M., Laine, J., Berglund, L. A., Österberg, M. and Ikkala, O., Colloidal ionic assembly between anionic native cellulose nanofibrils and cationic block copolymer micelles into biomimetic nanocomposites, *Biomacromolecules* 12:2074-2081(2011).

Wang, Q. Q., Zhu, J. Y., Gleisner, R., Kuster, T. A., Baxa, U. and Mcneil, S. E., Morphological development of cellulose fibrils of a bleached eucalyptus pulp by mechanical fibrillation, *Cellulose* 19:1631-1643 (2012).

Wang, W., Sabo, R. C., Mozuch, M. D. Kersten, P., Physical and mechanical properties of cellulose nanofibrils films from bleached eucalyptus pulp by endoglucanase treatment and microfluidization, *J Polm Environ* 23:551-402 558 (2015).

Wiśniewska, M., Influences of polyacrylic acid adsorption and temperature on the alumina suspension stability, *Powder Technology* 198:258-266 (2010).

Wu, C. N., Saito, T., Fujisawa, S., Fukuzumi, H. and Isogai, A., Ultrastrong and high gas-barrier nanocellulose/clay-layered composites, *Biomacromolecules* 13:1927-1932 (2012).

Wågberg, L., Decher, G., Norgren, M., Lindström, T., Ankerfors, M. and Axnäs, K., The build-up of polyelectrolyte multilayers of microfibrillated cellulose and cationic polyelectrolytes, *Langmuir* 24(3):784-795 (2008).

Xantheas, S. S., Theoretical study of hydroxide ion-water clusters *J. Am. Chem. Soc* 117: 10373-10380 (1995).

Xu, X., Liu F., Jiang, L., Zhu, J. Y., Haagenson, D. and Wiesenborn, D. P., Cellulose nanocrystals vs. cellulose nanofibrils: A comparative study on their microstructures and effects as polymer reinforcing agents, *ACS Appl. Mater. Interfaces* 5: 2999-3009 (2013).

Yokota, H., The mechanism of cellulose alkalization in the isopropyl alcohol-water- sodium hydroxide- cellulose system, *Journal of Applied Polymer Science* 30:263-277 (1985).

Zhang, F., Ren, H., Tong, G. and Deng, Y., Ultra-lightweight poly (sodium acrylate) modified TEMPO-oxidized cellulose nanofibrils aerogel spheres and their superabsorbent properties, *Cellulose* 23:3665-3676 (2015).

Zhang, L., Batchelor, W., Varanasi, S., Tsuzuki, T. and Wang, X., Effect of cellulose nanofiber dimensions on sheet forming through filtration. *Cellulose* 19:561-574 (2012).

Zhao, Y., Xu, C., Xing, C., Shi, X., Matuana, L. M., Zhou, H. and Ma, X., Fabrication and characteristics of cellulose nanofibrils films from coconut palm petiole prepared by different mechanical processing, *Industrial Crops and Product* 65: 96-101 (2015).

Zimmermann, T., Pöhler, E., and Geiger, T., Cellulose fibrils for polymer reinforcement, *Adv Eng Mater* 6: 754-761 (2004).

초 록

목재 및 비 목재 펄프 섬유로부터 그라인더, 호모게나이저 등과 같은 기계적 처리에 의하여 제조되는 셀룰로오스 나노피브릴(Cellulose nanofibrils, CNF)은 형태학적으로 100 nm 미만의 직경과 수 마이크로미터 수준의 길이를 갖는다. 식물로부터 유래되는 셀룰로오스 기반의 물질이기 때문에 재생가능하며, 생분해성이며, 높은 강도적 특성으로 인하여 고분자 복합체의 강도보강재, 투명 필름, 유변물성 개선제 등의 많은 분야로의 적용 가능성이 있는 물질이다. 하지만 CNF를 제조할 때 소비되는 높은 기계적 에너지 소비로 인하여 생산성 및 생산 원가가 매우 높아진다는 문제가 있으며 이러한 높은 가격은 CNF의 활용 범위를 넓히는데 하나의 한계로서 작용하고 있다. 다양한 전처리 방법 중 화학적 전처리를 통하여 제조된 CNF의 경우 낮은 에너지 소비만으로도 폭이 좁고 균일한 CNF의 제조가 가능하다고 알려져 있다. 대표적인 화학적 전처리 방법인 카르복시메틸화(Carboxymethylation) 전처리 반응은 알칼리 조건에서 펄프섬유와 모노클로로아세트산과의 에스테르화 반응을 통하여 진행된다. 일반적으로 널리 알려진 카르복시메틸화 전처리 반응 방법은 에탄올을 이용한 펄프의 용매 치환 과정과 메탄올과 아이소프로판올 혼합용매를 반응 용매로 사용하기 때문에 소비되는 유기용매의 양이 매우 많으며 용매 조건이 복잡하다는 단점이 있다. 또한 반응에 사용된 많은 양의 유기 용매들은 반응 후 버려지게 되기 때문에 추가적인 비용적, 환경적 문제를 야기하게 된다.

따라서 본 연구에서는 저비용의 CNF제조를 위한 카르복시메틸화 전처리 반응 및 반응 공정의 최적화에 대한 연구를 진행하였다. 첫째로, 카르복시메틸화 전처리 반응 시 다양한 반응 조건, 반응 순서 및 용매 조건의 변화를 통해 펄프 내 카르복실기의 함량을 높일 수 있는 방법을 연구하였다. 둘째로는 카르복시메틸화 전처리 시

일회성 사용에 그치는 반응 용매의 재활용 방안에 대한 연구를 진행하였으며, 이를 통하여 전처리를 통한 나노화에너지 저감효과와 더불어 전처리 비용의 절감을 통해 저비용의 CNF를 제조하고자 하였다. 또한 카르복시메틸화 전처리에 의해 도입된 이온성 작용기의 양에 따른 CNF의 형태학적 특성을 침전 양상 평가를 통하여 연구하였다.

카르복시메틸화 전처리 반응조건의 변화를 통하여 전처리 반응 시 펄프의 카르복실기 함량은 클로로아세트산의 투입량과 반응온도에 크게 영향을 받는 것으로 나타났다. 또한 본 연구에서는 반응조건의 최적화를 통하여 사용되는 반응 용매의 단순화 및 최소화 하는 방안에 대한 연구를 진행하였다. 용매 치환이 되지 않은 펄프를 사용하였으며, 반응 용매의 경우 아이소프로판올만을 단독으로 사용하였을 때 기존에 널리 알려진 전처리 반응 조건에 비하여 약 4배 이상의 높은 카르복실기 함량을 갖는 전처리 펄프를 제조할 수 있었다. 또한 최적화된 카르복시메틸화 전처리 반응의 경우 용매 치환되지 않은 펄프를 사용하기 때문에 펄프에서 유래된 수분이 반응성에 영향을 주었다. 약 4% 이상의 수분이 아이소프로판올 내에 존재할 경우 전처리 반응성은 감소하였다. 최적화된 카르복시메틸화 전처리 방법으로 제조된 전처리 펄프는 기존의 방식으로 제조한 펄프와 동일한 펄프 특성, 분화 양상, 그리고 CNF를 제조하였을 경우에도 동일한 폭을 갖는 것을 알 수 있었다. 이로 인하여 최적화된 카르복시메틸화 전처리를 통하여 수산화나트륨과 모노클로로아세트산의 사용량을 절감시킬 수 있었을 뿐만 아니라 반응 용매의 사용을 단순화시킬 수 있었다.

최적화된 전처리 반응 후 회수된 아이소프로판올을 동일한 조건에서 다음 전처리 반응의 반응 용매로 재 사용할 경우 펄프에서 유래된 수분량이 누적되어 반응성은 감소하는 결과를 나타내었다. 또한 아이소프로판올 내 수분량 증가에 의하여 알칼리화 단계에서 펄프

와 반응하지 못하는 수산화나트륨의 양이 증가하는 것을 알 수 있었다. 전처리 반응성에 영향을 미치지 않으며 반응용매의 반복적인 사용을 위해서는 아이소프로판올 내 수분량을 적절한 수준으로 관리해주어야 하나 물과 아이소프로판올은 공비 혼합물 (Azeotropic mixture)을 형성하여 분별 증류 방식으로는 87.4% 이상으로 아이소프로판올을 농축할 수 없는 문제점을 가지고 있다. 이를 위하여 본 연구에서는 분자체를 이용한 흡착 탈수 (Absorption dehydration) 방식을 이용하였다. 분자체를 공비 혼합물 내 침지시킴으로서 선택적인 수분의 제거가 가능하였으며, 이를 통해 수분이 제거된 아이소프로판올을 전처리 반응 용매로 재 사용해주었을 때 카르복시메틸화 전처리 반응성은 유지되었다.

전처리에 의하여 펄프에 도입된 카르복실기의 함량이 증가할수록 CNF를 제조할 때 소비되는 에너지는 감소하게 된다. 이러한 영향이 CNF의 특성에 미치는 영향에 대하여 평가하였다. 모노클로로아세트산 함량을 조절하여 카르복실기 함량이 상이한 세 조건의 펄프를 제조하였으며 이를 CNF로 제조하였다. 겔 포인트 (Gel point)와 크라우딩 넘버 (Crowding number)이론을 바탕으로 한 침전 양상평가를 통하여 카르복실기 함량과 기계적 에너지 소비량에 따른 CNF의 중형비를 산출 할 수 있었다. 또한 CNF의 물성을 유연성, 필름 특성과 연관지어 평가함으로써, 무처리 CNF 대비 카르복시메틸화 CNF의 특성을 제시 할 수 있었다.

주요어: 셀룰로오스 나노피브릴, 카르복시메틸화, 화학적 전처리, 용매 재사용, 전처리 반응성, 중형비, 유연특성, 기계적 강도

학번: 2014-31166